

NBER WORKING PAPER SERIES

PACK-CRACK-PACK:  
GERRYMANDERING WITH DIFFERENTIAL TURNOUT

Laurent Bouton (r)  
Garance Genicot (r)  
Micael Castanheira (r)  
Allison L. Stashko (r)



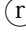
Working Paper 31442  
<http://www.nber.org/papers/w31442>

NATIONAL BUREAU OF ECONOMIC RESEARCH  
1050 Massachusetts Avenue  
Cambridge, MA 02138  
July 2023, Revised October 2024

Castanheira acknowledges the financial support of the FNRS. Genicot and Bouton acknowledge NSF grant SES 2242288. We are grateful to Luke Miller for his research assistance. We thank Wiola Dziuda, Kfir Eliaz, Adam Meirowitz, Debraj Ray, Alessandro Tarozzi, Philip Ushchev, Alexander Wolitzky, and seminar participants at numerous conferences as well as the California Institute of Technology, Columbia University, ECARES, Emory University, George Washington University, Hebrew University, HEC Montreal, London School of Economics, New York University, Penn State University, Queen Mary University London, Tel Aviv University, University College London, University of Chicago, University of New South Wales, University of Nottingham and University of Toronto for their comments. (r) indicates that author names are in random order. The views expressed herein are those of the authors and do not necessarily reflect the views of the National Bureau of Economic Research.


NBER working papers are circulated for discussion and comment purposes. They have not been peer-reviewed or been subject to the review by the NBER Board of Directors that accompanies official NBER publications.


© 2023 by Laurent Bouton (r) Garance Genicot (r) Micael Castanheira (r) Allison L. Stashko. All rights reserved. Short sections of text, not to exceed two paragraphs, may be quoted without explicit permission provided that full credit, including © notice, is given to the source.


Pack-Crack-Pack: Gerrymandering with Differential Turnout  
Laurent Bouton  Garance Genicot  Micael Castanheira  Allison L. Stashko  
NBER Working Paper No. 31442  
July 2023, Revised October 2024  
JEL No. D72

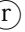
## **ABSTRACT**

This paper studies the manipulation of electoral maps by political parties, commonly referred to as gerrymandering. At the core of our analysis is the recognition that not all inhabitants of a district vote. This is important for gerrymandering as districts must have the same population size, but only voters matter for electoral outcomes. We propose a model of gerrymandering that allows for heterogeneity in voter turnout across individuals. This model reveals a new strategy for the gerrymanderers: the pattern is to pack-crack-pack along the turnout dimension. Specifically, parties benefit from packing low-turnout supporters and high-turnout opponents, while creating cracked districts that combine moderate-to-high-turnout supporters with lower-turnout opponents. These findings yield testable empirical implications about the relationship between partisan support, turnout rates, and electoral maps. Using a novel empirical strategy based on comparing maps proposed by Democrats and Republicans during the 2020 U.S. redistricting cycle, we test these predictions and find supporting evidence.

Laurent Bouton   
Georgetown University  
Department of Economics  
37th & O Streets, NW  
Washington, DC 20057  
and CEPR  
and also NBER  
boutonllj@gmail.com

Garance Genicot   
Georgetown University  
Department of Economics  
37th & O Streets, NW  
Washington, DC 20057  
and NBER  
gg58@georgetown.edu

Micael Castanheira   
ECARES, ULB CP 114  
50 Av. F.D. Roosevelt  
1050 Brussels, Belgium  
micael.casta@gmail.com

Allison L. Stashko   
Emory University  
Department of Quantitative Theory  
and Methods  
36 Eagle Row  
Atlanta, GA 30322  
allison.stashko@emory.edu

# 1. Introduction

Gerrymandering refers to the manipulation of electoral maps in order to gain a political advantage: the strategic redrawing of electoral districts by the incumbent party.<sup>1</sup> Most countries tackled this risk of manipulation by delegating redistricting to independent electoral commissions (Stephanopoulos 2013).<sup>2</sup> In contrast, in part with the support of enhanced data and software, gerrymandering is stronger than ever in the United States. Beyond producing “bizarrely-shaped” districts, that are not geographically compact or cohesive, gerrymandering appears to provide an unfair advantage to the party of the gerrymanderer and to impact policymaking. It affects the quality of political candidates (Stephanopoulos and Warshaw 2020), the ideological position of legislators (Jeong and Shenoy 2022; Caughey et al. 2017; Shotts 2003), roll-call voting behavior (Jones and Walsh 2018), the ideological slant of implemented policies (Caughey et al. 2017), and the allocation of public resources (Stashko 2020). Perhaps as a consequence, gerrymandering is viewed as a major problem of the U.S. political system by a majority of Americans.<sup>3</sup>

This paper focuses on the strategic incentives of gerrymanderers when they draw electoral maps.<sup>4</sup> We propose a novel model of gerrymandering and then bring some of its predictions to the data. We take into account a simple but important fact that has been mostly overlooked by the literature: not all inhabitants of a district vote (either because they are not eligible to vote or because they decide not to do so), and while districts must be equal in population size (counting voters and non-voters), only voters matter for electoral outcomes.

Differences in voting eligibility and voting propensity are large in practice. Only 72% of the U.S. population was eligible to vote in 2020, with significant heterogeneity across precincts.<sup>5</sup> Among eligible voters, the propensity to vote varies substantially with socio-demographic characteristics independently of their district characteristics. For instance, only 51.4% of those aged 18-24 voted in 2020, much below the 71% of those aged 65-74.<sup>6</sup> Together, variations in voting eligibility and voting propensity lead to large turnout rate

---

<sup>1</sup>The term is a portmanteau between the name of Governor Gerry and the salamander-like shape of a Massachusetts district from 1812, when the state legislature redrew the state senate districts.

<sup>2</sup>Exceptions include Hungary, Lebanon and, most notably, the U.S.

<sup>3</sup>APNORC Center for Public Affairs Research 2021.

<sup>4</sup>Understanding those incentives and what an optimally gerrymandered map look like is a necessary step to identify a gerrymandered map, develop measures of gerrymandering, evaluate the effects gerrymandering could have on electoral outcomes and policymaking, and assess potential regulations.

<sup>5</sup>The remaining 28% were ineligible for reasons such as being minors, convicted felons, or noncitizens.

<sup>6</sup>Similar gaps exist across race, income, and other socio-demographic characteristics (Census 2021, US Elections Project 2020).

differences (calculated as the share of all inhabitants who vote), both across precincts within states, and across and within partisan groups.<sup>7</sup> Importantly, these variations in turnout rates are largely predictable.<sup>8</sup> Gerrymanderers can thus easily exploit them. And indeed, there is evidence that gerrymanderers and the courts take turnout rates into account when drawing and assessing maps.<sup>9</sup>

How does a gerrymanderer want to draw their electoral map when voters differ not just in their ideological lean but also in their eligibility or propensity to vote? Do they want to “pack” some types of voters into some districts? Or to “crack” them and create districts that mix supporters and opponents? In the latter case, does the gerrymanderer want to mix higher turnout supporters with higher turnout opponents or with lower turnout ones? Does the gerrymanderer want their higher turnout supporters in strong or weak districts?

In order to answer these questions, we propose a new model of gerrymandering in which voters differ in terms of ideology and turnout rate. We anchor our model in the classic probabilistic voting model (see e.g., Lindbeck and Weibull 1987). The population is composed of various groups of individuals, which are characterized by their ideological lean—with Democrats having a higher probability to prefer the Democratic Party than Republicans do—and by their turnout rates (as in Strömberg 2004), which can depend on the composition of the district. Before the election, the gerrymanderer must draw the electoral map. This means allocating individuals from each group to districts, with the two-pronged constraint that each district must contain the same population mass and, naturally, that all of the population be allocated to a district. The gerrymanderer’s objective is to maximize the expected seat share of the incumbent party.

Our model uncovers a new force that shapes the map in the presence of turnout heterogeneity: gerrymanderers want to separate lower-turnout supporters from higher-turnout opponents and to mix higher-turnout supporters with lower-turnout opponents. This is because the election is more easily lost when a population of supporters gets diluted by an

---

<sup>7</sup>In recent presidential elections, the 25th and 75th percentiles of precinct-level turnout rates are 30% and 55%. See Table E.7 and Figure ?? in Appendix E.5 for more details.

<sup>8</sup>For example, when we predict precinct-level turnout rates for 25 states using only socio-demographic characteristics, the coefficient of correlation between predicted and realized turnout is 0.8 (Appendix E.4.1).

<sup>9</sup>The history of Texas’s 23rd congressional district is a case in point: as detailed by Levitt (2016, p282) “[S]tate officials in 2011 [...] drew a] district—that would look like it served the Latino population but was designed to do just the opposite. The court adjudicating the state’s 2011 preclearance submission found that [t]he map drawers consciously replaced many of the district’s active Hispanic voters with low-turnout Hispanic voters in an effort to strengthen the voting power of CD 23’s Anglo citizens”. Henderson et al. (2016) find systematic differences in turnout rates of Hispanic voters in majority-minority districts versus other districts in California, Florida, and Texas.

equally sized population of higher-turnout opponents, and more easily won when the same population of supporters outstrips an equally sized population of lower-turnout opponents.

Solving for the optimal map, we identify a “pack-crack-pack” strategy along the turnout dimension. The gerrymanderer’s incentives are to isolate both their lower-turnout supporters and their higher-turnout opponents in packed districts and to mix intermediate-turnout supporters and opponents in cracked districts. We show that this novel strategy comes on top of the typical “pack-and-crack” strategy along the ideology dimension identified by Owen and Grofman (1988), according to which the optimal map is composed of only two types of districts: packed districts with only opponents and cracked districts with more supporters than opponents. In this model, and other models in the literature (see Section 2), packed districts only concern opponents. Our model thus helps explain an otherwise puzzling pattern in the data, i.e., that gerrymanderers seem to often create districts packed with supporters (McCartan, et al. 2022).<sup>10</sup>

Our model generates two other predictions. First, the mixing of supporters and opponents in cracked districts should follow an assortative matching pattern: districts can be ordered along the turnout rates of both opponents and supporters. Second, in the optimal map, there is a negative correlation between the average turnout rate of individuals of each partisan leaning and the probability that the gerrymanderer wins their district.

We then examine recent gerrymandering attempts to determine whether our predictions find support in the data. To do so, we collect maps proposed by Republicans and Democrats in the most recent 2020 redistricting cycle. The district maps are combined with precinct-level data on population, turnout, and vote shares in recent presidential elections. This novel dataset, which includes 50 districting proposals for 25 states, allows us to compare redistricting proposals from both parties in the same state. The comparison of Democrat and Republican maps for a given state is key to attributing district characteristics to partisan strategy over other redistricting constraints and considerations.

Section 7.2 tests for the negative correlation between the turnout rate of the precincts composing a district and the anticipated vote share of the gerrymanderer’s party in the district. In line with the theoretical prediction, we find that Democrat and Republican maps tend to

---

<sup>10</sup>For instance, in the 2020 redistricting cycle, Democrat gerrymanderers in MA and MD created packed Democrat-leaning districts. In particular, the maps enacted by Democrat gerrymanderers include districts as safe for Democrats as the safest possible Democrat districts in 5,000 simulated maps (with the constraint that the simulated maps satisfy state redistricting rules and geographical distribution of preferences). For Republican gerrymanderers, maps in, e.g., IN and SC show similar patterns. This is based on the Figures at <https://alarm-redist.org/fifty-states/> on October 10, 2023.

treat the same precinct differently, depending on its turnout rate. In particular, a relatively low-turnout precinct tends to get allocated to a district that leans more strongly Democrat under the Democrat map than under the Republican map.

In Section 7.3, we provide empirical evidence that (i) information about precincts’ turnout rates is critical for identifying modifications to district borders that increase a party’s expected seat share, and (ii) gerrymanderers tend to identify these opportunities and exploit them in practice. To do so, we first construct many counterfactual districts by reallocating precincts along the border between two adjacent districts. We find that gerrymanderers have many more profitable deviations (i.e., those that would increase their expected number of seats) under their opponent’s proposal than under their own proposal. Moreover, gerrymanderers appear to extract essentially all of the available profitable deviations: starting from their own proposal, few deviations can produce non-trivial gains. To quantify the importance of turnout rate heterogeneity, we show that over half of the deviations that seem profitable when relying on ideological differences alone are actually detrimental when also taking turnout rates into account.

## 2. Literature

Theories of redistricting focus on partisan gerrymandering. Owen and Grofman (1988) is the germinal model of gerrymandering under uncertainty. Assuming two types of voters, opponents, and supporters, it rationalizes the so-called “pack and crack” strategy: to concentrate losses in as few districts as possible, the gerrymanderer should segregate (‘pack’) some opponents in select districts that heavily favor the opponent. To win as many districts as possible, they should mix (‘crack’) the remaining opponents with supporters in districts that narrowly favor the gerrymanderer. In the presence of a high degree of uncertainty, however, even the mixed districts can be strongly in favor of the gerrymanderer. Gul and Pesendorfer (2010) and Friedman and Holden (2008, 2020) generalize this intuition in the presence of a continuum of ideological preferences and both aggregate and individual uncertainty.

Under a unifying framework, Kolotilin and Wolitzky (2023) find that pack-and-pair patterns—which generalize pack-and-crack—are typically optimal for the designer. When individual uncertainty dominates, the gerrymanderer packs the stronger opponents in some districts and pairs the others into cracked districts. When aggregate uncertainty dominates, a gerrymanderer may sort voters by the intensity of preferences. High-intensity Republicans are matched with high-intensity Democrats. This is known as matching extremes, or

pairing, and is the districting strategy of focus in Friedman and Holden (2008, 2020). In all those models, individuals differ along one dimension, the intensity of their preferences for one party over the other, while individuals in our model differ along two dimensions: their preferences and their likelihood of voting.

The importance of incorporating turnout heterogeneity into redistricting models has also been recognized by Gomberg et al. (2023). They propose a model in which the gerrymanderer aims to align the ideology of the median district as closely as possible with their own ideology. That approach complements ours by confirming that the motivation to exploit turnout differentials exists irrespective of the gerrymanderer’s objective function. They find that a significant ideological gap can emerge when comparing a simplistic redistricting approach (ignoring turnout differentials) to a turnout-based strategy.

In addition to introducing a second dimension of heterogeneity into a model of strategic redistricting, our analysis also features two other important differences. First, we build on a standard probabilistic voting model à la Persson and Tabellini (2000). This simplifies the analysis and connects our results to the broader political economics literature. It also implies that our framework is amenable to study the redistributive politics implications of gerrymandering. Second, we draw concrete implications from the model that we can directly bring to the data.

Introducing turnout heterogeneity proves qualitatively important: in contrast to our paper, the above-mentioned theories cannot easily rationalize the gerrymanderer packing their own supporters, nor the resulting negative link between turnout and vote shares that we find in the data. The proposed alternative explanations for the creation of safe districts in favor of the gerrymanderer’s party are (i) a high degree of aggregate uncertainty (Owen and Grofman 1988), and (ii) the need to protect incumbent seats. However, the latter explanation, known as incumbency gerrymandering, has found little support in empirical work.<sup>11</sup> Our paper proposes an alternative explanation, which is that packing supporters can be optimal for the gerrymanderer in the presence of turnout disadvantages, even if there is little aggregate uncertainty.

Another strand of the literature focuses on how to evaluate redistricting in practice. Most measures of partisan gerrymandering are designed to assess the extent to which a party packs and cracks voters.<sup>12</sup> These include the Efficiency Gap (Stephanopoulos and McGhee

<sup>11</sup>Gelman and King (1994) and Friedman and Holden (2009) find that, if anything, gerrymandering works against the interests of incumbents. Similar conclusions are reached by Abramowitz et al. (2006).

<sup>12</sup>Others evaluate the shapes of districts (Chambers and Miller 2010, Niemi et al. 1990), or compare outcomes to simulated districts (Chen and Rodden 2013, Gomberg et al. 2023).

2015), Mean-Median difference (McDonald and Best 2015), Declination (Warrington 2018), and Partisan Dislocation (DeFord et al. 2022). The Efficiency Gap, perhaps the best-known among these, measures the number of votes ‘wasted’ by one party relative to the other. The idea is that if one party packs and cracks, then the other party’s votes are wasted because they win safe districts (votes over 50% of the vote share are wasted) and lose competitive districts (all votes in lost districts are wasted). Note that our pack-crack-pack strategy would not necessarily be detected by the Efficiency Gap and other measures designed to detect pack and crack strategies. In particular, the creation of partisan safe districts would conventionally be seen as ‘wasteful’ or non-strategic. In the conclusion, we discuss this issue in light of the case law surrounding partisan gerrymandering.

Though many measures of gerrymandering build on the predictions of a pack-and-crack strategy, few studies directly test whether gerrymanderers adhere to it. Jeong and Shenoy (2022) offers some evidence. For instance, they observe that African Americans, who predominantly support Democrats, are allocated differently across districts by Democrat and Republican gerrymanderers. However, while they find that the packing of African Americans *decreases* when Democrats gain control of redistricting, it does not disappear. This suggests that both pack-and-crack and pack-crack-pack are empirically relevant strategies. Note that their empirical strategy also relies on the comparison of Democrat and Republican maps. However, they compare maps drawn during different redistricting cycles, following a shift in control of the redistricting process, whereas our analysis compares the maps proposed by the two parties within a single redistricting cycle.

Instead of detecting partisan strategies, other measures are designed to evaluate the normative properties of a map. Common measures include the bias, asymmetry, and responsiveness of the seats-to-votes curve (Cox and Katz 2007, Grofman and King 2007, Katz et al. 2020).<sup>13</sup> Katz et al. (2020) define a map’s *bias* as the gap between the number of seats won by one party for each possible vote share, and those won by the other party with the same vote shares. A map displays *low responsiveness* if the number of seats won by a party does not change much as the vote share changes. They show that existing measures of partisan gerrymandering need not measure the actual bias and responsiveness of a map. Importantly for our setting, they also highlight that both the measures of gerrymandering and the estimates of a seats-to-votes curve are sensitive to the assumptions made about turnout rates. Thus, whether the intent is to detect a partisan gerrymander in practice or to determine how

<sup>13</sup>The seats-to-votes curve is the hypothetical relationship between the number of seats won by a party and its level of state-wide support.



gerrymandering affects fairness in theory, one needs to understand redistricting strategies in the presence of heterogeneous turnout rates.

### 3. The Model

Two parties, the Democrats ( $D$ ) and the Republicans ( $R$ ), will compete in a statewide election. The state is divided into  $J$  electoral districts, indexed by  $j$ . Each district elects one representative by first-past-the-post. Prior to the election, the incumbent has the opportunity to decide on the composition of each electoral district.

#### 3.1. The Population

Each individual belongs to one of a finite number of groups, indexed by  $k$ . These groups differ along two dimensions: partisan lean and turnout rates.

In this baseline model, we consider exactly two ideologies, where partisan lean is either Democratic or Republican: on average, Democrats assign a valence  $\nu_D \in \mathbb{R}$  to the Democratic Party, which is higher than the valence  $\nu_R \in \mathbb{R}$  assigned by Republicans to the Democratic Party:  $\nu_D > \nu_R$ . We discuss multiple ideological types in Section 3.4. Throughout, we shall often refer to  $\nu_K$  ( $K \in \{D, R\}$ ) as the voter's *ideology*.

The novelty of our model is to let population groups differ in turnout rates, denoted  $\tau_k \in [0, 1]$ .  $N_k (> 0)$  denotes the population size of each of these groups, and the total population size is 1:  $\sum_k N_k = 1$ .

To ease notation, we will often use subscripts  $d$  and  $d'$  to represent Democratic-leaning groups and subscripts  $r$  and  $r'$  to represent Republican-leaning groups. For instance, instead of writing “ $\tau_k$  with  $\nu_k = \nu_D$ ”, we will simply write  $\tau_d$ .

#### 3.2. Gerrymandering

The gerrymanderer designs an electoral map that allocates the population across electoral districts. An *electoral map*  $\mathbf{n} := (n_{kj})_{\forall k,j}$  (with  $n_{kj} \geq 0$ ) is a matrix that specifies how citizens of each group  $k$  are allocated to each district  $j$ .

We take the convention that the gerrymanderer belongs to party  $D$ . Their goal is to maximize the expected seat share of party  $D$ ,  $\pi(\mathbf{n})$ , subject to the constraints that each district must have an equal share of the population  $1/J$ , and that all individuals are allocated to a

district:

$$\max_{\mathbf{n}} \pi(\mathbf{n}) \text{ s.t. } \sum_k n_{kj} = \frac{1}{J}, \forall j \quad \& \quad \sum_j n_{kj} = N_k, \forall k. \quad (1)$$

### 3.3. Probabilistic voting

We now turn to voting behavior, which underpins the probability of winning a district. In the tradition of probabilistic voting models à la Lindbeck and Weibull (1987), we assume that the gerrymanderer is uncertain about the voters' preferences. Uncertainty is only resolved at the time of the election.

Following Persson and Tabellini (2000, chapter 3), we consider two types of shocks: first, an independently and identically distributed elector-level shock  $\eta_e$  toward party  $R$  captures preference heterogeneity among individuals within each group. Second, an aggregate shock  $\delta$  captures the valence of party  $R$  over party  $D$  at the time of the election.

The elector-level shock  $\eta_e \in \mathbb{R}$  is distributed according to the cumulative distribution function  $F$  and the aggregate shock  $\delta \in \mathbb{R}$  is distributed according to  $\Gamma$ , where  $F$  is symmetric, and  $F$  and  $\Gamma$  are strictly increasing and twice differentiable.

Due to preference heterogeneity, not all Democratic-leaning voters vote for party  $D$ , and not all Republican-leaning voters for  $R$ . Conditional on turning out, an elector  $e$  with political lean  $\nu_k$  votes for  $D$  iff  $\nu_k - \eta_e - \delta \geq 0$ . The share of voters from group  $k$  that cast their ballot for  $D$  conditional on turning out is  $F(\nu_k - \delta)$ , which is strictly increasing in  $\nu_k$  and strictly decreasing in  $\delta$ . The complementary fraction  $1 - F(\nu_k - \delta)$  votes for  $R$ .

However, only a share  $\tau_k$  of type- $k$  individuals turn out. The total number of ballots cast by  $n_{kj}$  individuals of type  $k$  in district  $j$  is thus:  $t_{kj} = n_{kj}\tau_k$ , where 't' stands for 'turnout'. For a given value of  $\delta$ , the share of these ballots that goes to  $D$  or  $R$  only depends on the groups' partisan leans,  $\nu_D$  or  $\nu_R$ . Therefore, we can usefully aggregate the total number of ballots cast by partisan lean: let  $K$  denote all groups  $k$  with ideological lean  $\nu_K \in \{\nu_D, \nu_R\}$ . Accordingly,  $t_j^K \equiv \sum_{k \in K | \nu_k = \nu_K} t_{kj}$  denotes the total turnout by ideological type  $K$  in district  $j$ . It follows that the number of *votes* in favor of  $D$  in district  $j$  is the turnout-weighted average of  $D$ 's support across all groups present in the district:

$$\sum_k t_{kj} F(\nu_k - \delta) = t_j^D F(\nu_D - \delta) + t_j^R F(\nu_R - \delta).$$

Party  $D$  wins district  $j$  whenever it collects more votes than  $R$ . The probability that this happens is:

$$\pi_j = \Pr_{\delta} \left( \sum_K t_j^K V_K(\delta) \geq 0 \right),$$

$$\text{where } V_K(\delta) \equiv F(\nu_K - \delta) - \frac{1}{2}. \quad (2)$$

$V_K(\delta)$  is the *excess vote share* of  $D$  among individuals with ideology  $\nu_K$  for a given realization of  $\delta$ . Like  $D$ 's vote share, this excess vote share is strictly increasing in  $\nu_K$  and strictly decreasing in  $\delta$ .

We impose that the two ideology shocks matter to determine whether a majority of each group votes for  $D$  or  $R$ :

**Assumption 1.** (i)  $F$  has full support over  $\Phi \supseteq [\nu_R - \nu_D, \nu_D - \nu_R]$  and (ii)  $\Gamma$  has full support over  $\Psi \supset [\nu_R, \nu_D]$

We show in Appendix A that under Assumption 1 (i) there is a unique realization  $\hat{\delta}_j$  of the aggregate shock  $\delta$  at which the number of votes for  $D$  is equal to the number of votes for  $R$ . This critical value  $\hat{\delta}_j \in [\nu_R, \nu_D]$  is a function of  $(t_j^D, t_j^R)$  and is implicitly defined by the condition:

$$t_j^D V_D(\hat{\delta}_j) + t_j^R V_R(\hat{\delta}_j) = 0. \quad (3)$$

Hence, the probability that party  $D$  wins district  $j$  is given by:<sup>14</sup>

$$\pi_j(\mathbf{n}_j) = \Gamma(\hat{\delta}_j). \quad (4)$$

We can think of  $\hat{\delta}_j$  as the expected position of the median voter in district  $j$ . In essence, (4) simply says that the gerrymanderer wins a district whenever the realization of the aggregate shock  $\delta$  is such that its median voter prefers  $D$  to  $R$ . In the case of uniform distributions for  $F$  for instance (see the discussion in Section 6),  $\hat{\delta}_j$  takes on a simple form:

$$\hat{\delta}_j := \sum_K \frac{t_j^K}{t_j} \nu_K, \text{ with } t_j := \sum_k t_{kj}.$$

Assumption 1 (ii) implies that each party has a non zero probability of winning each district.

<sup>14</sup>The probability that  $R$  wins district  $j$  is  $1 - \pi_j(\mathbf{n}_j)$ , making the problem symmetric for party  $R$ .

The expected seat share won by the Democrats being  $\frac{1}{J} \sum_j \pi_j$ ,<sup>15</sup> we can rewrite the gerrymanderer’s problem (1) as:

$$\begin{aligned} \max_{\mathbf{n}} \pi(\mathbf{n}) &= \frac{1}{J} \sum_j \Gamma(\hat{\delta}_j) \\ \text{s.t. } \sum_k n_{kj} &= \frac{1}{J}, \forall j \quad \& \quad \sum_j n_{kj} = N_k, \forall k. \end{aligned} \tag{5}$$

### 3.4. Discussion of Key Assumptions

Before moving to the analysis of the gerrymanderer’s behavior, we discuss five key assumptions of the model.

#### 3.4.1 Endogenous Turnout

In our base model, turnout rates differ between groups, but are exogenously fixed. In particular, this assumes away the possible influence of election closeness on turnout. Introducing that influence could, for instance, imply that voters of a given group turn out at a higher rate when they are assigned to a closely contested district, and at a lower rate when assigned to a strongly partisan district.

One reason why we abstract from endogenous turnout considerations in the baseline model is that exogenous socio-demographic variables account for most of the turnout variation. Different groups display large and systematic differences in turnout rates, independently of district composition. For example, at the 25th percentile of the precinct distribution, 63% of the total population are citizens of voting age. At the 75th percentile, this increases to 81%. Such differences do not disappear in close versus lopsided elections. Further, as we detail in Appendix E.4.1, socio-demographic variables alone explain 79% of the variation in observed turnout rates across precincts for the 2016 and 2020 presidential elections.

In Appendix E.4.2, we present a quantitative assessment of the impact of district competitiveness on voter turnout. Using a panel of precincts, we estimate the effect of changes in competitiveness on turnout, before and after the 2020 redistricting cycle. Our analysis finds that the effect of district competitiveness on turnout is small and statistically insignificant. Specifically, the 95% confidence intervals rule out any increase in turnout greater than 0.5

<sup>15</sup>To see why, order the districts from most likely to elect a  $D$  candidate to least likely. For values of  $\delta$  above  $\hat{\delta}_1$ ,  $D$  has zero seats. For values of  $\delta$  between  $\hat{\delta}_1$  and  $\hat{\delta}_2$ ,  $D$  has one seat (from district 1). For values of  $\delta$  between  $\hat{\delta}_2$  and  $\hat{\delta}_3$ ,  $D$  has two seats (from districts 1 and 2), and so on. The expected number of seats is:  $\sum_{j=1}^{J-1} j \times [\Gamma(\hat{\delta}_j) - \Gamma(\hat{\delta}_{j+1})] + J \times \Gamma(\hat{\delta}_J) = \sum_j \pi_j$ .

percentage points resulting from a 10 percentage point rise in competitiveness (e.g., from a 60-40 to a 50-50 split). This suggests that, compared to socio-economic factors, election competitiveness plays only a minor role in explaining turnout variation.

These findings are consistent with Moskowitz and Schneer (2019), who report a precise null effect of Congressional district competitiveness on voter turnout using a nationwide panel of voters. Their supplemental survey evidence indicates that voters often have low awareness of their district’s competitiveness, limiting its influence on turnout. Other studies, while identifying a statistically significant effect, estimate the impact to be modest. For instance, Bursztyn et al. (2020) find that a one standard deviation increase in competitiveness raises turnout by just 0.4 percentage points among eligible voters in Switzerland. Similarly, Jones et al. (2023) report a 2 percentage point increase in turnout following re-districting reforms in Pennsylvania and Ohio—an effect that remains small in comparison to the much larger turnout gaps observed across groups of voters (see Table E.7 and Figure ?? in Appendix E.5). Overall, these results suggest that while competitiveness can affect turnout, its impact is relatively minor compared to other drivers of voter behavior.

Yet, there may be other situations in which turnout rates do react noticeably to election closeness, and our theoretical setup can be extended to account for such effects. Appendix C proposes two generalizations of the baseline model to endogenize turnout. The first generalization is based on the calculus of voting tradition described, for example, in Riker and Ordeshook 1968 and Kawai et al. (2021). In that setup, an eligible voter will only turn out if the expected benefit of voting, accounting for the voters’ *perceived voting efficacy*, outweighs voting costs. While perceived voting efficacy (an extension of the concept of pivot probability) may differ across groups, it ought to vary in line with election closeness, which depends on the specifics of the electoral map. We find that, even when the impact of closeness is asymmetric across groups or parties, voting costs do not alter cross-district comparisons in an optimal map, and hence do not modify the essence of our results. To be more precise, endogenous turnout can affect the expected position of the median voter ( $\hat{\delta}$ ) in each district, which modifies the details of the gerrymanderer’s calculus. However, they do not modify eventual districting: whether a gerrymanderer prefers to assign, say, high-turnout supporters to some district  $i$  rather than another district  $j$  does not depend on the presence or absence of voting costs. The second generalization accounts for group-based effects, in line with, e.g., Morton (1987), Shachar and Nalebuff (1999), and Levine and Mattozzi (2020). For the same reason, all our results extend to that setup as well.

### 3.4.2 Objective Function

Our model assumes that the gerrymanderer draws the map to maximize their expected seat share. This assumption aligns with most of the gerrymandering models in the literature. Adhering to this approach thus ensures the comparability of our model with those of previous research. It is clear that there are various benefits for a party and its members of holding a larger number of seats and there is empirical evidence supporting this assumption (see, e.g., Jacobson and Kernell 1985; Incerti 2015; Snyder 1989 and see Genicot (r) al. 2021, pp. 3189-92, for a discussion).

Alternatively, we could assume that the gerrymanderer maximizes the probability of obtaining a majority of seats in the assembly like, for instance, Lizzeri and Persico (2001); Strömberg (2008); Gomberg et al. (2023). Such an objective would restore the incentive to draw a map following the typical “pack-and-crack” structure: creating several relatively strong districts that the gerrymanderer expects to win with the same probability, and giving up on the others.

In practice, gerrymanderers’ objectives go beyond pure partisan gains (Katz et al. 2020). For instance, parties may draw maps to protect incumbents or to hurt incumbents of the other party (and even encourage them to retire). While our model abstracts from those objectives, our empirical strategy takes them into account. In particular, we focus on Congressional districts, which are drawn by state legislatures, leaving little role for incumbents.

### 3.4.3 Two Ideology Types

In our base model, we focus on the case of two ideologies: Democratic ( $\nu_D$ ) and Republican ( $\nu_R$ ). Yet, the reasoning and the propositions extend to the case of multiple ideologies. There are at least two reasons to favor the two-type model in the body of the paper: First, as discussed in Appendix F.2, empirically, several states appear to have a bimodal distribution of types. Second, the intuition of the results is much simpler with two ideologies. When extending the model to an arbitrary number of groups, with each group  $k$  having its own partisan lean,  $\nu_k \in [\nu_R, \nu_D]$ , and turnout  $\tau_k$ , our three Propositions hold verbatim.<sup>16</sup> However, the interpretation of the results is less intuitive since intermediary types in a given district will be treated as Democrats or Republicans depending on their *relative* ideology in the district.

---

<sup>16</sup>The proofs are written to apply to this multi-type case.

### 3.4.4 Geographical and Legal Constraints

Our model, like much of the existing literature, places minimal constraints on the actions of gerrymanderers. Specifically, we abstract from legal constraints such as geographic contiguity, adherence to political boundaries, and compliance with the Voting Rights Act of 1965, which are typically observed to varying degrees in practice (Sherstyuk, 1998). These constraints will be revisited in the empirical section (see Section 7.1).

### 3.4.5 Other Sources of Heterogeneity

We consider only one source of heterogeneity other than partisanship here – differential turnout. Other sources of heterogeneity could be introduced, including swingness or information (Strömberg 2004), as long as they enter the sensitivity of the group (Genicot & Bouton 2021). That is, the results that follow extend to a case where voters differ along several dimensions and where the gerrymanderer observes both the partisan lean and sensitivity of each population group.

## 4. Basic Swaps

Since districts must be well apportioned and the number of districts is fixed, comparing two feasible electoral maps is equivalent to assessing the effect of a sequence of population exchanges or “swaps” across districts. The key question will be whether a (sequence of) swap(s) increases or decreases the expected number of seats controlled by the gerrymanderer’s party.

As a convention, we always denote by  $d$  and  $r$  the types who originate from district  $i$  and by  $d'$  and  $r'$  the types who originate from district  $j$ . We denote by “ $k \stackrel{i}{\rightleftharpoons}_j k'$  swap” the reallocation of an  $\varepsilon$  mass of individuals of type  $k \in \{d, r\}$  from district  $i$  to district  $j$ , in exchange for an equal mass of citizens of type  $k' \in \{d', r'\}$  from district  $j$ .

We can distinguish (i) swaps of individuals sharing the same ideology, either two different types of Democrats ( $d \stackrel{i}{\rightleftharpoons}_j d'$ , or DD swaps for short) or two different types of Republicans ( $r \stackrel{i}{\rightleftharpoons}_j r'$ , or RR swaps), and (ii) swaps of Republicans for Democrats ( $d \stackrel{i}{\rightleftharpoons}_j r'$  and  $r \stackrel{i}{\rightleftharpoons}_j d'$ , or DR and RD swaps for short).

Swapping two types  $k$  and  $k'$  who share ideology  $\nu_K$  may increase or decrease the expected number of seats, depending on two factors: first, which group has the highest turnout rate? Second, does increasing the number of votes by this group increase or decrease the probability of winning the district? Quantitatively, we consider  $\varepsilon \rightarrow 0$  to compute the

marginal effect of a DD or RR swap on the joint probability of winning in  $i$  and  $j$ :

$$\left( \frac{\partial \pi_i}{\partial n_{k'i}} - \frac{\partial \pi_i}{\partial n_{ki}} \right) - \left( \frac{\partial \pi_j}{\partial n_{k'j}} - \frac{\partial \pi_j}{\partial n_{kj}} \right) = (\tau_{k'} - \tau_k) \left( \frac{\partial \pi_i}{\partial t_i^K} - \frac{\partial \pi_j}{\partial t_j^K} \right). \quad (6)$$

Instead, in a  $k \stackrel{i}{\rightleftharpoons} j$  swap where  $\nu_k \neq \nu_{l'}$ , we must take account of the different ideologies in each district:

$$\left( \frac{\partial \pi_i}{\partial n_{l'i}} - \frac{\partial \pi_i}{\partial n_{ki}} \right) - \left( \frac{\partial \pi_j}{\partial n_{l'j}} - \frac{\partial \pi_j}{\partial n_{kj}} \right) = \tau_{l'} \left( \frac{\partial \pi_i}{\partial t_{li}} - \frac{\partial \pi_j}{\partial t_{lj}} \right) + \tau_k \left( \frac{\partial \pi_j}{\partial t_{kj}} - \frac{\partial \pi_i}{\partial t_{ki}} \right). \quad (7)$$

We can readily draw three inferences from (6) and (7):

- (1) With a DD-swap ( $k$  and  $l'$  are Democrats),  $\frac{\partial \pi}{\partial t^D}$  is strictly positive in both districts  $i$  and  $j$ . Hence, gerrymanderers want to assign higher turnout supporters to the district where they have the largest impact (i.e., the district where  $\frac{\partial \pi}{\partial t^D}$  is larger).
- (2) With an RR-swap ( $k$  and  $l'$  are Republicans),  $\frac{\partial \pi}{\partial t^R}$  is strictly negative in both districts. Hence, gerrymanderers want to assign higher turnout opponents to the district where they have the least negative impact (i.e., where  $\frac{\partial \pi}{\partial t^R}$  is larger, which means closer to zero).
- (3) With DR-swaps, gerrymanderers still want to assign supporters to the district where they have the largest positive impact and opponents to the district where they have the least negative impact. There might thus be a tension in DR-swaps if the gerrymanderer prefers to send both supporters and opponents to the same district. Then one term is positive and the other negative in (7)) and the sign of the effect of the swap depends on the relative turnout rates of the groups.

It remains to identify the determinants of the magnitude of  $\frac{\partial \pi}{\partial t^D}$  and  $\frac{\partial \pi}{\partial t^R}$ . Using the definition of  $\hat{\delta}$  in (3) and the implicit function theorem, we find that:

$$\frac{\partial \pi_j}{\partial t_j^K} = \gamma(\hat{\delta}_j) \frac{V_K(\hat{\delta}_j)}{\left| \sum_X t_j^X \frac{\partial V_X(\hat{\delta}_j)}{\partial \hat{\delta}_j} \right|}, \quad (8)$$

where  $V_K(\hat{\delta}_j)$  is the excess vote share for ideology  $\nu_K$ , as defined in (2), evaluated at  $\hat{\delta}_j$ . Notice that this *critical excess vote share* and therefore Equation (8) must be positive for Democrat-leaning groups and negative for Republican-leaning groups (such that the excess vote share for the district is zero).



Equation (8) tells us that the magnitude of  $|\partial\pi/\partial t_j^K|$  is larger in districts where (i) the likelihood of the district being tied,  $\gamma(\hat{\delta}_j)$ , is larger; (ii) the critical excess vote share among the corresponding ideological groups in the district  $|V_K(\hat{\delta}_j)|$  (keeping the denominator constant) is larger in magnitude; (iii) the overall turnout in the district is lower (see the denominator).

The forces in (i) imply that gerrymanderers want to place their supporters in districts that are more likely to be tied. This is because  $\partial\pi_j/\partial t_j^D > 0$ , since  $V_D(\hat{\delta}_j) > 0$ . On the contrary, gerrymanderers want to place their opponents in districts that are *less* likely to be tied. This is because  $\partial\pi_j/\partial t_j^R < 0$ , since  $V_R(\hat{\delta}_j) < 0$ . This force drives the classical pack-and-crack strategy along the ideological dimension widely discussed in the literature. The two other forces are new and stem from the heterogeneity in turnout rates.

The forces in (ii) imply that the gerrymanderer prefers to place supporters in districts with large  $V_D(\hat{\delta}_j)$ . These are districts with weak support for party  $D$  (weak districts require strong support from all  $D$ -leaning voters in order to tie). Importantly, they also want to place opponents in weak districts. Since such districts are largely pro-Republican, so is the median voter. Hence,  $V_R(\hat{\delta}_j)$  is close to zero, implying that opponents only have a minor negative impact on the probability of winning the district. Based on these forces only, there would thus always be a tension in DR-swaps: the gerrymanderer would want to send both supporters and opponents to the weak district.

Finally, since  $V_D(\hat{\delta}_j) > 0$  and  $V_R(\hat{\delta}_j) < 0$ , the forces in (iii) create incentives to place high-turnout supporters in low-turnout districts since the effect of their additional votes is then amplified. Conversely, they want to allocate high-turnout opponents to districts with high overall turnout, to dilute the effect of their votes.

## 5. Optimal Gerrymandering

This section presents our main theoretical results, which identify three key patterns of an optimal gerrymander.

Before doing so, we introduce the concepts of “packed” and “cracked” districts, as well as additional pieces of notation. We refer to a district as “packed” if it comprises solely supporters or solely opponents. A packed  $D$  district is defined as one where  $\sum_d n_{dj} = 1/J$ , whereas a packed  $R$  district is one where  $\sum_r n_{rj} = 1/J$ . Conversely, if a district includes both supporters and opponents, it will be called a “cracked” district. We denote the lowest and highest turnout rates within each political faction as:  $\underline{r} := \arg \min_r \tau_r$  and

$\bar{r} := \arg \max_r \tau_r$  for the Republicans, and  $\underline{d} := \arg \min_d \tau_d$  and  $\bar{d} := \arg \max_d \tau_d$  for the Democrats.

Our first proposition shows that the optimal map displays what we call a ‘*pack-crack-pack*’ pattern. That is, gerrymanderers rely on a cutoff strategy, splitting supporters and opponents according to their turnout rates: low-turnout supporters and high-turnout opponents get “packed” in separate districts, whereas the others are mixed in “cracked” districts.

For expositional clarity, we always state our findings from the viewpoint of a Democratic gerrymanderer. By symmetry, equivalent results hold for a Republican gerrymanderer.

**Proposition 1.** *In an optimal map, the allocation of voters to districts is characterized by two cutoffs,  $\tau_{d*} \in [\tau_{\underline{d}}, \tau_{\bar{d}}]$  and  $\tau_{r*} \in [\tau_{\underline{r}}, \tau_{\bar{r}}]$  such that:*

- (1) *High-turnout supporters, with  $\tau_d > \tau_{d*}$ , are assigned to cracked districts, whereas low-turnout supporters, with  $\tau_d < \tau_{d*}$ , are assigned to packed districts;*
- (2) *High-turnout opponents, with  $\tau_r > \tau_{r*}$ , are assigned to packed districts, whereas low-turnout opponents, with  $\tau_r < \tau_{r*}$ , are assigned to cracked districts.*

The intuition of the proof is as follows: If a gerrymanderer packs some high-turnout supporters, but not some low-turnout ones, a DD swap is necessarily profitable. Such a swap does not affect the probability of winning the packed district whereas it increases the probability of winning the cracked district. Similarly, if a gerrymanderer packs some opponents, it must be the higher turnout ones.

To understand why the gerrymanderer may have incentives to pack supporters in the first place, consider a weak and a strong D district. With force (ii) in mind, the gerrymanderer wants to send both opponents and supporters to the weak D district. To resolve this tension, and determine which of the supporters or opponents the gerrymanderer allocates to that district, their relative turnout rates are key (this is the effect of  $\tau_{l'}$  and  $\tau_k$  in (7)). If the supporters have the lower turnout rate, then the benefit of sending them to the weak D district is relatively small. The gerrymanderer then prefers to assign opponents to that district. This creates an incentive to pack lower-turnout supporters in strong Democrat districts.

This is not to say that gerrymanderers *always* pack their lower-turnout supporters ( $\tau_{d*}$  need not be interior). Indeed, a potential countervailing force is an incentive to place supporters in districts that are more likely to be tied (force (i) above works against force (ii) if packed districts are less likely to be tied). We discuss this issue further in Section 6.

Figure 1 illustrates the result for a case in which all three types of districts co-exist: when the two cutoffs are strictly interior, there are (a) districts packed with low-turnout supporters, (b) cracked districts, and (c) districts packed with high-turnout opponents. Of course, whether all of the three zones displayed in the figure should actually be present in a map depends on the distribution of types (Section 6 discusses concrete examples).

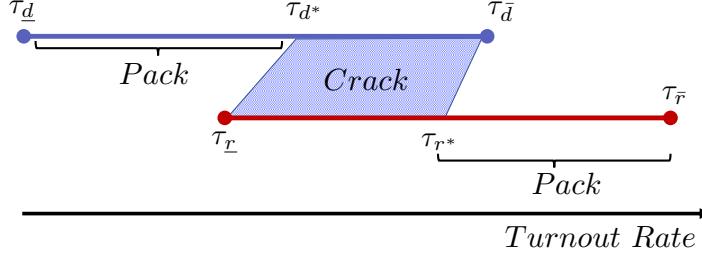


FIGURE 1. ILLUSTRATION OF PROPOSITION 1

This pack-crack-pack pattern complements the existing literature. First, it identifies differential turnout rates as a novel reason why gerrymanderers may prefer to pack and crack their opponents. In the classical “pack and crack” strategy proposed by Owen and Grofman (1988) or its generalized “segregate-pair” version by Kolotilin and Wolitzky (2023), the gerrymanderer sorts opponents based on the intensity of their preferences, with the stauncher opponents allocated to packed districts. In contrast, in our model, the gerrymanderer also sorts opponents based on their turnout rates, with the higher turnout rate opponents allocated to packed districts. This is a novel prediction since the above-mentioned papers implicitly assume equal turnout rates for all ideology types. Second, our model identifies a novel incentive for gerrymanderers to pack their lower-turnout supporters. Such a strategy cannot be optimal when individuals only differ along the partisan dimension. Indeed, packing supporters is conventionally seen as an inefficient or ‘wasteful’ allocation of voters.

The next proposition focuses on the question of the composition of cracked districts and shows that turnout rates cannot diverge across districts: there is positive assortative matching of supporters and opponents in terms of turnout rates.

**Proposition 2.** *In an optimal map, there cannot be two cracked districts  $i$  and  $j$  with  $\tau_k < \tau_{k'}$  and  $\tau_l > \tau_{l'}$ , when  $\pi_i \neq \pi_j$  and ideology types  $\nu_k = \nu_{k'} = \nu_K$  and  $\nu_l = \nu_{l'} = \nu_L$ .*

The intuition of the proof is as follows. First, note that we cannot have two districts  $i$  and  $j$  such that supporters have a larger positive impact on the probability of winning in district  $i$  (i.e.,  $\partial\pi_i/\partial t_i^D > \partial\pi_j/\partial t_j^D$ ) but opponents have the least negative impact on the probability of winning in district  $j$  (i.e.,  $\partial\pi_i/\partial t_i^R < \partial\pi_j/\partial t_j^R$ ). Indeed, in such a case, the gerrymanderer would want to implement an RD-swap (i.e., assigning supporters to district  $i$  and opponents to district  $j$ ). Thus, in an optimal map, districts in which supporters have the largest positive impact must be the same as those in which opponents have the least negative impact. Second, when one district has that twin feature, then we know from DD and RR swaps that the gerrymanderer wants to assign both higher turnout supporters and higher turnout opponents to that district. This leads to positive assortative matching along the turnout dimension.

This result complements the existing literature. The “pack-moderates-and-pair” strategy identified in Kolotilin and Wolitzky (2023) requires negative assortative matching along the partisanship dimension: the most extreme opponents should be matched with the most extreme supporters. We show assortative matching along the turnout dimension: individuals who turn out the most for the Democrats are matched with those who turn out the most for the Republicans. Both results have similar flavors in the sense that the most intense supporters and opponents are matched together. However, while in Kolotilin and Wolitzky (2023) districts composed of more extreme supporters and opponents have a higher probability of winning, our model predicts the opposite correlation. Indeed, the following proposition identifies a negative relationship between turnout rates and winning probabilities across districts:

**Proposition 3.** *Consider any pair of cracked districts  $i$  and  $j$  including, respectively, voters  $k$  and  $k'$  of the same ideology  $\nu_k = \nu_{k'} = \nu_K$ . If  $\pi_i < \pi_j$ , then it must be that  $\tau_k \geq \tau_{k'}$ .*

As we have seen, the gerrymanderer wants to assign individuals (both supporters and opponents) with higher turnout to the district(s) in which they have the largest positive (or least negative) impact. Proposition 3 shows that these districts are the ones with a lower  $\hat{\delta}$  (and hence a lower probability of winning). This is driven by the second of the three forces shaping the optimal map (i.e., the gerrymanderer prefers to allocate both high-turnout supporters and high-turnout opponents into weak D districts, see Section 4). The other two forces, related to the probability of a tie and the overall turnout in the districts, may interfere with that pattern. Yet, the proposition shows that they can never dominate.

Note that this ordering is also present across D- and R-packed districts. Proposition 1 indicates that D-packed districts, which are most likely to be won by the Democratic party,

must have lower turnout rates than Democratic voters allocated to cracked districts (in D-packed districts,  $\tau_d \leq \tau_{d^*}$ ). Conversely, R-packed districts, which are least likely to be won by the Democratic party, are composed of the highest Republican turnout rates ( $\tau_r \geq \tau_{r^*}$ ).<sup>17</sup>

## 6. Pack-Crack-Pack versus Pack-and-Crack

In this section, we isolate the role of heterogeneous turnout rates in the model and discuss how the pack-crack-pack incentives and the traditional pack-and-crack incentives interact.

### Effects of Turnout Differentials

Consider a specification of the model with uniform distributions for  $F$  and  $\Gamma$ . This specification neutralizes the classical forces behind pack-and-crack à la Owen and Grofman (1988), thereby isolating the new results brought about by turnout heterogeneity.

To see this, first note that, under a uniform  $F$ , the critical value  $\hat{\delta}$  that equalizes the number of votes for  $D$  and for  $R$  becomes a simple average of the voters' ideology weighted by their turnout:

$$\hat{\delta}_j = \frac{t_j^D \nu^D + t_j^R \nu^R}{t_j^D + t_j^R}.$$

If all turnout rates were the same,  $\hat{\delta}_j$  would be the average partisanship of the *individuals* in the district.<sup>18</sup> Moreover, when uniformly distributed,  $\Gamma$  is also linear, and hence the objective of the gerrymanderer to maximize the expected share of districts won,  $\frac{1}{J} \sum_j \Gamma(\hat{\delta}_j)$ , is also linear in  $\hat{\delta}_j$ . In other words, the joint linearity of  $F$  and  $\Gamma$  implies that the probability of winning a district behaves as a Tullock contest function of the (turnout-weighted) average ideology of its population.

In the absence of turnout differentials, that is if all groups have the same turnout rate  $\tau$ , the sum of the different  $\hat{\delta}_j$  is constant: the expected number of seats is independent of the allocation of voters to districts. That is, the gerrymanderer would be indifferent between all feasible maps because the classical incentive to pack and crack identified by Owen and Grofman (1988) is neutralized.<sup>19</sup> This implies that, with this specification, the optimal map with turnout differential is purely driven by our effects.

<sup>17</sup>The gerrymanderer is indifferent to the specific distribution of types within D-packed districts and within R-packed districts. Creating identical districts or ordering them based on turnout rates would both be optimal.

<sup>18</sup>All intermediate developments can be found in the Online Appendix.

<sup>19</sup>Another way to see this is to note that as  $\gamma$  is independent of  $\hat{\delta}$  in (8), the first force discussed in Section 4 disappears.

Uniform distributions have the added advantage of delivering closed-form solutions. This allows us to identify sufficient conditions for the coexistence of the three types of districts in our pack-crack-pack pattern along the turnout dimension. As we detail in the online Appendix, for the case of a large number of districts, the presence of sufficiently low-turnout supporters becomes a sufficient condition for the creation of at least one district packed with supporters (in particular,  $\tau_d < \tau_r$  is sufficient). Conversely, the presence of sufficiently high-turnout opponents is sufficient for the creation of at least one district packed with opponents (in particular,  $\tau_d < \tau_r$  is sufficient). These sufficient conditions are satisfied in Figure 1 (see p17), where low enough Democrats ( $\tau_d < \tau_d^*$ ) are packed in Democratic districts, high enough Republicans ( $\tau_r > \tau_r^*$ ) are packed in Republican districts, and intermediate turnout Democrats and Republicans ( $\tau_d > \tau_d^*$  and  $\tau_r < \tau_r^*$ ) are assigned to cracked districts.

A disadvantage of the uniform specification is that it can predict maps with counterfactual features precisely because it neutralizes the classical pack-and-crack forces. In particular, for some parameters, it is optimal to draw a map with multiple cracked districts composed of a majority of opponents. Such districts would be lost with a high probability. This is an artifact of the uniform distribution: because  $\gamma$  is a constant, increasing one's expected vote share by 1% increases the probability of winning a lopsided district as much as that of winning a closely contested district. This artifact disappears when the aggregate shock is distributed according to, e.g., a single-peaked distribution such that  $\gamma(\nu_R) \ll \gamma(0)$ . That is, one more democratic vote has a much lower probability of swinging an  $R$  stronghold than a closely contested district.

### Bringing Back Traditional Pack-and-Crack

A single-peaked  $\Gamma$  reintroduces the incentives that lead to the traditional pack-and-crack strategy identified by Owen and Grofman (1988) and Kolotilin and Wolitzky (2023). The probability of winning a district  $\pi_j$  then exhibits an S-shaped relationship between the average ideology of the district  $\hat{\delta}$  and the probability of winning it.

Let us first return to the case in which all turnout rates are the same. The convexity of  $\Gamma$  for low probabilities of winning generates an incentive to create two distinct types of districts. Some districts get packed with opponents, while all others are cracked with an identical average ideology when turnout rates are homogeneous. In essence, if they cannot be strong in all districts, gerrymanderers prefer to abandon some districts (packed- $R$  districts) to reinforce their supporters' position in the other (cracked) districts.

When turnout rates are heterogeneous, both the traditional pack-and-crack incentives and our turnout differential incentives are present. These two sets of incentives generate two different but congruent reasons to pack high-turnout opponents. By contrast, these incentives pull in opposite directions when it comes to packing low-turnout supporters. Which effect dominates then depends on the curvature of the distribution compared to the difference in turnout rates. To illustrate this point, consider two districts: district  $i$  is packed with one type of democrats  $d$ , whereas district  $j$  is cracked. Under a uniform  $F$ , the profitability of a  $d^i \rightleftharpoons_j r'$  swap in (7) depends on the sign of:

$$\gamma_j \frac{\tau_d t_j^R + \tau_{r'} t_j^D}{t_j^2} - \gamma_i \frac{\tau_{r'}}{t_i^D}, \text{ with } \gamma_i \leq \gamma_j.$$

Since  $t_i^D = \tau_d n_{di} (= \tau_d / J)$ , a sufficiently low  $\tau_d$  is a sufficient condition for the swap not to be profitable (i.e., the gerrymanderer does not want to unpack district  $i$ ). Keeping  $\tau_d$  fixed, increasing  $\gamma_j / \gamma_i$  (i.e., making  $\Gamma$  more S-shaped) reduces the incentive of the gerrymanderer to pack their supporters. Note that sufficiently large values of  $\gamma_j / \gamma_i$  are needed to reverse the sign of the above expression, hence making the swap profitable.

As illustrated in the following example, when  $\gamma_j / \gamma_i$  is larger than one –but not too large– the gerrymanderer has incentives to pack their supporters and not create weak cracked districts. Our pack-crack-pack incentives thus come on top of the traditional pack-and-crack incentives.

Let  $\nu_D = 1 = -\nu_R$  and the population is partitioned in four groups: 3/8th are low-turnout Republicans  $\underline{r}$ , with  $\tau_{\underline{r}} = 0.4$ ; 1/4th are high-turnout Republicans  $\bar{r}$ , with  $\tau_{\bar{r}} = 0.8$ ; 1/4th are low-turnout Democrats  $\underline{d}$  ( $\tau_{\underline{d}} = 0.2$ ), and 1/8th high-turnout Democrats  $\bar{d}$  ( $\tau_{\bar{d}} = 0.5$ ).

Figure 2 contrasts the optimal maps for the uniform case,  $\Gamma(\delta) \sim U[-5, 5]$ , and the Normal case,  $\Gamma(\delta) \sim N(0, 1)$ . In both cases, both  $\underline{d}$ -types and  $\bar{r}$ -types are packed. Under the uniform distribution, two cracked districts are created by mixing the high-turnout Democrats and the low-turnout Republicans, despite the fact that these districts have a low expected probability of winning. Under the normal distribution instead, the gerrymanderer prefers creating only one such mixed district. The strong convexity of  $\Gamma$  makes it profitable to increase support in District 2 despite the cost of packing low-turnout opponents in District 3.

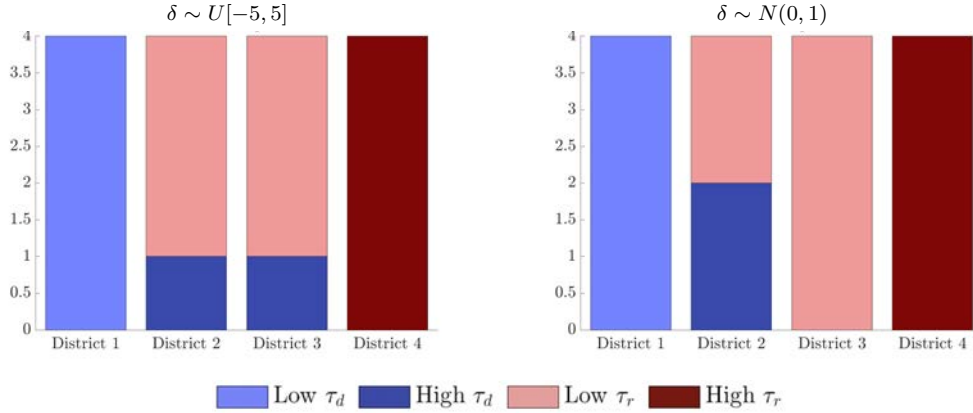


FIGURE 2. Pack-Crack-Pack.

## 7. Empirical Analysis

In this section, we examine recent instances of gerrymandering to assess whether our model is substantiated by empirical data and to quantify the extent to which heterogeneous turnout rates influence partisan gerrymandering proposals. In Section 7.2, we focus on a key testable implication of the model: whether we observe a negative correlation between turnout rates and expected vote shares, as predicted by Proposition 3. In Section 7.3, we evaluate the optimality of gerrymanderers’ decisions by assessing the extent to which gerrymanderers exhaust swaps at the borders of actual gerrymandering proposals that our model deems profitable.

For this empirical analysis, we collected data from 25 states where both Republicans and Democrats submitted a proposal for congressional districts in the 2020 redistricting cycle.<sup>20</sup> We assembled precinct-level data to evaluate these redistricting proposals. Our final dataset includes 94,304 precincts across the 25 states (see Appendix E for more information).

### 7.1. From Theory to Data

In practice, gerrymanderers draw maps using electoral precincts as the building blocks of districts.<sup>21</sup> Using electoral precincts to create districts means moving a discrete number of individuals at a time, which contrasts with our model where we assume a continuum

<sup>20</sup>Specifically, we have a total of 50 redistricting proposals from the states of Alabama, Arizona, Arkansas, Connecticut, Florida, Georgia, Kansas, Louisiana, Maryland, Minnesota, Montana, Nebraska, North Carolina, New Hampshire, New Jersey, New Mexico, Nevada, New York, Ohio, Oklahoma, Pennsylvania, South Carolina, Texas, Washington, and Wisconsin.

<sup>21</sup>Only 2% of the precincts in our sample are split across proposed congressional districts under either the Democrat or Republican proposals.



of individuals. Yet, given that most precincts are very small in comparison to the size of a district (average population is 2,000 for precincts vs. more than 700,000 for districts), it is unlikely that this discrepancy will create a substantial difference between theoretical predictions and actual maps. This is why we use precincts as the base unit of observation for the empirical analysis and think of precincts as small groups in our model. As in our model, actual gerrymanderers have information about the average ideology and turnout rates of precincts. In fact, precincts are the smallest possible geographic units at which electoral data are available. We thus treat precinct characteristics as the fixed parameters of the model: they have a set ideological lean and turnout rate. The question is: to which district should they be assigned? The average ideology and turnout of the districts are endogenous to that allocation.

The biggest challenge in testing the predictions of our theoretical model is to take into account the geographic and legal redistricting constraints mentioned in Section 3.4.4 that can strongly affect district composition, but that the model abstracts from (e.g., geographic contiguity, respect for political boundaries, and adherence to the Voting Rights Act of 1965). Scholars have long noted that these factors make it difficult to identify a partisan gerrymander from an ‘unintentional’ gerrymander (Erikson, 1972; Chen and Rodden, 2013; Stephanopoulos, 2023): is a precinct in a particular district because this increases the seat share of the gerrymanderer or because of a legal or geographical constraint? For this reason, it is impossible to test if a gerrymanderer follows a particular strategy by simply looking at the composition of districts in a single map.<sup>22</sup>

To overcome this challenge, we combine two strategies. First, we focus on *differences* between the Democrat and Republican proposals for the same redistricting cycle. The idea is that if a precinct has to be assigned to a particular district due to legal constraints, both the Democrat and the Republican proposals will have to respect them. Instead, the difference between the two proposals ought to reflect the gerrymanderer’s incentives, while filtering out common geographic or legal constraints. This is a variation on a strategy adopted by

---

<sup>22</sup>As an example, consider the case of a majority-Latino community of interest. Under certain conditions, the Voting Rights Act would prohibit the community of interest from being divided across multiple districts. Majority-Latino precincts also tend to have relatively low turnout rates and to lean Democrat. The prediction from our model is for a Democrat gerrymanderer to pack the community of interest into a safe Democrat district. But if we observe this in practice, it could be due to the Voting Rights Act, rather than partisan gerrymandering, a false positive. Similarly, if the community of interest is in a strong Democrat district under the Republican proposal, we might improperly reject the theoretical prediction, a false negative.

others in the literature who have compared redistricting proposals *across time* (e.g., Jeong and Shenoy 2022, Friedman and Holden 2009, Shotts 2003, Cox and Katz 2007).<sup>23</sup>

However, taking the difference between the two proposals is not enough to capture the intent of the gerrymanderers. This is because not all precincts can easily be moved from one district to another: we call these “unmovable.” While the overall characteristics of a district (in terms of, e.g., lean and turnout) depend on the characteristics of both movable and unmovable precincts, the gerrymanderer can only make decisions on the former. Let us consider a district with 70% of unmovable precincts. The Republican and Democratic proposals will only differ through their decisions on the 30% of movable precincts allocated to that district. If the Democratic gerrymanderer allocates movable precincts that are leaning more Democrat to that district compared to the Republican gerrymanderer, then the district will be measured as leaning more Democrat under the  $D$  map than under the  $R$  map. The problem is that all precincts, including the unmovable ones, will appear to have been intentionally allocated to a more Democratic-leaning district under the  $D$  map. In our example, with 70% of unmovable precincts, any inference about the gerrymanderers’ choices made based on the allocation of precincts to districts would mainly be driven by unmovable precincts. Hence, our second strategy is to focus on movable precincts to make inferences about the gerrymanderer’s intent. To identify movable precincts, we will focus on precincts that are near district borders (more details on this point below).

## 7.2. A Reduced-Form Test: Turnout and Vote Shares

Proposition 3 and the discussion that follows predict a negative relationship between the turnout rate of the precincts composing a district and the probability that the gerrymanderer’s party wins that district. Importantly, Proposition 3 and its extension to multiple types hold among groups that share a common ideological lean. Empirically, we thus need to compare precincts that differ in turnout rates but share a common partisan lean.

---

<sup>23</sup>A limitation of comparing proposals across time is that many other factors change in a ten-year redistricting cycle, including the population and the number of districts per state. In 2020, 18 states had a different number of congressional districts than in the previous redistricting cycle. Given the small number of congressional districts per state, any change in the number of districts makes it difficult to compare maps over time. It is also rare to observe a change in partisan control within a state. In 2020, only two states (Arkansas and West Virginia) experienced a change in full partisan control over redistricting, and only Arkansas had both a change in partisan control and no change in the number of districts. Even for the 2010 cycle, when there was a nationally coordinated effort by Republicans to control the redistricting cycle, only 4 states switched control, and only 2 switched control with no change in the number of districts (party control of redistricting cycles by state and year are available at <https://redistricting.lls.edu/>).

Take all precincts of a given partisan lean in a state, assume that they are all movable, and order them by increasing turnout rates. Now, consider the probability that the Democrat wins the district to which each precinct is assigned. This probability of winning should be decreasing with the turnout rates under the Democrat proposal, but increasing under the Republican proposal. Across the two maps, the *difference* in the probability that Democrats win a district in the Democrat proposal versus the Republican proposal should be decreasing in turnout rates.

As detailed above, we expect this difference to only hold for *movable precincts*. We thus test whether, for the set of movable precincts, lower turnout precincts of a given partisan lean are placed in bluer districts in a Democratic map compared to in a Republican map:

**Empirical Prediction 1.** *Among sets of movable precincts of a given partisan-lean in a given state, there is a negative relationship between the precinct turnout rate and the difference in the expected Democratic vote share of its assigned district under the Democrat versus Republican map.*

### *Empirical Methodology*

The first step to test the above prediction is to define the sub-sample of movable precincts. We define those as the precincts that are adjacent to the congressional district borders in the *baseline map*.<sup>24</sup> We expect precincts to be especially movable if they lie on preexisting congressional district borders that do not coincide with county borders. Figure F.6 in the Appendix documents that the differences between Democratic and Republican redistricting proposals are indeed greater for this sub-sample. This is because congressional districts should follow county borders “where possible,” with some states limiting the total number of counties that can be split into multiple districts.

For the sub-samples of movable precincts, we measure turnout rate and partisan lean and estimate the following empirical specification:

$$\text{Difference in Democratic Vote Share}_{kpbs} = \beta \text{Turnout}_{kps} + \theta_{ps} + \kappa_{bs} + \varepsilon_{kpbs}, \quad (9)$$

where  $\text{Difference in Democratic Vote Share}_{kpbs}$  is the difference in the district-wide expected Democratic vote share under the Democrat proposal versus the Republican proposal for a precinct  $k$ , of partisan-lean  $p$ , along pre-existing border  $b$ , in state  $s$ .  $\theta_{ps}$  is a vector

<sup>24</sup>Perhaps as a result of movability constraints, redistricting proposals tend to resemble the status quo map, with changes made along the borders. We avoid using precincts that are adjacent to borders in the *proposed* maps due to endogeneity problems.

of state-specific partisan-lean fixed effects,  $\kappa_{bs}$  is a vector of congressional district border fixed effects, and  $\varepsilon_{kpbs}$  is an error term. The coefficient of interest is  $\beta$ , which we predict is negative. We include state-specific partisan-lean fixed effects,  $\theta_{ps}$ , so that the variation used to estimate  $\beta$  comes from comparisons within precincts of the same partisan-lean in the same state, in line with the theory. We include border fixed effects,  $\kappa_{bs}$ , to ensure that comparisons come from within precincts that could be feasibly moved or ‘swapped’ across two districts.<sup>25</sup>

To determine the partisan lean of a precinct, we use the share of registered Democrats as a proxy for the ideology of a precinct. Party registration data has the advantage of relying on individuals’ ideology, as revealed by their party affiliation, and not being affected by voting decisions. However, since not all voters choose to register with a party, it may fail to accurately represent the average ideology of the precinct at large.<sup>26</sup> As a robustness check, we use precinct-level past vote shares to proxy for ideology. Precinct-level past vote shares take independent voters into account, but are sensitive to turnout decisions. For precincts with large turnout heterogeneity across party lines, vote shares may not give an accurate measure of average ideology.

We consider four ideological groups in each state, defined as the state-specific quartiles of these proxies for partisanship. Hence, we test for a negative correlation within precincts that are strongly Democrat-leaning, weakly Democrat-leaning, weakly Republican-leaning, or strongly Republican-leaning in each state.<sup>27</sup> We show that results are not sensitive to the number of quantiles used to define partisan lean in Appendix F.2.

We measure the expected *Democratic vote share* of a district as the average votes of the two most recent presidential elections prior to redistricting. We test our predictions on three different definitions of  $Turnout_{kps}$ , detailed in Appendix E.4: past turnout rate, predicted turnout rate, and percent citizen voting age population (CVAP).<sup>28</sup> We use all three measures

<sup>25</sup>To see why border fixed effects are needed, note that the correlation could be negative when comparing precincts of a given partisan lean across the state, but positive within each border (and vice versa). Due to geographic constraints, we expect that within-border correlations are more likely to reflect intentional decisions by gerrymanderers than cross-border correlations.

<sup>26</sup>On average, 25% of registered voters in our sample are not affiliated with either the Democratic or Republican party, while only 3% of the ballots go to third-party candidates.

<sup>27</sup>In Figures F.2 and F.3 in Appendix F.2 we show that there is a bimodal distribution of percent Democrats across all precincts, as well as within several states. This suggests that, in some states, it may be sufficient to consider only two ideological groups (Democrat-leaning versus Republican-leaning precincts). In other states, we may improperly reject the empirical prediction by mistakenly including too few partisan-lean fixed effects.

<sup>28</sup>Note that, in line with the theory, each measure of turnout uses the total population in the denominator. Four states in the sample use prison-adjusted populations when creating congressional districts, meaning they

to address concerns that turnout could be endogenous to redistricting. Predicted turnout is our preferred measure because it uses only exogenous sociodemographic variables to predict past turnout. We prefer this measure over past turnout because we can more confidently rule out endogeneity concerns. We also prefer predicted turnout over percent CVAP since the latter is a crude proxy and gerrymanderers are likely aware of other salient correlates of turnout like race, education, and income.<sup>29</sup> Finally, we estimate standard errors allowing for spatial correlation across precincts using the approach of Colella et al. (2019).<sup>30</sup>

## Results

Table 1 reports the coefficients from OLS estimations of Equation (9) for each of the three measures of turnout. Columns 1-3 report coefficients for the sample of all border precincts, and columns 4-6 report coefficients for the subsample of border precincts that excludes county borders, leaving only those we expect to be “most movable.” In all regressions, the measure of turnout is negatively correlated with the difference in Democratic vote share, in line with the theoretical prediction.

As anticipated, the correlations are stronger in the sub-sample that excludes county borders. In both samples, the coefficients are largest in magnitude for predicted turnout, relative to CVAP or realized turnout. As mentioned above, our preferred measure of turnout is predicted turnout.<sup>31</sup> The point estimates in columns (2) and (5) suggest that a one standard deviation increase in predicted turnout (10 p.p.) is associated with a 0.65-1.12 p.p. decrease in the difference in the expected Democratic vote share of districts across proposals (which represents 8-14% of the mean of the absolute value of the difference in district vote shares).<sup>32</sup>

---

reassign incarcerated individuals to their last known residence. For those four states, we also use prison-adjusted population counts in the denominator for turnout. See Appendix E.1 for detail.

<sup>29</sup>The aim is to use a measure of turnout that best approximates the information that gerrymanderers use in reality. Even if previous turnout is endogenous to past redistricting decisions, it might be a good measure if gerrymanderers use it to evaluate maps in practice. Without knowing the exact information used by the various proposers in our dataset, we risk attenuation bias due to measurement error. This is another reason why it is useful to use three different proxies for turnout.

<sup>30</sup>We allow for arbitrary correlation among precincts that are within 50 kilometers of each other, measured as the Euclidean distance between the centroids of precincts. We use the Stata command `acreg`.

<sup>31</sup>Consistent with the idea that CVAP is a crude proxy for anticipated turnout, we observe a relatively weak correlation between the precinct-level turnout rate in 2022 midterm elections and percent CVAP (coefficient of correlation is 0.35). By comparison, the average turnout rate for 2016 and 2020 presidential elections and predicted turnout have a coefficient of correlation with 2022 turnout of 0.85 and 0.83, respectively.

<sup>32</sup>In a competitive district, a 0.65 p.p. change in expected vote shares can translate into large changes in the probability of winning a district. In Section 7.3, we calibrate the probability of winning a district as a function of expected vote shares. This calibration implies that a small increase in the expected change in vote shares

In Appendix F.2, we show that the negative correlation is robust to alternative definitions of partisan lean. The coefficients for all three measures of turnout are negative if we use two levels of partisan lean and for up to ten levels of partisan lean. The results are also robust to using vote shares rather than ideology to measure precinct-level ideology. We show that the negative correlation is not sensitive to the selection of states with a leave-one-out exercise in Appendix F.4. We also consider alternative definitions of movable precincts in Appendix F.3 by including precincts that are increasingly far away from the existing borders. In line with our hypothesis that precincts near the borders of baseline congressional districts are more likely to be movable, the negative correlation grows weaker as we include precincts that are further and further from the border. In the full sample, the negative correlation is small and statistically insignificant. This suggests that geographic and legal constraints do limit a gerrymanderer's ability to optimize a map to some extent. Overall, the negative correlations between turnout rates and the difference in expected vote shares among movable precincts support the idea that gerrymanderers exploit differences in turnout rates in a pattern consistent with the predictions of the theoretical model.

TABLE 1. Turnout and difference in district-level Democratic vote share.

	Border precincts			Border precincts, excluding county borders		
	(1)	(2)	(3)	(4)	(5)	(6)
Percent CVAP	-0.020** (0.009)			-0.007 (0.013)		
Predicted turnout rate		-0.066*** (0.023)			-0.112*** (0.030)	
Turnout rate			-0.045*** (0.015)			-0.085*** (0.021)
N	17635	17635	17635	9068	9068	9068
$R^2$	0.049	0.051	0.050	0.054	0.062	0.060
Outcome variable mean	-0.004	-0.004	-0.004	-0.001	-0.001	-0.001
State-partisan lean FE	X	X	X	X	X	X
Border FE	X	X	X	X	X	X

*Note:* OLS estimates. The dependent variable is the difference in the two-party Democratic vote share between the Democratic and Republican maps (D map - R map). Percent CVAP is the share of citizens aged 18 and older. The turnout rate is the average of Democratic and Republican votes as a share of the total population in the 2016 and 2020 presidential elections. Predicted turnout rate is based only on demographic and socioeconomic variables. Regressions include border and state-specific partisan-lean fixed effects, with partisan lean defined by state-specific quartiles of registered Democrats. Standard errors are clustered within 50 kilometers to account for spatial correlations. \*  $p < 0.1$ , \*\*  $p < 0.05$ , \*\*\*  $p < 0.01$ .

would have large effects on the probability of winning a highly competitive district. A 0.65 p.p. increase in expected vote shares would increase the probability of winning a 50-50 district by 13 p.p..

### 7.3. Swapping Precincts at the Border

In this section, our objective is to test whether, in practice, gerrymanderers exploit profitable deviations (i.e., changes in the map that would increase their party’s expected number of seats) and, if they do, the extent to which turnout rates matter for optimizing a map.

These tests require taking the model seriously when evaluating actual redistricting proposals. In theory, there should be no profitable deviation from one’s own proposal and plenty from the opponent’s proposal. We can test this directly by creating counterfactual districts and evaluating whether these “swaps” reveal gains that were left unexploited. Given the geographical and legal limitations discussed earlier, there may of course remain some apparently unexploited profitable deviations. Consequently, we compare profitable deviations within a party across different proposed maps:

**Empirical Prediction 2.** *The share of unexploited profitable deviations for a party should be lower under its proposal than under the one of the other party.*

Naturally, the number of possible counterfactual maps is extensive. Hence, we concentrate on counterfactual districts created by redistributing precincts along the district boundaries of proposed maps. This has the added benefit of increasing the likelihood of feasibility of the counterfactual scenarios, in particular in view of the contiguity constraint.

#### *Counterfactual Maps*

For each pair of adjacent districts, we identify all precincts along the border, then independently randomly assign each of these precincts to either of the two districts with 50% probability. A random allocation of precincts is considered a feasible counterfactual map only if it satisfies the equal population constraint.<sup>33</sup> For a border with  $n$  precincts, there are  $2^n$  possible redistricting proposals. The median number of precincts per border is 20, but some borders have hundreds of precincts. Due to computational limitations, we sample until we generate 1,000 feasible maps per border, resulting in 824,000 simulated maps.<sup>34</sup>

<sup>33</sup>As in reality, we impose strict population constraints for the counterfactual districts. The total population of the counterfactual district must be within 1% of the size of an ideal district in the state. The size of an ideal district is the total population of the state divided by the number of districts. Given these tight population constraints, we reassign precincts one border at a time. Otherwise, assessing a large number of feasible counterfactual maps is a computational challenge.

<sup>34</sup>Moreover, there are a few borders for which there is no feasible swap due to the strict population constraints. We exclude such borders from the analysis. In total, we simulate 416,000 maps for Democrat proposals and 408,000 for Republican proposals.

Relative to existing redistricting simulation methods, ours has the advantage of generating a sample of districts that only differ ‘at the margin’ from proposed maps. Existing redistricting algorithms generate maps that differ greatly from the proposals and were never considered by gerrymanderers. Hence, focusing on counterfactual maps not too different from the proposals is best to evaluate the extent to which turnout rates affect gerrymanderers’ decision-making. Moreover, our method allows for district-level comparisons between enacted maps and counterfactual maps. This is useful because we can focus on areas of a map that are less likely to be influenced by legal constraints. For example, as in Section 7.2, we can focus on district borders that do not coincide with county borders, since these borders were not drawn to respect existing political boundaries.

### *Profitable Deviations*

We can determine if a deviation is profitable by mapping vote shares into win probabilities. Let  $\pi_1 + \pi_2$  be the sum of the probability of winning the two districts along a border under the baseline proposal and  $\tilde{\pi}_1 + \tilde{\pi}_2$  be the same for the counterfactual map. A counterfactual redistricting is a profitable deviation if  $\tilde{\pi}_1 + \tilde{\pi}_2 > \pi_1 + \pi_2$ .

To calculate the probabilities of winning, we need to parameterize the aggregate and individual-level shocks. We choose a normal distribution for the aggregate shock  $\delta$ , which implies an S-shaped relationship between vote shares and the probability of winning a district. For simplicity, we assume a uniform distribution for the individual-level shocks. We calibrate the standard deviation of the aggregate shock,  $\sigma$ , using the state-wide standard deviation of the Democratic two-party vote share in presidential elections from 2008-2020.<sup>35</sup> The values for  $\sigma$  range from 0.006 to 0.08 (see Appendix F.5). These values imply that gerrymanderers only meaningfully benefit from swaps in competitive districts. In our model, the standard deviation of the normal distribution is equal to the standard deviation in vote shares, divided by the density of individual shocks,  $\phi$ . Thus, we risk over-estimating  $\sigma$  if there is a relatively large degree of individual-level uncertainty and under-estimating  $\sigma$  if there is a relatively low degree of individual-level uncertainty. Rather than calibrate  $\phi$ , we present results for a range of values of  $\sigma$  between 0.005 and 0.3 (Figure F.10 in Appendix F.6). Concretely, this means that a district with 60% of the expected vote share is won with probability greater than 99% if  $\sigma = 0.005$  and with probability 63% if  $\sigma = 0.3$ .

<sup>35</sup>We use presidential elections rather than congressional elections to avoid imputing values for uncontested races. We are able to use more presidential elections for this state-level analysis than in the precinct-level analysis of Section 7.2 since precinct borders change over time.



## Results

The vast majority of swaps have a negligible effect on either party’s payoff, with 76% of swaps affecting the payoff function by less than 0.5 p.p. in absolute value (The median effect size of a swap is  $2.4 \times 10^{-6}$  p.p.). However, the standard deviation is large (4 p.p.), with a tiny number of swaps affecting the payoff by up to 60 p.p. Figure F.9 in Appendix F.6 shows the distribution of the change in the payoff for a Democratic gerrymanderer for all counterfactual districts.

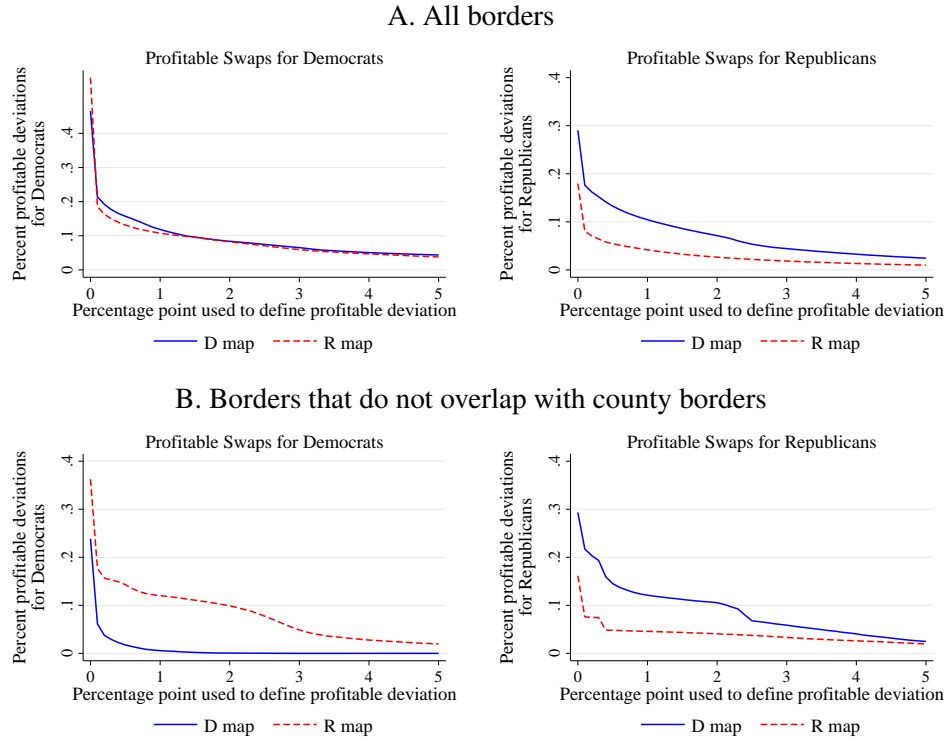


FIGURE 3. SHARE OF SIGNIFICANTLY PROFITABLE SWAPS. The y-axis is the percent of feasible counterfactual maps (‘swaps’) that are profitable for Democrats (left) and Republicans (right). A swap is profitable if the change in payoff exceeds the threshold on the x-axis. The payoff is the expected number of seats. To compute the expected number of seats, we assume that the aggregate shock is normally distributed with mean zero and standard deviation calibrated using statewide presidential election returns from 2008-2020 (see Table F.1).

Figure 3 reports the share of swaps that are “profitable” for each party under Democrat and Republican proposals, using different thresholds to define a *non-negligible profitable deviation*. Part A depicts the share of swaps that are profitable for all district borders, including

precincts that are unlikely to be movable as they overlap with county borders. In that sample, the share of profitable deviations is relatively large, suggesting that gerrymanderers might fail to exhaust all profitable swaps. Moreover, the share of unexploited profitable deviations for a party is not much lower under its own proposal than under the one of the other party.

Part B of Figure 3 instead isolates the most movable precincts by focusing on the subset of borders that do not overlap with county borders. Here, a clear pattern emerges: each party has much fewer profitable deviations in its own proposal than under its opponent’s proposal, and the number of profitable deviations is very small under the party’s own map. For instance, under the Democratic Proposal, only 0.5% of swaps are profitable for Democrats by at least 1 percentage point. In comparison, 12% of swaps are profitable by at least 1 p.p. under the Republican proposal. Likewise, under the Republican proposal, 5% of swaps are profitable for Republicans by at least 1 p.p., compared to 12% of swaps under the Democrat proposal. Note that each party also has strictly fewer profitable deviations than their opponents, within each proposal. These patterns remain regardless of the threshold used to define a profitable deviation (the x-axis of Figure 3). The comparison between the two parts of Figure 3 provides supportive evidence that gerrymanders exploit profitable deviations whenever they can and that legal and geographic constraints reduce this exploitation.

These results are robust to different levels of  $\sigma$ , the standard deviation of the aggregate shock (see Figure F.10 in Appendix F.6). To confirm that our results are not driven by minority maps being less aggressive, Figure F.12 shows that the results are similar when comparing the shares of profitable swaps for the party with majority versus minority control of the state legislature.

### *Isolating the turnout rate effect*

The above exercise demonstrates that gerrymanderers propose maps that exploit swaps that are deemed profitable by our model. However, it leaves open the question of the relative role of ideological heterogeneity as opposed to turnout heterogeneity. To disentangle these two, we repeat the above exercise with the difference that we artificially suppress turnout heterogeneity from the gerrymanderers’ calculations.

Technically, in the original exercise above, we computed  $\hat{\delta}_i$  (and hence the probabilities of winning any given district,  $\pi_j$  and  $\tilde{\pi}_j$ ) using precinct population ( $n_k$ ), past turnout rates ( $\tau_k$ ), and each of the two proxies for ideology,  $\nu_k$ , discussed in Section 7.2 (namely, the

share of registered Democrats or the Democratic vote share):

$$\hat{\delta}_i = \sum_k \frac{n_k \tau_k \nu_k}{\sum_k n_{kj} \tau_k}. \quad (10)$$

What if a gerrymanderer were to mistakenly ignore turnout heterogeneity? If we impose  $\tau_k = \tau$  for all precincts  $k$ , then the median ideology of the district would simply be the average ideology of each precinct, weighted by the precinct’s total population:

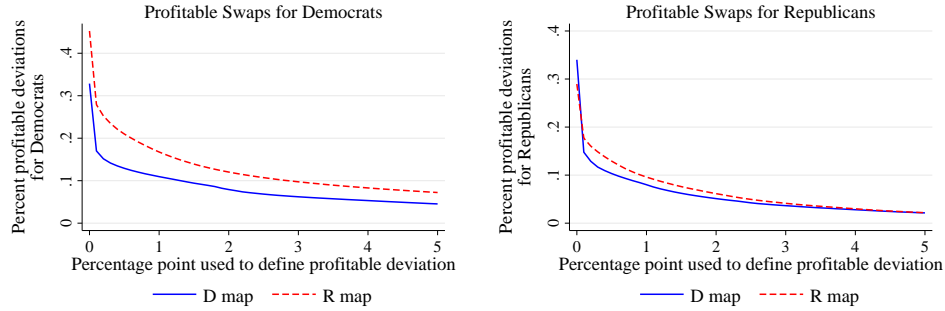
$$\bar{\delta}_j = \sum_k \frac{n_{kj} \nu_k}{\sum_k n_{kj}}. \quad (11)$$

We compute  $\bar{\delta}_i$  and the resulting  $\tilde{\pi}(\bar{\delta}_i)$  for each proposed and counterfactual district using precinct population and the same proxies for  $\nu_k$ . The two measures of a district’s median ideology allow us to compare profitable deviations under the assumption that a gerrymanderer uses an ‘ideology only’ model (with  $\bar{\delta}_i$ ) versus our ‘ideology and turnout’ model (with  $\hat{\delta}_i$ ). To the extent that turnout heterogeneity matters for gerrymanderers’ payoffs in practice, we expect to find only weak support for Prediction 2 using the ideology-only model.

In addition, we can quantify the importance of turnout rate heterogeneity for optimizing a map by evaluating the rate at which a gerrymanderer would make mistakes by ignoring turnout rates. There may be some swaps that are profitable based on ideology alone, but not after taking turnout rate heterogeneity into account. For a gerrymanderer who mistakenly ignores turnout rates, these would be type I errors (false positives). We can also determine the frequency of type II errors (false negatives): those swaps that are not profitable with ideology alone, but that are profitable after taking turnout rate heterogeneity into account.

The results are starkly different when turnout heterogeneity is not taken into account: we no longer find strong evidence in support of Empirical Prediction 2. Figure 4 shows the rate of profitable swaps for Democrats and Republicans when using an ideology-only measure of  $\bar{\delta}_i$  based on voter registration data. With this “ideology-only” approach, Republicans would have a similar share of swaps that are profitable under their own proposals and under the Democratic proposals, whether looking at the full sample or the sample of borders that do not coincide with county borders. Worse, Democrats have *fewer* profitable swaps under their own proposal than Republicans in the full sample. For borders that do not coincide with county borders, the result depends on the threshold used to define “profitable” swaps: for low (respectively, high) thresholds, Democrats have fewer (resp. more) profitable swaps

### A. All borders



### B. Borders that do not coincide with counties

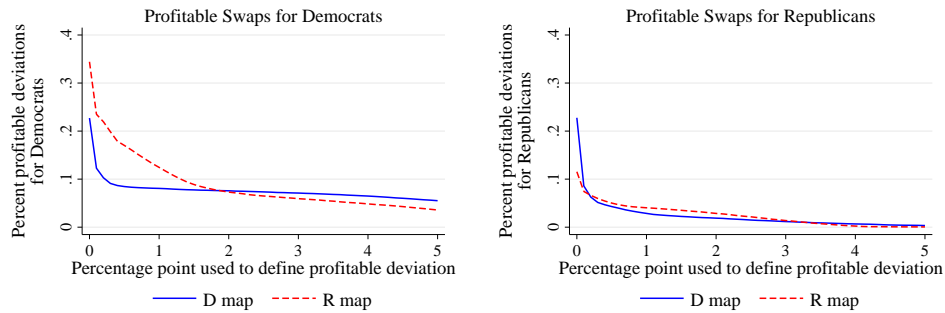


FIGURE 4. SHARE OF SIGNIFICANTLY PROFITABLE SWAPS, MEASURING PAYOFFS WITH IDEOLOGY ONLY. The y-axis is the percent of feasible counterfactual maps (‘swaps’) that are profitable for Democrats (left) and Republicans (right). A swap is profitable if the change in payoff exceeds the threshold on the x-axis. The payoff is the expected number of seats. To compute the expected number of seats we assume that the aggregate shock is normally distributed with mean zero and standard deviation calibrated using statewide presidential election returns from 2008-2020 (see Table F.1). For this exercise, we assume that the vote share of a district is the weighted average of the precinct-level ideology, where ideology is measured with party registration.

under their own proposal than under the Republican proposal. Evidence in support of the empirical prediction is similarly weak with the other proxy for a precinct’s ideology, namely previous vote shares (Figure F.11 in Appendix F.6).

This reveals the central importance of turnout heterogeneity to identify profitable deviations: the interaction between turnout and ideology appears to play an important role in defining the district borders proposed by actual gerrymanderers. In contrast, trying to determine whether a swap is profitable without taking turnout into account results in a hit-and-miss pattern with a high rate of both type I and type II errors.<sup>36</sup>

<sup>36</sup>Of the swaps that are profitable by at least 1 p.p. for the gerrymanderer’s party using ideology only (using registered voters to measure ideology), only 33% are profitable after adding information about turnout rate differences. Of the swaps that are profitable when incorporating information about turnout rates, 60% are not

## 8. Conclusions

This paper studies the strategic incentives of gerrymanderers when drawing electoral maps, introducing a novel aspect by considering that not all individuals vote. We first present a formal theory of redistricting that accounts for heterogeneity in turnout. Our findings show that gerrymanderers, aiming to maximize their party’s number of seats, allocates supporters and opponents differently across electoral districts. Specifically, low-turnout supporters are packed into safe districts to prevent dilution by higher-turnout opponents, thereby ensuring their influence on the final outcome. Conversely, high-turnout opponents are packed in losing districts, minimizing their influence by concentrating losses. The remaining groups are placed in mixed districts, where opponents are paired with higher-turnout supporters. We term this strategy “pack-crack-pack”: as turnout increases, supporters are packed, then mixed in cracked districts, followed by packing high-turnout opponents. Our model predicts (i) assortative matching by turnout in cracked districts, and (ii) that districts can be ranked by turnout, with the probability of winning decreasing as average turnout rises.

In the second part of the paper, we empirically test two key predictions of the model: (i) a negative correlation between turnout rates and expected vote shares of the gerrymanderer’s party across districts; (ii) gerrymanderers exploiting any swaps of precincts across districts that would increase their party’s expected number of seats. To test these predictions, we compared the actual proposals put forth by both the Democrats and the Republicans in 25 U.S. states during the 2020 redistricting cycle. We found patterns in the data that were in line with both predictions, an indication that turnout-based gerrymandering is already happening in practice.

The empirical relevance of turnout-based gerrymandering adds complexity to building legally valid evidence against partisan gerrymandering in an already long and winding road of contradictory court cases.<sup>37</sup> The Supreme Court’s engagement with partisan gerrymandering began with *Davis v. Bandemer* (1986), where it recognized partisan gerrymandering as a potential violation of the Equal Protection Clause. However, the Court failed to establish a clear and workable standard, proposing a test that required showing intent to harm an identifiable political group and proof that the plan would consistently degrade that group’s influence. This vague standard proved unmanageable. The lack of a clear standard persisted until *Vieth v. Jubelirer* (2004), where the Court rejected the *Bandemer* criterion. Justice

---

profitable if you use ideology only, based on registered voters, and 38% are not profitable if you use ideology only, based on vote shares.

<sup>37</sup>For more details, see Stephanopoulos and McGhee (2015, 2018) and Stephanopoulos (2023).

Kennedy, in his concurring opinion, acknowledged the harms of partisan gerrymandering but expressed uncertainty about the proper standard, leading to a period of doctrinal limbo.

In *LULAC v. Perry* (2006), Justice Kennedy signaled an openness to considering “partisan symmetry” as a metric of partisan gerrymandering, while expressing reservations about its practical implementation. This led to the development of the “Efficiency Gap” by Stephanopoulos and McGhee (2015).<sup>38</sup> This metric gained traction in lower courts but, in 2018, the Supreme Court rejected the Efficiency Gap and other statewide measures as insufficient to establish harm to individual voters’ rights and demanded a more district-specific analysis. Finally, in *Rucho v. Common Cause* (2019), the Supreme Court ruled that partisan gerrymandering claims are nonjusticiable, effectively leaving the issue to state courts. Since then, several state courts have shown a willingness to utilize a statistical approach and other objective metrics, although without converging on a consistent approach (see Cervas et al. 2023).

Our findings contribute to the development of ex-post measures of gerrymandering. As discussed in Section 2, most existing measures evaluate the degree to which a party uses packing and cracking strategies. However, we found that in cases of heterogeneous turnout rates, gerrymanderers adopt a pack-crack-pack strategy, deviating from traditional approaches. This alternative strategy could produce maps that appear unbiased according to existing measures of gerrymandering. For instance, if a pack-crack-pack strategy is employed, the Efficiency Gap might not detect partisan bias and may even suggest the map favors the opposing party, given that safe districts are traditionally viewed as a ‘waste’ of votes.

Our results suggest that existing measures like the Efficiency Gap should be complemented by accounting for systematic differences in turnout between districts. A systematic association of “weak opponents” with “strong supporters” could serve as district-specific evidence of partisan gerrymandering. Similarly, the presence of packed districts with low-turnout supporters and high-turnout opponents could also be indicative gerrymandering. While this understanding is important, developing more comprehensive yet coherent measures of gerrymandering remains a major challenge. We need a deeper understanding of how local conditions may result in different district-specific symptoms of individual voter injuries.

---

<sup>38</sup>The Efficiency Gap quantifies the extent to which a party follows the conventional pack-and-crack strategy by adding up the number of votes ‘wasted’ by one party relative to the other. Concretely, packing opponents generates a lot of wasted votes for the opponent (say, they win with a 91% margin when 51% of the votes would suffice, hence wasting 40%), whereas cracking supporters reduces the number of votes wasted for the gerrymanderers’ party.

Only then can we develop a single statistic that captures both the extent of gerrymandering and the intent to discriminate against specific groups.

## References

- Abramowitz, Alan I., Brad Alexander, and Matthew Gunning (2006) “Incumbency, Redistricting, and the Decline of Competition in U.S. House Elections,” *Journal of Politics*, 68 (1), 75–88.
- Bouton, Laurent, Micael Castanheira, and Allan Drazen (2024) “A Theory of Small Campaign Contributions,” *The Economic Journal*, 2351–2390.
- Bursztyn, Leonardo, Davide Cantoni, Patricia Funk, Felix Schönenberger, and Noam Yuchtman (2020) “Identifying the Effect of Election Closeness on Voter Turnout: Evidence from Swiss Referenda,” Working Paper 23490, NBER.
- Caughey, Devin, Chris Tausanovitch, and Christopher Warshaw (2017) “Partisan Gerrymandering and the Political Process: Effects on Roll-Call Voting and State Policies,” *Election Law Journal: Rules, Politics, and Policy*, 16 (4), 453–469.
- Cervas, Jonathan, Bernard Grofman, and Scott Matsuda (2023) “The Role of State Courts in Constraining Partisan Gerrymandering in Congressional Elections,” Technical Report 12584, IZA Discussion Paper.
- Chambers, Christopher P and Alan D Miller (2010) “A measure of bizarreness,” *Quarterly Journal of Political Science*, 5 (1), 27–44.
- Chen, Jowei and Jonathan Rodden (2013) “Unintentional gerrymandering: Political geography and electoral bias in legislatures,” *Quarterly Journal of Political Science*, 8 (3), 239–269.
- Colella, Fabrizio, Rafael Lalive, Seyhun Orcan Sakalli, and Mathias Thoenig (2019) “Inference with Arbitrary Clustering,” *The University of New Hampshire Law Review*, 21 (2), 421–494.
- Cox, Gary W. and Jonathan N. Katz (2007) *Elbridge Gerry’s Salamander: The Electoral Consequences of the Reapportionment Revolution*: Cambridge University Press.
- DeFord, Daryl R., Nicholas Eubank, and Jonathan Rodden (2022) “Partisan Dislocation: A Precinct-Level Measure of Representation and Gerrymandering,” *Political Analysis*, 30, 403–425.
- Erikson, Robert S. (1972) “Malapportionment, Gerrymandering, and Party Fortunes in Congressional Elections,” *American Political Science Review*, 66 (4), 1234–1245.

- Friedman, Jeffrey N. and Richard Holden (2009) “The Rising Incumbent Reelection Rate: What’s Gerrymandering Got To Do with It?” *Journal of Politics*, 593–611.
- Friedman, John N. and Richard Holden (2020) “Optimal Gerrymandering in a competitive environment,” *Economic Theory Bulletin*, 8 (2), 347–367.
- Friedman, John N. and Richard T. Holden (2008) “Optimal Gerrymandering: Sometimes Pack, but Never Crack,” *American Economic Review*, 98 (1), 113–44.
- Gelman, Andrew and Gary King (1994) “Enhancing democracy through legislative redistricting,” *American Political Science Review*, 88 (3), 541–559.
- Genicot, Garance (r) Laurent Bouton (r) Micael Castanheira (2021) “Electoral Systems and Inequalities in Government Interventions,” *Journal of the European Economic Association*.
- Gomberg, Andrei, Romans Pans, and Tridib Sharma (2023) “Electoral Maldistricting,” *Working Paper*.
- Grofman, Bernard and Gary King (2007) “The Future of Partisan Symmetry as a Judicial Test for Partisan Gerrymandering after LULAC V. Perry,” *Election Law Journal*, 6 (1), 2–35.
- Gul, Faruk and Wolfgang Pesendorfer (2010) “Strategic Redistricting,” *American Economic Review*, 100 (4), 1616–1641.
- Henderson, John A, Jasjeet S Sekhon, and Roc’io Titunuk (2016) “Cause or Effect? Turnout in Hispanic Majority-Minority Districts,” *Political Analysis*, 24 (3), 404–412.
- Incerti, Giovanni (2015) “Mixed-Member Electoral Systems and the Objective of Maximizing the Expected Seat Share,” *American Journal of Political Science*, 59 (2), 393–408.
- Jacobson, Gary C and Samuel Kernell (1985) *Strategy and choice in congressional elections*: Yale University Press.
- Jeong, Dahyeon and Ajay Shenoy (2022) “The Targeting and Impact of Partisan Gerrymandering: Evidence from a Legislative Discontinuity,” *Review of Economics and Statistics*, 1–47.
- Jones, Daniel B, Neil Silveus, and Carly Urban (2023) “Partisan Gerrymandering and Turnout,” *Journal of Law & Economics*, Forthcoming.
- Jones, Daniel B. and Randall Walsh (2018) “How do voters matter? Evidence from US congressional redistricting,” *Journal of Public Economics*, 158, 25–47.
- Katz, Jonathan N., Gary King, and Elisabeth Rosenblatt (2020) “Theoretical Foundations and Empirical Evaluations of Partisan Fairness in District-Based Democracies,” *American Political Science Review*, 114 (1), 164–178.



- Kawai, Kei, Yuta Toyama, and Yasutora Watanabe (2021) "Voter turnout and preference aggregation," *American Economic Journal: Microeconomics*, 13 (4), 548–586.
- Kolotilin, Anton and Alexander Wolitzky (2023) "The Economics of Partisan Gerrymandering," unsw economics working paper.
- Levine, David K and Andrea Mattozzi (2020) "Voter turnout with peer punishment," *American Economic Review*, 110 (10), 3298–3314.
- Levitt, Justin (2016) "Lulac v. perry: The frumious gerry-mander, rampant," *Mazo (Eds.), Election Law Stories*, 233–284.
- Lindbeck, Assar and Jörgen Weibull (1987) "Balanced-budget redistribution as the outcome of political competition," *Public Choice*, 52 (3), 273–297.
- Lizzeri, Alessandro and Nicola Persico (2001) "The Provision of Public Goods under Alternative Electoral Incentives," *American Economic Review*, 91 (1), 225–239.
- McDonald, Michael D. and Robin E. Best (2015) "Unfair Partisan Gerrymanders in Politics and Law: A Diagnostic Applied to Six Cases," *Election Law Journal*, 14 (4), 312–330.
- Morton, Rebecca B (1987) "A group majority voting model of public good provision," *Social Choice and Welfare*, 4 (2), 117–131.
- (1991) "Groups in rational turnout models," *American Journal of Political Science*, 758–776.
- Moskowitz, Daniel J. and Benjamin Schneer (2019) "Reevaluating Competition and Turnout in U.S. House Elections," *Quarterly Journal of Political Science*, 14 (2), 191–223.
- Niemi, Richard G, Bernard Grofman, Carl Carlucci, and Thomas Hofeller (1990) "Measuring compactness and the role of a compactness standard in a test for partisan and racial gerrymandering," *The Journal of Politics*, 52 (4), 1155–1181.
- Owen, G. and B. Grofman (1988) "Optimal Partisan Gerrymandering," *Political Geography Quarterly*, 7, 5–22.
- Persson, Torsten and Guido Tabellini (2000) *Political Economics: Explaining Economic Policy*, MIT Press Books: The MIT Press.
- Riker, William H and Peter C Ordeshook (1968) "A Theory of the Calculus of Voting," *American political science review*, 62 (1), 25–42.
- Shachar, Ron and Barry Nalebuff (1999) "Follow the leader: Theory and evidence on political participation," *American Economic Review*, 89 (3), 525–547.
- Sherstyuk, Katerina (1998) "How to gerrymander: A formal analysis," *Public Choice*, 27–49.

- Shotts, Kenneth W. (2003) “Racial Redistricting’s Alleged Perverse Effects: Theory, Data, and “Reality”,” *Journal of Politics*, 65 (1), 238–243.
- Snyder, James M (1989) “The effect of party activity on campaign spending,” *Legislative Studies Quarterly*, 14 (1), 95–110.
- Stashko, Allison (2020) “Crossing the District Line: Border Mismatch and Targeted Redistribution,” working paper, University of Utah.
- Stephanopoulos, Nicholas (2023) “Partisan Gerrymandering,” *SSRN Electronic Journal*, 10.2139/ssrn.4294248.
- Stephanopoulos, Nicholas O. (2013) “Our Electoral Exceptionalism,” *University of Chicago Law Review*, 80 (2).
- Stephanopoulos, Nicholas O and Eric M McGhee (2015) “Partisan gerrymandering and the efficiency gap,” *U. Chi. L. Rev.*, 82, 831.
- Stephanopoulos, Nicholas O. and Christopher Warshaw (2020) “The Impact of Partisan Gerrymandering on Political Parties,” *Legislative Studies Quarterly*, 45 (4), 609–643.
- Strömberg, David (2004) “Radio’s Impact on Public Spending,” *The Quarterly Journal of Economics*, 119 (1), 189–221.
- (2008) “How the Electoral College Influences Campaigns and Policy: The Probability of Being Florida,” *American Economic Review*, 98 (3), 769–807.
- Warrington, Gregory S. (2018) “Quantifying Gerrymandering Using the Vote Distribution,” *Election Law Journal: Rules, Politics, and Policy*, 17 (1), 39–57.

# Appendices

As stated in Section 3.4.3, the Properties and the proofs in this Appendix are written for the case of multiple ideologies:  $\nu_k \in [\nu_R, \nu_D]$ . We therefore maintain the notation that ideology  $\nu_R$  is the most republican, i.e., with the lowest value of  $\nu$ , and  $\nu_D$  the most democratic, with the highest value of  $\nu$ .

## A. Properties

**Proof of Existence and Uniqueness of  $\hat{\delta}_j$  and that  $\nu_R \leq \hat{\delta}_j \leq \nu_D$ .** To see that  $\hat{\delta}_j$  exists and is unique and that  $\hat{\delta}_j \in [\nu_R, \nu_D]$ , note that the sum of excess vote shares of  $D$  in district  $j$  (3) is: (i) strictly positive for  $\delta_j = \nu_R$  since  $V_R(\nu_R) = 0$  and  $V_K(\nu_K) > 0$  for all  $\nu_K > \nu_R$ ; (ii) strictly negative for  $\delta_j = \nu_D$  since  $V_D(\nu_D) = 0$  and  $V_K(\nu_K) < 0$  for all  $\nu_K < \nu_D$ ; (iii) continuous in  $\delta_j$  by the continuity of  $F$ ; and (iv) strictly decreasing in  $\delta_j$ , since  $F$  is strictly increasing over its support  $\Phi$ . ■

As remarked earlier, changes in the population of a district affect the probability of winning a district  $\pi_j = \Gamma(\hat{\delta}_j)$  only via its effect on the turnout of the ideological groups  $\{t_j^K\}_{\forall K}$  and how it affects  $\hat{\delta}_j$ . We can also show the following basic properties:

**Property 1.** *If  $F$  and  $\Gamma$  are strictly increasing, then:*

- i. *For all  $t^D > 0$ ,  $\frac{\partial \pi}{\partial t^D} > 0$  if  $t^R > 0$ , and  $\frac{\partial \pi}{\partial t^D} = 0$  if  $t^R = 0$ ,*
- ii. *For all  $t^R > 0$ ,  $\frac{\partial \pi}{\partial t^R} < 0$  if  $t^D > 0$ , and  $\frac{\partial \pi}{\partial t^R} = 0$  if  $t^D = 0$ .*

**Proof of Property 1.** Recall that the definition of  $\hat{\delta}$  is such that:

$$\sum_K t^K V_K(\hat{\delta}) = 0.$$

Hence,

$$\frac{\partial \hat{\delta}}{\partial t^K} = - \frac{V_K(\hat{\delta})}{\sum_L t^L V'_L(\hat{\delta})}. \quad (\text{A.1})$$

Notice that if the district is packed  $K$ , then  $t^L = 0$  for all  $L \neq K$ . The definition of  $\hat{\delta}$  then implies that  $V_K(\hat{\delta}) = 0$  and therefore  $\hat{\delta} = \nu_K$ .

Now if the district is not packed  $K$  then the sign of (A.1) is given by the sign of  $V_K(\hat{\delta})$  (recall that  $V'_L < 0$ ). If the district is not packed  $D$ , it follows from the strict monotonicity of  $F$  that  $\hat{\delta} < \nu_D$  and

therefore  $V_D(\hat{\delta}) > 0$ . This proves Property 1.i. Similarly, if the district is not packed  $R$ , it follows from the strict monotonicity of  $F$  that  $\hat{\delta} > \nu_R$  and therefore  $V_R(\hat{\delta}) < 0$ . This proves Property 1.ii. ■

**Property 2.** Consider any two ideologies,  $\nu_L < \nu_H$  (for instance,  $\nu_R < \nu_D$ ). Then,  $V_L(\delta)/V_H(\delta)$  is strictly decreasing in  $\delta$  for all  $\delta \in (\nu_R, \nu_D)$ .

**Proof of Property 2.** We must prove that  $\partial \left( \frac{V_L(\delta)}{V_H(\delta)} \right) / \partial \delta$  is always negative. It is immediate to see that it has the same sign as:

$$\frac{\partial V_L(\delta)}{\partial \delta} V_H(\delta) - \frac{\partial V_H(\delta)}{\partial \delta} V_L(\delta). \quad (\text{A.2})$$

We note that (i)  $\nu_H > \nu_L \Rightarrow V_H(\delta) > V_L(\delta), \forall \delta$ , and (ii)  $\partial V_K(\delta) / \partial \delta < 0, \forall K \in \{L, H\}$ .

We now show that (A.2) must be negative for any value of  $\delta \in (\nu_L, \nu_H)$ . First, remember that:

$$V_k(\delta) \equiv F(\nu_k - \delta) - \frac{1}{2},$$

and hence that, from the symmetry of  $F$ , we have that  $V_k(\delta) = 0$  if  $\delta = \nu_k$ . Combined with  $\frac{\partial V_K(\delta)}{\partial \delta} < 0, \forall K \in \{L, H\}$ , this gives us that for all  $\delta \in (\nu_L, \nu_H)$ , then  $V_H(\delta) > 0 > V_L(\delta)$ . Hence, (A.2) is strictly negative. ■

## B. Proofs: Main Results

**Proof of Proposition 1.** Suppose that district  $i$  is packed  $R$  ( $\frac{t_i^R}{t_i} = 1$ ) while  $j$  is cracked ( $\frac{t_j^R}{t_j} < 1$ ) and consider an  $r \stackrel{i}{\rightleftharpoons}_j r'$  swap with  $\tau_r < \tau_{r'}$

First, note that, given that  $\frac{t_i^R}{t_i} = 1$  we know that  $\frac{\partial \pi_i}{\partial t_i^R} = 0$  by Property 1ii. Hence, an  $r \stackrel{i}{\rightleftharpoons}_j r'$  swap does not affect  $\pi_i$ . We can thus focus on  $\pi_j$ , for which the marginal effect is:

$$-(\tau_{r'} - \tau_r) \frac{\partial \pi_j}{\partial t_j^R},$$

which is positive by Property 1ii. The proof for D voters follows the same steps. ■

**Proof of Proposition 2.** Suppose not. Then there exists a district  $i$  with types  $k$  and  $l$  and a district  $j$  with types  $l'$  and  $k'$  where  $\tau_k < \tau_{k'}, \tau_l > \tau_{l'}, \nu_k = \nu_{k'}$  and  $\nu_l = \nu_{l'}$ , with  $\pi_i \neq \pi_j$  (which requires  $\hat{\delta}_i \neq \hat{\delta}_j$ ).

Wlog, we assume  $\nu_K \geq \nu_L$  and start by considering the case where  $\nu_K > \nu_L$ .

In an optimal map, the effect of a  $k \stackrel{i}{\rightleftharpoons} k'$  swap must be non-positive. From (6) and  $\tau_k < \tau_{k'}$ , this requires:

$$\left( \frac{\partial \pi_i}{\partial t_i^K} - \frac{\partial \pi_j}{\partial t_j^K} \right) \leq 0. \quad (\text{B.1})$$

The effect of a  $l \stackrel{i}{\rightleftharpoons} l'$  swap must also be non-positive. From (6) and  $\tau_l > \tau_{l'}$ , this requires:

$$\left( \frac{\partial \pi_i}{\partial t_i^L} - \frac{\partial \pi_j}{\partial t_j^L} \right) \geq 0. \quad (\text{B.2})$$

Plugging those inequalities in (7), we obtain that a  $k \stackrel{i}{\rightleftharpoons} l'$  swap is necessarily weakly profitable:

$$\underbrace{\tau_{l'} \times \left( \frac{\partial \pi_i}{\partial t_i^L} - \frac{\partial \pi_j}{\partial t_j^L} \right)}_{\geq 0} + \underbrace{\tau_k \times \left( \frac{\partial \pi_j}{\partial t_j^K} - \frac{\partial \pi_i}{\partial t_i^K} \right)}_{\geq 0} \geq 0. \quad (\text{B.3})$$

Now, inequality (B.3) is strict unless both terms between parentheses are equal to zero, that is:

$$\frac{\partial \pi_i}{\partial t_i^L} = \frac{\partial \pi_j}{\partial t_j^L}, \quad \text{and} \quad (\text{B.4})$$

$$\frac{\partial \pi_i}{\partial t_i^K} = \frac{\partial \pi_j}{\partial t_j^K}. \quad (\text{B.5})$$

Using the expressions in (8) and dividing (B.4) by (B.5) implies that

$$\frac{V_L(\hat{\delta}_i)}{V_K(\hat{\delta}_i)} = \frac{V_L(\hat{\delta}_j)}{V_K(\hat{\delta}_j)}.$$

Property 2 tells us that  $\frac{V_L(\delta)}{V_K(\delta)}$  is strictly decreasing in  $\delta$ . As a result, the previous equality cannot hold unless  $\hat{\delta}_i = \hat{\delta}_j$ , a contradiction. This proves the proposition for  $\nu_K \neq \nu_L$ .

Now suppose that  $\nu_K = \nu_L$ . Inequalities (B.1) and (B.2) then imply that (B.5) holds.

Since the districts are cracked, we know that they contain at least some voters of types  $q$  and  $m$ , with ideology  $\nu_Q \neq \nu_M$  that are present either in district  $i$  and/or district  $j$ . Moreover, we select types  $q$  in  $i$  and  $m'$  in  $j$  that lean more democratic than  $\nu_K$  if  $K$  is more republican than the median, and more republican than  $\nu_K$  if  $K$  is more democratic than the median. That is:  $\nu_Q, \nu_{M'} \gtrless \nu_K$ , if  $\nu_K \gtrless \min\{\hat{\delta}_i, \hat{\delta}_j\}$  (with more than two ideologies,  $\nu_M$  could be distinct or equal to  $\nu_Q$ ).

Given (B.5), in order not to have a profitable  $q \stackrel{i}{\rightleftharpoons} k'$  swap we must have that

$$\frac{\partial \pi_i}{\partial t_i^Q} \geq \frac{\partial \pi_j}{\partial t_j^Q}. \quad (\text{B.6})$$

Similarly in order not to have a profitable  $k \stackrel{i}{\rightleftharpoons} m'$  swap we must have that

$$\frac{\partial \pi_i}{\partial t_i^M} \leq \frac{\partial \pi_j}{\partial t_j^M}. \quad (\text{B.7})$$

Dividing these equations by (B.5) tells us that,

$$\begin{aligned} \frac{V_Q(\hat{\delta}_i)}{V_K(\hat{\delta}_i)} &\geq \frac{V_Q(\hat{\delta}_j)}{V_K(\hat{\delta}_j)}, \quad \text{and} \\ \frac{V_M(\hat{\delta}_i)}{V_K(\hat{\delta}_i)} &\leq \frac{V_M(\hat{\delta}_j)}{V_K(\hat{\delta}_j)}. \end{aligned}$$

If  $\nu_K > \hat{\delta}_i$ , with both inequalities reversed if  $\nu_K < \hat{\delta}_i$ . Given the monotonicity of Property 2, the only way for both inequalities to hold is  $\hat{\delta}_j = \hat{\delta}_i$ , a contradiction. ■

**Proof of Proposition 3.** The claim is that all cracked districts can be ordered by increasing turnout rates and decreasing winning probabilities.

Take any two districts  $i$  and  $j$  such that  $\pi_i(\mathbf{n}_i) < \pi_j(\mathbf{n}_j)$ , which requires  $\hat{\delta}_i < \hat{\delta}_j$ . Consider two types,  $k$  and  $k'$  with the same ideology  $\nu_K$ . We now prove that  $\tau_k < \tau_{k'}$  always leads to a contradiction.

From (6), a  $k \stackrel{i}{\rightleftharpoons} k'$  swap is profitable unless:

$$\frac{\partial \pi_i}{\partial t_i^K} - \frac{\partial \pi_j}{\partial t_j^K} \leq 0. \quad (\text{B.8})$$

Next, consider a type  $m'$  with an ideology different from  $\nu_K$ : a  $k \stackrel{i}{\rightleftharpoons} m'$  swap is profitable unless

$$\tau_{m'} \left( \frac{\partial \pi_i}{\partial t_i^M} - \frac{\partial \pi_j}{\partial t_j^M} \right) + \underbrace{\tau_k \left( \frac{\partial \pi_j}{\partial t_j^K} - \frac{\partial \pi_i}{\partial t_i^K} \right)}_{\geq 0} \leq 0,$$

where the sign of the second term follows from (B.8). As a result, we need:

$$\frac{\partial \pi_i}{\partial t_i^M} \leq \frac{\partial \pi_j}{\partial t_j^M}. \quad (\text{B.9})$$

Now recall from (8) that:

$$\frac{\partial \pi_m}{\partial t_m^X} = \gamma(\hat{\delta}_m) \frac{V_X(\hat{\delta}_m)}{\left| \sum_Y t_m^Y \frac{\partial V_Y(\hat{\delta}_m)}{\partial \hat{\delta}_m} \right|}, \quad (\text{B.10})$$

and consider the different possibilities.

**Case 1:**  $\nu_K < \hat{\delta}_i < \hat{\delta}_j < \nu_M$ . In this case, we have that  $0 > V_K(\hat{\delta}_i) > V_K(\hat{\delta}_j)$  (where the second inequality follows from  $\hat{\delta}_i < \hat{\delta}_j$ ).

Using this together with (B.10), we see that (B.8) implies that  $\frac{\gamma(\hat{\delta}_i)}{|\sum_Y t_i^Y V_Y'(\hat{\delta}_i)|} > \frac{\gamma(\hat{\delta}_j)}{|\sum_Y t_j^Y V_Y'(\hat{\delta}_j)|}$ . Given this, for (B.9) to hold, we must have that:

$$0 < V_M(\hat{\delta}_i) < V_M(\hat{\delta}_j),$$

which contradicts  $\hat{\delta}_i < \hat{\delta}_j$ .

**Case 2:**  $\nu_K > \hat{\delta}_j > \hat{\delta}_i > \nu_M$ . In this case, we have that  $V_K(\hat{\delta}_i) > V_K(\hat{\delta}_j) > 0$  (where the first inequality follows from  $\hat{\delta}_i < \hat{\delta}_j$ ). Hence, (B.8) implies that  $\frac{\gamma(\hat{\delta}_i)}{|\sum_Y t_i^Y V_Y'(\hat{\delta}_i)|} < \frac{\gamma(\hat{\delta}_j)}{|\sum_Y t_j^Y V_Y'(\hat{\delta}_j)|}$ . Given this, for (B.9) to hold, we must have that:

$$V_M(\hat{\delta}_i) < V_M(\hat{\delta}_j) < 0,$$

which contradicts  $\hat{\delta}_i < \hat{\delta}_j$ .

**Case 3:**  $\hat{\delta}_i < \nu_K < \hat{\delta}_j$ . That is, there is (at least) one type with an ideology strictly between the two district medians (note that this requires multiple ideological types).

This case can simply not materialize: for  $\nu_K \in [\hat{\delta}_i, \hat{\delta}_j]$ , we have  $V_K(\hat{\delta}_i) \geq 0 \geq V_K(\hat{\delta}_j)$ . This implies that  $\frac{\partial \pi_i}{\partial t_i^K} \geq 0$  and  $\frac{\partial \pi_j}{\partial t_j^K} \leq 0$ , with at least one strict inequality. Hence, (B.8) cannot hold. ■

## Online Appendix to “Pack-Crack-Pack: Gerrymandering with Differential Turnout”

L. Bouton  G. Genicot  M. Castanheira  A. Stashko

### C. Endogenous Turnout

In the baseline model, turnout rates are group-specific but exogenously set at  $\tau_k$ . This overlooks the possibility that such turnout rates may also depend on the competitiveness of the election or other factors related to local circumstances. When this happens, voters from a same group may display a different turnout rate depending on the district in which they are. In this section, we extend the model to incorporate such district-specific effects: the probability that a voter turns out and votes for  $D$  can be decomposed into a group-specific factor  $\tau_k$  and a district-specific factor  $\lambda_j^k$ . To simplify the exposition, we can think of  $\tau_k$  as the share of individuals from group  $k$  who are eligible to vote. That is, there is a share  $1 - \tau_k$  who are ineligible; they cannot vote, e.g., because of legal constraints such as age or citizenship, or of external factors such as having to work on election day. In contrast, conditional on being eligible,  $\lambda_j^k$  captures decisional, or preference, factors, i.e., their *decision* to vote or not. The share of group- $k$  voters who turn out and vote for  $D$  and  $R$  are then:

$$\tau_k \times \lambda_j^D \text{ and } \tau_k \times \lambda_j^R.$$

We consider two different models of costly voting from the literature to endogenize  $\lambda_j^P$ : (i) Calculus of voting à la Riker and Ordeshook (1968), and (ii) Group-based voting à la Shachar and Nalebuff (1999).

#### Calculus of Voting

This first model of endogenous voting follows the traditional calculus of voting model described, for example, in Riker and Ordeshook (1968), and extended by Kawai et al. (2021). The logic is as follows: the voters’ preference intensity reveals how much they value the election of their preferred candidate over that of the opponent. We follow the same probabilistic voting specification as in Lindbeck and Weibull (1987): preference intensity is captured by  $\nu_k - \eta_e - \delta$ , and going to the voting booth has a cost  $c_k \geq 0$  that can be group specific. One’s personal vote also only matters insofar as it may affect the election outcome. In Riker and Ordeshook (1968), this is captured by the probability of being pivotal. In Kawai et al. (2021), the central element is the voters’ *perceived voting efficacy*, which we denote  $p_k(\mathbf{n}_j) > 0$ , and which depends both on group-specific factors that affect their beliefs about how their vote may influence policy and on the actual composition



of the district,  $\mathbf{n}_j$ . In particular, voters might believe their vote to have a larger impact in a closely contested district than in a highly partisan district.

An eligible voter turns out and votes for  $D$  when her expected benefit of doing so is larger than the cost of voting:

$$(\nu_k - \eta_e - \delta) p_k(\mathbf{n}_j) \geq c_k \text{ or } \eta_e \leq \nu_k - \delta - \frac{c_k}{p_k(\mathbf{n}_j)},$$

and she votes for  $R$  when:

$$\eta_e \geq \nu_k - \delta + \frac{c_k}{p_k(\mathbf{n}_j)}.$$

The share of eligible voters who cast a ballot for  $D$  is therefore increasing in  $\nu_k$  and decreasing in  $\delta$ , like in the absence of voting costs. Conversely, the share of eligible voters who cast a ballot for  $R$  is decreasing in  $\nu_k$  and increasing in  $\delta$ . The new element is that the share of voters who turn out is now decreasing in  $c_k/p_k(\mathbf{n}_j)$ : turnout decreases with the cost of voting ( $c_k$ ) and increases with a voter's perceived voting efficacy ( $p_k(\mathbf{n}_j)$ ).

To simplify exposition, we assume that  $c_k/p_k(\mathbf{n}_j)$  is the same for all individuals with the same ideology  $\nu_k$ . We thus have  $c_k/p_k(\mathbf{n}_j) \in \{c_D/p_D(\mathbf{n}_j), c_R/p_R(\mathbf{n}_j)\}$ . We could easily relax this assumption.

We slightly modify Assumption 1 to guarantee that both parties receive some votes despite these costs. Equivalently, it amounts to assuming that voting costs are not prohibitively high:

**Assumption 1bis.** (i)  $\Gamma$  has full support over  $\Psi = [\delta_{\min}, \delta_{\max}] \supset [\nu_R, \nu_D]$  and (ii)  $F$  has full support over  $\Phi \supset [\min_{K,j}(\nu_R - c_K/p_K(\mathbf{n}_j) - \delta_{\max}), \max_{K,j}(\nu_D + c_K/p_K(\mathbf{n}_j) - \delta_{\min})]$ .

A second natural assumption is that, irrespective of the map and in each given district, the median individual in group  $D$  leans more toward candidate  $D$  than the median individual in group  $R$ :

**Assumption 2.**  $\nu_D - \frac{c_D}{p_D(\mathbf{n}_j)} > \nu_R - \frac{c_R}{p_R(\mathbf{n}_j)}$  and  $\nu_D + \frac{c_D}{p_D(\mathbf{n}_j)} > \nu_R + \frac{c_R}{p_R(\mathbf{n}_j)}$  for all  $\mathbf{n}_j$ .

It remains to characterize  $p_K(\mathbf{n}_j)$ . We want to capture the fact that voting efficacy is expected to be higher in close districts than in safe districts. Whether a district is close or safe depends on  $\hat{\delta}$  (more details on the definition of that critical value of the aggregate shock below): close districts are characterized by values of  $\hat{\delta}$  close to 0. Conversely, safe  $D$  and  $R$  districts are characterized respectively by values of  $\hat{\delta}$  close to  $\nu_D$  and  $\nu_R$  respectively. Hence, we impose that voting efficacy peaks at 0, and is monotonically decreasing away from it. Let's assume that a district map implies a belief  $\tilde{\delta}$  regarding the critical value of the aggregate shock for which the district is tied (we will impose rational expectation below). Abusing slightly notation, we assume that:

$$p_K(\mathbf{n}_j) = p_K(\tilde{\delta}), \text{ with } \partial p_K(\tilde{\delta})/\partial \tilde{\delta} \leq 0 \text{ for } \tilde{\delta} \geq 0.$$

Under Assumptions 1bis and 2, an eligible voter with type  $k$ , when in district  $j$ , casts a  $D$ -ballot and an  $R$ -ballot respectively with probabilities:

$$F\left(\nu_K - \delta - \frac{c_K}{p_K(\tilde{\delta}_j)}\right) \text{ and } 1 - F\left(\nu_K - \delta + \frac{c_K}{p_K(\tilde{\delta}_j)}\right),$$

whereas “moderate” voters abstain. The probability that  $D$  wins district  $j$  is then:

$$\pi_j = \Pr_{\delta} \left[ \sum_K t_j^K W_K(\delta, \tilde{\delta}_j) \right], \text{ with } W_K(\delta, \tilde{\delta}_j) \equiv F\left(\nu_K - \delta - \frac{c_K}{p_K(\tilde{\delta}_j)}\right) + F\left(\nu_K - \delta + \frac{c_K}{p_K(\tilde{\delta}_j)}\right) - 1.$$

Still like in the baseline model, there is a unique realization of  $\delta$  for which the number of votes for  $D$  and for  $R$  are equal. In particular, for any value of  $\tilde{\delta}_j$ , there is a critical value  $\delta_j^*(\tilde{\delta}_j)$  such that:

$$\sum_K t_j^K \times W_K(\delta_j^*(\tilde{\delta}_j), \tilde{\delta}_j) = 0. \quad (\text{C.1})$$

To see that  $\delta_j^*(\tilde{\delta}_j)$  exists and is unique, note that the LHS of (C.1): (i) is strictly positive for  $\delta = \nu_R$  since, by Assumption 2, we have that  $W_D(\delta, \tilde{\delta}) > W_R(\delta, \tilde{\delta})$ ,  $\forall \delta$  and that, by the symmetry of  $F$ ,  $W_R(\nu_R, \tilde{\delta}) = 0$ ; (ii) is strictly negative for  $\delta = \nu_D$  since  $W_R(\nu_D, \tilde{\delta}) < W_D(\nu_D, \tilde{\delta}) = 0$ ; (iii) is continuous in  $\delta$  by the continuity of  $F$ ; and (iv) is strictly decreasing in  $\delta$ , since  $F$  is a strictly increasing function.

Finally, an equilibrium also requires a consistency requirement on the beliefs of the voters, i.e.,  $\tilde{\delta}_j = \hat{\delta}_j$ . Thus, the consistent critical value  $\hat{\delta}_j$  that we are interested in solves the fixed point  $\hat{\delta}_j = \delta_j^*(\hat{\delta}_j)$ . It is implicitly defined as

$$\sum_K t_j^K V_K(\hat{\delta}_j) = 0, \quad (\text{C.2})$$

where  $V_K(\hat{\delta}_j) = W_K(\hat{\delta}_j, \hat{\delta}_j)$  is the *excess vote share of  $D$*  in district  $j$  among voters with ideology  $K$  at  $\hat{\delta}_j$ .

The uniqueness of the consistent critical value  $\hat{\delta}_j$  is guaranteed by the following assumption:

**Assumption 3.**  $dV_k(\hat{\delta}_j)/d\hat{\delta}_j < 0$  for both  $K = D, R$ .

It requires that for any ideological group  $K$ , the excess vote share of  $D$  in district  $j$  is decreasing in the critical value of the aggregate shock  $\hat{\delta}_j$ . This prevents situations in which, e.g., the change in the voting efficacy is such that the excess vote share of  $D$  goes up when the aggregate shock is more in favor of  $R$ . It is easy to show that this assumption is necessarily satisfied if any one of  $|p'_K(\delta)|$  or  $c_K$ , or  $|f(x - c_K/p_K(\delta')) - f(x + c_K/p_K(\delta'))|$ ,  $\forall x \in \mathbb{R}$ , is sufficiently close to zero.

For any given cutoff  $\hat{\delta}_j$ , we thus have that  $D$  wins district  $j$  for all values of  $\delta \leq \hat{\delta}_j$  and  $R$  wins for all  $\delta > \hat{\delta}_j$ . That is, like in the base model:

$$\pi_j = \Gamma(\hat{\delta}_j),$$

with the only difference being that the value of this cutoff now depends on the groups' cost of voting and perceived voting efficacy, on top of the heterogeneity of their eligibility rates,  $\tau_k$ .

It is then easy to check that, under Assumptions 1bis, 2, and 3, the proof of Property 1 (in Appendix A) applies verbatim with this modified  $V_K$  function.<sup>39</sup> The following property proves the equivalent of Property 2 (also in Appendix A) for this endogenous turnout model.

**Property 2bis.**  $\frac{V_R(\delta)}{V_D(\delta)}$  is strictly decreasing in  $\delta \in (\nu_R, \nu_D)$ .

**Proof.** Notice that the sign of the effect of  $\delta$  on  $\frac{V_R(\delta)}{V_D(\delta)}$  is the same as the sign of:

$$\frac{\partial V_R(\delta)}{\partial \delta} V_D(\delta) - \frac{\partial V_D(\delta)}{\partial \delta} V_R(\delta). \quad (C.3)$$

From Assumption 2bis, we have that  $\nu_D - \frac{c_D}{p_D(\hat{\delta}_j)} > \nu_R - \frac{c_R}{p_R(\hat{\delta}_j)}$  and  $\nu_D + \frac{c_D}{p_D(\hat{\delta}_j)} > \nu_R + \frac{c_R}{p_R(\hat{\delta}_j)}$ ,  $\forall \hat{\delta}_j$ , and hence that  $V_D(\delta) > V_R(\delta) \forall \delta$ . From Assumption 3, we know that  $\frac{\partial V_K(\delta)}{\partial \delta} < 0 \forall K \in \{D, R\}$ .

We now show that (C.3) must be negative for any value of  $\delta \in (\nu_R, \nu_D)$ . First, note that from the symmetry of  $F$ , we have that  $V_k(\delta) = 0$  if  $\delta = \nu_k$ . Combined with  $\frac{\partial V_K(\delta)}{\partial \delta} < 0 \forall K \in \{D, R\}$ , this gives us that if  $\delta \in (\nu_R, \nu_D)$  then  $V_D(\delta) > 0$  and  $V_R(\delta) < 0$ . Then, we have that  $\frac{\partial V_R(\delta)}{\partial \delta} V_D(\delta) < 0$  and  $\frac{\partial V_D(\delta)}{\partial \delta} V_R(\delta) > 0$ , implying that (C.3) is strictly negative. ■

It then follows that the proofs of Propositions 1, 2, and 3 extend directly to the present setup.

## Group-based Voting

An alternative approach to endogenize  $\lambda_j^k$  is that it is not voters who spontaneously change their voting behavior depending on the composition of their district because they themselves perceive that they have higher or lower voting efficacy. Instead, it is the parties/candidates (or some group-specific leaders) that exert some costly effort to mobilize their supporters. Our approach is in the spirit of the follow-the-leader trend of the group-based voting literature (see, e.g., Morton 1987, 1991; Shachar and Nalebuff 1999; Levine and Mattozzi 2020; Bouton et al. 2024).

In each district, both running candidates can exert effort to mobilize individuals leaning their way: that is, candidate  $D$  mobilizes individuals leaning Democrat and candidate  $R$  mobilizes individuals leaning Republican. In particular, candidate  $D$  chooses  $\lambda_j^D \in (0, 1]$  and candidate  $R$  chooses  $\lambda_j^R \in (0, 1]$ . (More on the objective function of the candidates below.)

<sup>39</sup>Note that, in this case, the use of the symmetry of  $F$  around 0 is key to have that  $V_K(\hat{\delta}) = 0$  requires  $\hat{\delta} = \nu_K$ .

Voting costs are uniformly distributed between 0 and 1 within each group  $k$ . Among group  $k$  individuals, a share  $\tau_k$  are mobilizable in the sense that they turn out if their voting cost is below  $\lambda_j^K \in (0, 1]$ . The remaining individuals abstain. Hence, the share of individuals in group  $k$  who actually vote is  $\tau_k \lambda_j^K$ .

As in the baseline model, an individual in group  $k$  prefers  $D$  if and only if  $\nu_k - \eta_e - \delta \geq 0$ . The share of voters from group  $k$  that prefer  $D$  over  $R$  is therefore  $F(\nu_k - \delta)$ . We can then derive the number of votes for  $D$  in a given district for any given realization of the aggregate shock  $\delta$ . With  $n_{kj}$  voters of type  $k$  in district  $j$ , they cast a total of  $t_{kj} \lambda_j^K = n_{kj} \tau_k \lambda_j^K$  ballots for either party. It follows that the number of votes in favor of  $D$  in district  $j$  is the turnout-weighted average of  $D$ 's support across all groups present in the district:

$$\sum_K t_j^K \lambda_j^K F(\nu_k - \delta)$$

where  $t_j^K \equiv \sum_{k \in K | \nu_k = \nu_K} t_{kj}$ .

For any given pair of effort levels  $(\lambda_j^D, \lambda_j^R)$ , there is a unique realization of the aggregate shock,  $\hat{\delta}_j$ , such that the support for  $D$  and  $R$  in district  $j$  is identical. This critical value is defined implicitly by:

$$V_D(\hat{\delta}_j) \lambda_j^D t_j^D + V_R(\hat{\delta}_j) \lambda_j^R t_j^R = 0 \quad (\text{C.4})$$

where  $V_K(\delta_j)$  is defined as in the baseline model and is decreasing in  $\delta_j$ . Like in the other versions of the model,  $D$  wins for  $\delta < \hat{\delta}_j$ , i.e., with probability  $\pi_j = \Gamma(\hat{\delta}_j)$ .

It follows from (C.4) that a variation in  $\lambda_j^D$  modifies  $\hat{\delta}_j$  by:

$$\frac{d\hat{\delta}_j}{d\lambda_j^D} = \frac{V_D(\hat{\delta}_j)}{f_{Dj} \lambda_j^D t_j^D + f_{Rj} \lambda_j^R t_j^R} t_j^D, \quad (\text{C.5})$$

where we write  $f_{Kj}$  as a short form for  $f(\nu_K - \hat{\delta}_j)$  for  $K = D, R$ .

The objective function of candidate  $D$  in district  $j$  is to maximize their probability of winning the district, net of mobilization costs:

$$\max_{\lambda_j^D > 0} \pi_j(t_j^D, t_j^R, \lambda_j^D, \lambda_j^R) - c(t_j^D, \lambda_j^D),$$

with  $c(t_j^D, \lambda_j^D) = \kappa(t_j^D)^\alpha (\lambda_j^D)^\beta / \beta$ , with  $\alpha \in [0, 1]$  and  $\beta > 1$ . Like in Shachar and Nalebuff (1999), this specification allows for costs to also depend on the size of the target population (i.e., eligible voters). In our specification, for  $\alpha = 0$ , mobilization effort is a pure public good. For  $\alpha = 1$ , mobilization effort is a pure private good.

Assuming that  $\beta$  is large enough for the objective function to be quasi-concave, and hence to display a unique maximum, the optimal level of effort,  $\lambda_j^{D*}$ , solves the first order condition:

$$\gamma(\hat{\delta}_j) \times \frac{d\hat{\delta}_j}{d\lambda_j^D} = \kappa(t_j^D)^\alpha (\lambda_j^{D*})^{\beta-1}, \text{ or:}$$

$$\lambda_j^{D*} = \sqrt[\beta-1]{\frac{\gamma(\hat{\delta}_j) (t_j^D)^{1-\alpha}}{\kappa} \frac{V_D(\hat{\delta}_j)}{f_{Dj}\lambda_j^{D*}t_j^D + f_{Rj}\lambda_j^{R*}t_j^R}},$$

where the second line is obtained by using (C.5) to substitute for  $\frac{d\hat{\delta}_j}{d\lambda_j^D}$ .

By symmetry:

$$\lambda_j^{R*} = \sqrt[\beta-1]{-\frac{\gamma(\hat{\delta}_j) (t_j^R)^{1-\alpha}}{\kappa} \frac{V_R(\hat{\delta}_j)}{f_{Dj}\lambda_j^{D*}t_j^D + f_{Rj}\lambda_j^{R*}t_j^R}}.$$

Combining the FOCs on  $\lambda_j^{D*}$  and  $\lambda_j^{R*}$  yields:

$$\frac{\lambda_j^{D*} t_j^D}{\lambda_j^{R*} t_j^R} = \sqrt[\beta-1]{-\frac{(t_j^D)^{\beta-\alpha} V_D(\hat{\delta}_j)}{(t_j^R)^{\beta-\alpha} V_R(\hat{\delta}_j)}}.$$

Plugging this ratio into (C.4) we obtain:

$$V_D(\hat{\delta}_j) (t_j^D)^{\frac{\beta-\alpha}{\beta}} + V_R(\hat{\delta}_j) (t_j^R)^{\frac{\beta-\alpha}{\beta}} = 0. \quad (\text{C.6})$$

This highlights that, if  $\alpha > 0$ , then the strategic mobilization effort by each candidate generates an ‘underdog effect’: the candidate who has comparatively more support in the district faces higher mobilization cost. Hence, she exerts lower mobilization effort in equilibrium.<sup>40</sup> Indeed, for  $\alpha = 0$ ,  $\hat{\delta}_j$  is defined by the ratio  $\frac{t_j^D}{t_j^R} = -\frac{V_R(\hat{\delta}_j)}{V_D(\hat{\delta}_j)}$  as in the baseline model. It implies that the probability of winning is not affected by the endogenous turnout. If instead  $\alpha > 0$ , then  $\hat{\delta}_j$  is defined by the ratio  $\left(\frac{t_j^D}{t_j^R}\right)^{\frac{\beta-\alpha}{\beta}} = -\frac{V_R(\hat{\delta}_j)}{V_D(\hat{\delta}_j)}$  with  $\frac{\beta-\alpha}{\beta} \in (0, 1)$ . Hence, when  $\frac{t_j^D}{t_j^R} > 1$ ,  $\hat{\delta}_j$ , and hence  $\pi_j$ , become smaller than in the baseline model.

Differentiating equality (C.6) with respect to  $t_j^D$  yields:

$$\frac{d\hat{\delta}_j}{dt_j^D} = \frac{V_D(\hat{\delta}_j)}{f_{Dj} t_j^D + f_{Rj} t_j^R \left(\frac{t_j^D}{t_j^R}\right)^{\frac{\alpha}{\beta}}} \frac{\beta - \alpha}{\beta}. \quad (\text{C.7})$$

<sup>40</sup>Note that, by relaxing the assumption that  $\beta < \alpha$ , we could also obtain a ‘bandwagon effect’: the candidate with comparatively less support in the district has higher mobilization costs and hence exerts lower mobilization effort. Our results would also hold in that case.

Similarly:

$$\frac{d\hat{\delta}_j}{dt_j^R} = \frac{V_R(\hat{\delta}_j)^{\frac{\beta-\alpha}{\beta}}}{f_{Dj} t_j^D \left(\frac{t_j^D}{t_j^R}\right)^{\frac{-\alpha}{\beta}} + f_{Rj} t_j^R}. \quad (\text{C.8})$$

We prove the equivalent of Property 1 below, and it is easy to check that Property 2bis and its proof from the previous section hold.

**Property 1bis.** If  $F$  and  $\Gamma$  are strictly increasing, then:

- i. For all  $t^D > 0$ ,  $\frac{\partial \pi}{\partial t^D} > 0$  if  $t^R > 0$ , and  $\frac{\partial \pi}{\partial t^D} = 0$  if  $t^R = 0$ ,
- ii. For all  $t^R > 0$ ,  $\frac{\partial \pi}{\partial t^R} < 0$  if  $t^D > 0$ , and  $\frac{\partial \pi}{\partial t^R} = 0$  if  $t^D = 0$ .

**Proof.** From (C.6) and  $V_D(\delta) > V_R(\delta)$  for all  $\delta$ , we have that, if  $\frac{t_j^D}{t_j} < 1$ , then  $V_D(\hat{\delta}_j) > 0 > V_R(\hat{\delta}_j)$ . Together with C.7 and  $\frac{\beta-\alpha}{\beta} > 0$ , we obtain that

$$\frac{d\hat{\delta}_j}{dt_j^D} = \frac{V_D(\hat{\delta}_j)}{f_{Dj} t_j^D + f_{Rj} t_j^R \left(\frac{t_j^D}{t_j^R}\right)^{\frac{\alpha}{\beta}}} \frac{\beta - \alpha}{\beta} > 0.$$

For  $\frac{t_j^D}{t_j} = 1$ , (C.6) requires  $V_D(\hat{\delta}_j) = 0$ , and hence  $\frac{d\hat{\delta}_j}{dt_j^D} = 0$ . This proves point i.

The proof of point ii follows similar steps. ■

It follows that the proofs of Propositions 1, 2, and 3 extend directly to the present setup.

## D. Probabilistic Voting with Uniform Shocks

Following (Persson and Tabellini, 2000, chapter 3), consider two uniform shocks: first, the independently and identically distributed elector-level shock  $\eta_e$  follows a uniform distribution  $U[-\frac{1}{2\phi}, \frac{1}{2\phi}]$ . Second, the aggregate shock  $\delta$ , which captures the valence of party  $R$  over party  $D$  at the time of the election, follows another uniform distribution  $\Gamma = U[-\frac{1}{2\gamma}, \frac{1}{2\gamma}]$ .

With that specification, the share of voters from group  $k$  that cast their ballot for  $D$  is:

$$\sigma_k(\delta) = \frac{1}{2} + \phi(\nu_k - \delta).$$

Throughout, we assume that vote shares in each district are “interior”:<sup>41</sup>

<sup>41</sup>This assumption is but a sufficient condition that simplifies the algebra. It can be relaxed to allow for  $\sigma_k$  to equal 0 or 1. With two types, our results hold as long as  $\nu_D + \nu_R < \frac{1}{2\phi}$  and  $|\nu_k| < \frac{1}{2\gamma}$ .

**[A1U] Assumption Interior:** We assume that  $\sigma_k$  is strictly between 0 and 1 for any realization of  $\delta$  by imposing that  $|\nu_k| < \frac{1}{2\phi} - \frac{1}{2\gamma}$  for all  $k, p$ . Moreover, we assume  $|\nu_k| < \frac{1}{2\gamma}$ : depending on the realization of  $\delta$ ,  $\sigma_k$  can be strictly above or strictly below 1/2.

Under that assumption, the vote share of each party in district  $j$  given a realisation of the aggregate shock  $\delta$  is:

$$\sum_k t_j^k \sigma_k(\delta) = \frac{\sum_k t_j^k}{2} + \sum_k t_j^k \phi (\nu_k - \delta).$$

Like in the general model, this number of votes is increasing in  $\nu_k$  for all  $k$  and strictly decreasing in  $\delta$ . For the simplicity of exposition, we normalize  $\phi$  to 1 for most of the analysis.

Denoting *total turnout in district  $j$*  by  $t_j := \sum_k t_j^k$ , under Assumption A1, the probability that  $D$  wins district  $j$  is:

$$\pi_j = \Pr \left( \frac{t_j}{2} + \sum_k t_{kj} (\nu_k - \delta) \geq \frac{t_j}{2} \right) = \Pr \left( \delta \leq \hat{\delta}_j := \sum_k \frac{t_j^k \nu_k}{t_j} \right).$$

By the distribution of  $\delta$  and Assumption [A1U], this simplifies into:  $\pi_j = \frac{1}{2} + \gamma \hat{\delta}_j$ .

## E. Data Appendix

### E.1. Dataset

We compile precinct-level political and demographic data from various sources and use geospatial data to assign these characteristics to congressional districts under both Democratic and Republican proposals from the 2020 redistricting cycle.<sup>42</sup>

A central aspect of our analysis is the ability to compare how a precinct is treated under a Democratic versus a Republican proposal. As a result, we limit our focus to states where proposals from both political parties are available. Notably, detailed data for redistricting proposals, rather than just the final maps, became widely accessible only after the 2020 redistricting cycle. These maps were drawn by redistricting committees, party caucuses, independent organizations, or individual representatives (see Appendix E.2).

At the precinct level, we compile information on demographics, voter registration, and presidential election returns from 2016 and 2020. Precincts are geographic areas used to administer elections. They are the smallest possible geographic unit to observe election returns. The precinct-level data

<sup>42</sup>We focus on U.S. congressional districts rather than state legislative districts to minimize incumbency gerrymandering. Since most maps are drawn by state legislators, the incentives for incumbency gerrymandering are stronger at the state level. Additionally, most states have a small number of congressional districts, making our theoretical framework more manageable by considering a finite number of districts.

come from multiple sources. We use precinct-level population counts from the 2020 Census and information about age, race/ethnicity, sex, income, and education from the American Community Survey. Four states in our sample (MD, NJ, NV, and WA) use prison-adjusted populations when redistricting for congressional districts. In these states, the total population counts for precincts are adjusted by reassigning incarcerated individuals to their last known residence. These data were obtained from the state redistricting websites and by a public records request to the Washington Secretary of State.

The Redistricting Data Hub compiles voter registration data, election returns, and Citizen Voting Age Population (CVAP, the number of citizens aged 18 and older).<sup>43</sup>

## **E.2. Redistricting Proposals**

We collect redistricting proposals from the 2020 cycle for all states where both Democratic and Republican proposals are available. The sources vary by state, with most proposals coming from state legislature redistricting committees, which typically align with the majority party. Therefore, we assign committee maps to the majority party, while minority party proposals are sourced from party caucuses or individual representatives. When multiple proposals exist for the minority party, we prioritize caucus maps over individual submissions. In some states, independent or bipartisan redistricting commissions submitted maps endorsed by either party. For more details, see Table E.1. Geospatial data for each proposal were gathered from state legislature websites or requested directly. Two states were excluded from the analysis despite having two partisan proposals: Maine, due to missing voter registration data for many precincts, and West Virginia, due to missing geospatial data.

## **E.3. Geospatial Analysis**

We use geospatial data to merge precinct-level data in Python. The precinct boundaries vary slightly across the precinct-level data sources for election returns, party registration, and demographics. We aggregate all precinct-level data to the boundaries used by the 2020 Census. Where necessary, we use block-level population data to disaggregate precincts and voter registration data. Due to the discrepancies in precinct borders, we expect some measurement error in the final precinct-level dataset, especially when computing ratios like turnout rates in small precincts. We drop 4,633 precincts (8.3% of precincts) in which there is either a) a total population under 50, b) reportedly more votes than people, c) reportedly more registered voters than people, or d) reportedly more citizens of voting age than people. These tend to be small precincts, accounting for 2.3% of the total population in the sample.

<sup>43</sup>The Redistricting Data hub geocodes and validates precinct-level data. Their source for voter registration data is L2, their source for election returns is the Voting and Election Science Team (VEST), and their source for CVAP is the American Community Survey.



TABLE E.1. REDISTRICTING PROPOSALS

State	Party	Proposer	Proposal Name	Notes
AL	D	State Senator Rodger Smitherman	Singleton Congressional Plan 1	Senator Smitherman is the minority party leader.
AL	R	Alabama Legislature	US House Second Special Session 2021 Draft	This plan was passed by Republican dominated state legislature, but later invalidated by the Supreme Court.
AZ	D	Arizona Independent Redistricting Commission	CD Test Map Version 10.1.2	Proposed by Democratic members of the redistricting commission.
AZ	R	Arizona Independent Redistricting Commission	CD Test Map Version 10.1.1	Proposed by Republican members of the redistricting commission.
AK	D	State Senator Greg Leding	SB724	Amendment proposed by Democratic state senator.
AK	R	Arkansas General Assembly	Arkansas Final Congressional Plan	Plan passed by Republican majority legislature.
CT	D	Democrat Members of Connecticut Reapportionment Committee	Democrat Members' Proposed Map	Presented by members of the Democratic party to the state's Supreme Court.
CT	R	Republican Members of Connecticut Reapportionment Committee	Republican Members' Proposed Map	Presented by members of the Republican party to the state's Supreme Court.
FL	D	State Senator Darryl Rouson	S019C8062	Of the proposals from Democrats, this was submitted most recently.
FL	R	Governor Ron DeSantis	PP000C0109109	Governor DeSantis rejected the legislature's plan and proposed this one, which was later enacted and challenged in state court.
GA	D	House and Senate Democratic Caucuses	House Bill 5EX	Amenment proposed by democratic caucuses.
GA	R	Senate and House Committee Chairs	Senate Bill 2EX	Plan enacted state legislature and later invalidated by state supreme court.
KS	D	State Senator Dinah Sykes	United	Senator Sykes is the minority party leader.
KS	R	Kansas House Committee on Redistricting	Ad Astra 2	The Democratic governor vetoed this proposal and the legislature overrode the veto. The state supreme court ultimately rejected the map.
LA	D	State Senator Gary Smith	SB11	Of the proposals from Democrats, this plan was from the most senior member of the state legislature.
LA	R	State Representative Clay Schexnayder	House Bill 1	The Democratic governor vetoed this proposal and the legislature overrode the veto. An appeals court rejected the map, but the U.S. Supreme Court allowed it to be used in 2022 elections.
MD	D	Legislative Redistricting Advisory Commission	LRAC Final Recommended Congressional Plan	This map was enacted and upheld by the Maryland Court of Appeals.
MD	R	Maryland Citizens Redistricting Commission	CRC Final Recommended Congressional Map	The governor traditionally proposes a map. The Republican Governor delegated this job to a task force called the Maryland Citizens Redistricting Commission.
MN	D	Democratic Farmer-Labor (DFL) Caucus	House DFL plan/ Murphy plan	Plan proposed by the Democratic caucus in the state legislature.
MN	R	State Representative Paul Torkelson	C2102-0	Plan proposed on behalf of state Republican caucus.

TABLE E.1 CONTINUED. REDISTRICTING PROPOSALS

State	Party	Proposer	Proposal Name	Notes
MT	D	Democrats on Redistricting Commission	CP 13	Most recent plan proposed by Republican members of redistricting commission.
MT	R	Republicans on Redistricting Commission	Montana Congressional Adopted	Most recent plan proposed by Democratic members of redistricting commission.
NC	D	Senator Jay Chaudhuri	CST-6	Of the proposals submitted by Democrats, this proposal was later used in court cases challenging the Republican map.
NC	R	North Carolina General Assembly	Congressional Plan Senate Bill 740 / SL 2021-174	Plan enacted and later rejected by the state supreme court. The following year the state supreme court overturned their previous opinion.
NE	D	Democratic State Senator Justin Wayne	LB2	Although Nebraska has a nonpartisan legislature, this map was endorsed by the state Democratic party.
NE	R	Nebraska Legislature Redistricting Committee	LB1	Plan enacted by state legislature.
NH	D	State Representative Paul Bergeron	Amendment 2022 - 1736h	Plan proposed by Democrats after the democratic governor vetoed the original plan.
NH	R	State Representative Berry Ross	i-93 Corridor Plan	Plan proposed by Republicans after the democratic governor vetoed the original plan.
NJ	D	New Jersey Congressional Redistricting Commission	New Jersey Congressional Districts 2022-2031	Plan proposed by Democratic members of the Redistricting commission.
NJ	R	New Jersey Congressional Redistricting Commission	Republican Proposal	Plan proposed by Republican members of the Redistricting commission.
NM	D	New Mexico Legislature	New Mexico Final Congressional Plan	Plan enacted by state legislature.
NM	R	Citizen Redistricting Committee	Map A	Authored by a non-partisan redistricting committee, but endorsed by the Republican party.
NV	D	Democrats in the Nevada Legislature	Nevada Final Congressional Plan	Plan enacted by state legislature and later challenged in state court.
NV	R	Republicans in the Nevada Legislature	Congressional Minority Plan	Plan submitted by the Legislature Joint Minority Committee.
NY	D	Democrats in the New York Legislature	New York State Assembly Congressional Plan	The New York State Independent Redistricting Commission submitted two maps: one from Democrats and one from Republicans. The democratic legislature then proposed this map, which was enacted and later rejected by the state supreme court.
NY	R	Republican-appointed members of the New York Independent Redistricting Commission	Plan B	Plan proposed by Republicans appointed to the New York State Independent Redistricting Commission.
OH	D	Democratic members of Ohio Redistricting Commission	Proposed Sub SB 237 - Senate Dem Caucus	Plan proposed by Democratic member of redistricting commission.
OH	R	Republican members of Ohio Redistricting Commission	Senate Bill 258	Plan passed by state legislature and later invalidated by the state's Supreme Court.

TABLE E.1 CONTINUED. REDISTRICTING PROPOSALS

State	Party	Proposer	Proposal Name	Notes
OK	D	Oklahoma Senate Democrats	Oklahoma Congressional Draft - Democrat Proposal	Amendment proposed by state senators.
OK	R	Oklahoma State Legislature	Oklahoma Congressional District Maps 2022-2031	Plan passed by the Republican majority legislature.
OR	D	State Senator Peter Courtney	Oregon Congress Plan B	Plan was sponsored by Senator Peter Courtney, president of the state Senate.
OR	R	Republican members of Interim Committee On Redistricting	Oregon Congressional Plan SB 881A	Plan was sponsored by Republican members of the redistricting committee.
PA	D	Senate Democratic Caucus	Senate Democratic Caucus	Plan submitted by the Senate Democratic Caucus in the state supreme court case.
PA	R	General Assembly	Updated Preliminary Congressional Plan	Plan enacted by state legislature and later vetoed by the democratic governor.
SC	D	State Senator Brad Hutto	Floor Amendment 4 - Hutto / Greene Fix Map	Amendment proposed by the minority party leader.
SC	R	South Carolina legislature	South Carolina Congressional Districts House Plan 2 Amendment 1 (ACT 118)	Plan passed by Republican majority state legislature.
TX	D	State Representative Yvonne Davis	PLANC2165	Amendment proposed by Democrats. Of the three Democratic proposals found, this proposal was from the most senior-ranking representative.
TX	R	Republican members of state legislature	Texas Congressional Plan 2193	Plan proposed and passed by state legislature.
WI	D	Democratic legislators	SB622 - amendment 1	Plan proposed by state senators Bewley, Erpenbach, Ringhand, Roys and Wirsch. This map was originally written by the People's Commission, a bipartisan group organized by the Democratic governor.
WI	R	Republican legislators	SB622	Plan passed by Republican majority state legislature, but vetoed by Democratic governor.
WA	D	State Representative April Sims	Sims	Plan proposed by the House Democratic Caucus appointee to the redistricting committee.
WA	R	State Representative Paul Graves	Graves	Plan proposed by the House Republican Caucus appointee to the redistricting committee.

Finally, we assign precincts to congressional districts for each map. We compute the percent of a precinct's land area that falls inside a district. A precinct is assigned to a unique district if at least 98% of its land area is inside one district. Otherwise, a precinct may be assigned to multiple districts. Precincts are split relatively infrequently: 1.7% of precincts are split in the Democrat proposals and 2.2% of precincts are split in the Republican proposals.

Where precincts span multiple districts, we disaggregate precinct characteristics using the percentage of precinct population in each district. To measure the population in a part of a precinct, we use block-level population data from the Census. In the rare case that a block is split across a precinct,

we use the land area of the block to disaggregate its population. We drop split precincts from the regression analysis in Section 7.2, since we use precincts as the unit of analysis and make comparisons across Democrat and Republican proposals. We do, however, include split precincts in the analysis of counterfactual maps in Section 7.3. There, we allow parts of split precincts to be swapped along the border when we construct counterfactual maps.

For each precinct, we identify the district it is assigned to under both proposals, enabling us to compute district-level characteristics. Additionally, we identify precincts adjacent to district borders in the previous congressional map or in both partisan proposals. This subset of border precincts helps us isolate movable precincts and construct and evaluate counterfactual maps. Using Census adjacency files, we then identify precincts adjacent to these border precincts, continuing the process iteratively. The final precinct-level dataset includes 96,307 precincts across the 25 states (summary statistics are reported in Section E.5).

#### **E.4. Measures of Turnout Rate**

A challenge in measuring turnout rates is that we do not know exactly which information gerrymanderers use in practice to anticipate vote shares. At a minimum, redistricting committees must use information about total population and race. They might also incorporate election data with varying degrees of sophistication. Another concern is that observed turnout might be endogenous to redistricting. We use three measures of turnout rates to address both potential measurement errors and endogeneity concerns.

First, we use data from elections prior to redistricting to measure turnout. We compute the turnout rate of a precinct as the average of the total number of votes in the 2016 and 2020 presidential elections, divided by the population of the precinct in 2020.<sup>44</sup> Note that these elections happened before the 2020 redistricting proposals, but might still be endogenous to redistricting proposals if districts in the 2020 cycle are similar to districts in the 2010 cycle.

In a second approach, we predict the measure of turnout just described using only demographic and socioeconomic characteristics, which are difficult for political parties to manipulate: population, race and ethnicity, citizenship, age, education, and income.

Just in case one worries that our prediction model is overly sophisticated compared to the information at hand for partisan gerrymanderers, in a third approach we use Citizen Voting Age Population (CVAP) as an exogenous proxy for the turnout rate. However, the coefficient of correlation between

---

<sup>44</sup>We take the average of the two presidential elections to limit noise. We use presidential elections instead of congressional elections or state-level elections because we do not need to impute values for uncontested elections and because within-state contest effects, which could depend on redistricting, only indirectly affect presidential elections.

TABLE E.2. CANDIDATE VARIABLES FOR TURNOUT PREDICTION MODELS

<i>Population, Race, and Ethnicity</i>	<i>Age, Education, and Income</i>
Total Population	Population aged 0 to 17
Voting Age Population (aged 18+)	Population aged 18 to 24
Total Hispanic or Latino	Population aged 25 to 34
Total White, non-Hispanic	Population aged 35 to 44
Total Black, non-Hispanic	Population aged 45 to 54
Total AI/AN, non-Hispanic	Population aged 55 to 64
Total Asian, non-Hispanic	Population aged 65 and up
Total NHOPI, non-Hispanic	Percent aged 0 to 17
Total Other Race, non-Hispanic	Percent aged 18 to 24
Percent Hispanic or Latino	Percent aged 25 to 34
Percent White, non-Hispanic	Percent aged 35 to 44
Percent Black, non-Hispanic	Percent aged 45 to 54
Percent AI/AN, non-Hispanic	Percent aged 55 to 64
Percent Asian, non-Hispanic	Percent aged 65 and up
Percent NHOPI, non-Hispanic	Population with no high school degree
Percent Other Race, non-Hispanic	Population with high school degree
	Population with some college
<i>Citizen Voting Age Population (CVAP)</i>	Population with Bachelor's degree
CVAP, Total	Population with graduate degree
CVAP, American Indian or Alaska Native	Percent with no high school degree
CVAP, Asian	Percent with high school degree
CVAP, Black or African American	Percent with some college
CVAP, Native Hawaiian, Pacific Islander	Percent with Bachelor's degree
CVAP, White	Percent with graduate degree
CVAP, Hispanic or Latino	Median household income
	Labor force population
	Percent of adults in labor force

percent CVAP and turnout rate is low (0.41) compared to the coefficient of correlation between predicted turnout and observed turnout (0.89). The downside of using percent CVAP as a proxy is that it assumes that gerrymanderers are naive enough to ignore correlations between turnout rates and other factors like race, income, and education.

#### *E.4.1 Predicted Turnout*

To predict turnout at the precinct level, we measure precinct-level demographic and socioeconomic factors using data from the American Community Survey and Census. The candidate variables are in Table E.2. Population, race, and ethnicity variables are from the 2020 Census: P.L. 94-171 Redistricting Data Summary File (downloaded at the Census Voting Tabulation District level from

NHGIS).<sup>45</sup> The Citizen Voting Age Population variables are from the Redistricting Data Hub.<sup>46</sup> The Redistricting Data Hub uses the 2019 special CVAP tabulation files from the American Community Survey (ACS) 5-Year Estimates (2016-2020). They disaggregate Census Block group-level estimates to the Census Block level. We then aggregate the block-level data to the precinct level, as in section E.1. Age, education, and income variables are from the 2020 American Community Survey: 5-Year Data (2016-2020). We download these data at the Census Tract level from NHGIS. To aggregate to the precinct level, we first disaggregate to the block level (using the percent of tract population in a block), then aggregate to the precinct level.

TABLE E.3. TURNOUT PREDICTION: MODEL PERFORMANCE

Model	MSE	Correlation
Lasso, state-specific model	0.0083	0.7423
Lasso, pooled model	0.0115	0.6054
Random Forest	0.0052	0.8449
Gradient Boosting	0.0048	0.8573

We compare the performance of three different models, namely Lasso, Random Forest, and Gradient Boosting. The dataset was divided into training and test data. The training data, comprising 75% of the precincts, was used to train each model, and the remaining 25% was used to evaluate accuracy.

The state was included as a categorical variable in all models. We additionally train a LASSO model separately for each state.<sup>47</sup> Table E.3 reports the MSE and the correlations between turnout and predicted turnout for the test data. We use predictions from the Gradient Boosting model in our main analysis since it has the lowest MSE. Figure E.1 plots the distribution of turnout and predicted turnout across all precincts. If we regress turnout on predicted turnout in the full sample, the  $R^2$  is 0.79, with Root MSE of 0.06. The coefficient of correlation between predicted turnout and turnout is 0.89 ( $p < 0.001$ ). The most important predictors are reported in Table E.4, ranked by feature importance. Higher numbers indicate that the candidate variable has a larger effect on the model's performance.<sup>48</sup>

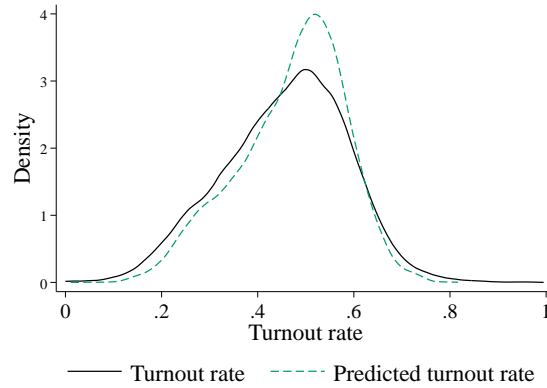


FIGURE E.1. DISTRIBUTION OF TURNOUT RATE AND PREDICTED TURNOUT RATE.

TABLE E.4. TOP PREDICTORS, RANKED BY FEATURE IMPORTANCE

Variable	Feature Importance
Percent White, non-Hispanic	0.2721
Total population	0.2281
State categorical variable	0.1598
Citizen Voting Age Population	0.0817
Voting Age Population	0.0515
Percent with no high school degree	0.0417
Total Hispanic population	0.0416
Percent below poverty rate	0.0288
Percent age 65 and up	0.0263
Percent with college degree	0.0216

#### E.4.2 District Competitiveness and Turnout Rates

In this section, we study associations between district competitiveness and turnout. The aim is to determine if endogenous turnout responses might be large in magnitude and whether there are asymmetric responses between Democratic- and Republican-leaning precincts.

We use a differences-in-differences approach, comparing changes in turnout amongst similar precincts that experienced changes in competitiveness during the 2020 redistricting cycle. For the states in

<sup>45</sup>Steven Manson, Jonathan Schroeder, David Van Riper, Tracy Kugler, and Steven Ruggles. IPUMS National Historical Geographic Information System: Version 17.0 [dataset]. Minneapolis, MN: IPUMS. 2022. <http://doi.org/10.18128/D050.V17.0>.

<sup>46</sup>Available at: <https://redistrictingdatahub.org/>.

<sup>47</sup>We used the `LassoCV` function from `scikit-learn`, which automatically selects the alpha value that minimizes the Mean-squared error (MSE) by cross-validation. The maximum number of iterations was set to 100. For Gradient Boosting we use their `HistGradientBoostingRegressor` algorithm.

<sup>48</sup>Feature importance measures the decrease in model performance when the values of a variable are randomly reassigned. For each candidate variable, we randomly reassign values within the dataset, then train the model and measure MSE for the test data. We repeat this process 10 times for each variable. The feature importance score is the average difference in MSE caused by the permutation of the values of a given variable.

TABLE E.5. DISTRICT COMPETITIVENESS AND TURNOUT

A. Closeness measured using Cook's PVI (2016 and 2020 presidential votes)			
	(1)	(2)	(3)
Competitiveness (PVI)	0.0023*** (0.0006)	0.0001 (0.0002)	-0.0002 (0.0003)
N	187923	187923	187923
$R^2$	0.251	0.763	0.936
Outcome variable mean	0.408	0.408	0.408
Year FEs	X	X	X
State FEs	X		
Precinct FEs			X
Group-district FEs		X	
B. Closeness measured using registered voters			
	(1)	(2)	(3)
Competitiveness (voter reg.)	0.0024*** (0.0004)	-0.0002 (0.0002)	0.0000 (0.0002)
N	187923	187923	187923
$R^2$	0.266	0.936	0.763
Outcome variable mean	0.408	0.408	0.408
Year FEs	X	X	X
State FEs	X		
Precinct FEs		X	
Group-district FEs			X

*Note:* Standard errors clustered at the level of pre-redistricting congressional districts. Additional controls are the log of total population, log of citizen voting age population, percent Black, non-Hispanic, percent Hispanic, percent Asian, percent American Indian/Alaska Native, percent below the poverty line, median household income, percent with a bachelor's degree or higher, percent ages 18-24, percent ages 65 and older, and percent registered democrats. Group-district fixed effects (FEs) indicate groups of similar turnout rates and ideology within the same pre-redistricting congressional district. We use state-specific quartiles of predicted turnout and of share of registered democrats to define groups. \*  $p < 0.1$ , \*\*  $p < 0.05$ , \*\*\*  $p < 0.01$ .

our main dataset, we construct a precinct-level panel. In the pre-redistricting period, we measure turnout as the average of the 2016 and 2020 presidential elections. In the post-redistricting period, we observe turnout in the 2022 midterm elections.<sup>49</sup> Following Moskowitz and Schneer (2019), we measure competitiveness using the Cook Partisan Voting Index (PVI). PVI measures how partisan a district is, relative to the nation, using average vote shares from the 2016 and 2020 presidential elections. If the nationwide Democratic vote share is 50% then a district with 55% Democratic votes is  $-5$  and a district with 55% Republican votes is  $+5$ . Competitiveness is measured as  $-abs(PVI_d)$ . A 10-unit increase in competitiveness is equivalent to, for example, a district moving from a 60-40 split to a 50-50 split in two-party vote shares. Since PVI uses turnout to measure competitiveness, we complement this measure with a measure of competitiveness that uses party registration

<sup>49</sup>Precinct-level election data for 2022 is available only for senate and gubernatorial elections, not house elections.



data from 2010:  $-\lvert\text{two-party share of registered voters that are Democrats} - 50\%\rvert$ . Note that we observe voter registration data and PVI in the pre-redistricting period only. Since the same voter registration and PVI data are used to measure competitiveness in both the pre- and post-redistricting periods, any variation in competitiveness comes from redistricting alone.

We estimate the effect of congressional district competitiveness on turnout with the following specification:

$$turnout_{pt} = \beta competitiveness_{pt} + \theta_p + \epsilon_{pt}, \quad (\text{E.1})$$

where  $turnout_{pt}$  is the number of votes per population in precinct  $p$  at time  $t$ ,  $competitiveness_{pt}$  is one of the two measures listed above, and  $\theta_p$  are precinct-fixed effects. The coefficient  $\beta$  captures the effect of competitiveness on turnout if, conditional on time-invariant precinct characteristics, changes in competitiveness are uncorrelated with other factors that might affect turnout. This identification strategy is similar to the differences-in-differences approach of Moskowitz and Schneer (2019), but instead of an individual-level panel, we use a precinct-level panel. A concern with this approach arises if the change in competitiveness is non-random due to strategic redistricting. In an additional specification, we compare changes in turnout amongst precincts that were assigned to the same initial congressional district and that have similar ideology and predicted turnout rate (i.e., group-district FEs). According to the model, precincts that belong to the same group should be treated similarly by gerrymanderers. Any difference in changes in competitiveness amongst these similar precincts is perhaps due to a geographic or legal constraint, which is unlikely to be related to precinct-level turnout within the group-district. The group-district fixed effects specification is akin to the ‘block fixed effects’ approach in Moskowitz and Schneer (2019).

Estimates are reported in Table E.5. There is a small positive and statistically significant association between competitiveness and turnout when including only state and year fixed effects (Panel A, Column 1). The point estimate suggests that a 10-point increase in competitiveness would increase turnout by 2.3 percentage points ( $\beta = 0.0023$ ,  $SE = 0.0006$ ; a standard deviation in PVI competitiveness is 9.4). However, this drops to a 0.1 percentage point increase in turnout per 10-point increase in competitiveness when including county fixed effects, and the point estimate is not statistically significant (Column 2,  $\beta = 0.0001$ ,  $SE = 0.0002$ ). The estimated coefficient is slightly negative and statistically insignificant when including group-district fixed effects (Column 3,  $\beta = -0.0002$ ,  $SE = 0.0003$ ). The 95% confidence interval implies that a 10-point increase in competitiveness would increase turnout by no more than 0.5 percentage points. We see the same results using voter registration to measure competitiveness (Panel B). These findings are very similar to those from Moskowitz and Schneer (2019). Using a nationwide panel of voters, they estimate a 0.1 p.p. increase in turnout per 10-point increase in competitiveness.

TABLE E.6. HETEROGENEOUS AND UNDERDOG COMPETITIVENESS EFFECTS

A. Closeness measured using Cook's PVI (2016 and 2020 presidential votes)				
	(1)	(2)	(3)	(4)
Competitiveness (PVI)	0.0003 (0.0003)	0.0006** (0.0003)	-0.0001 (0.0003)	0.0001 (0.0002)
Competitiveness (PVI) $\times$ D-leaning	-0.0008** (0.0004)	-0.0008*** (0.0003)		
D-leaning		0.0067 (0.0142)		
Underdog (PVI)			-0.0054 (0.0045)	-0.0058 (0.0037)
N	187929	187929	187929	187929
$R^2$	0.936	0.763	0.936	0.763
Outcome variable mean	0.408	0.408	0.408	0.408
Year FEs	X	X	X	X
Precinct FEs	X		X	
Group-District FEs		X		X
B. Closeness measured using registered voters				
	(1)	(2)	(3)	(4)
Competitiveness (voter reg.)	0.0002 (0.0003)	0.0004 (0.0003)	-0.0002 (0.0002)	0.0000 (0.0002)
Competitiveness (voter reg.) $\times$ D-leaning	-0.0007** (0.0003)	-0.0006** (0.0003)		
D-leaning		0.0087 (0.0137)		
Underdog (voter reg.)			0.0011 (0.0027)	0.0006 (0.0026)
N	187929	187929	187929	187929
$R^2$	0.936	0.763	0.936	0.763
Outcome variable mean	0.408	0.408	0.408	0.408
Year FEs	X	X	X	X
Precinct FEs	X		X	
Group-District FEs		X		X

*Note:* Standard errors clustered at the level of pre-redistricting congressional districts. Additional controls are the log of total population, log of CVAP, percent Black, non-Hispanic, percent Hispanic, percent Asian, percent American Indian/Alaska Native, percent below the poverty line, median household income, percent with a bachelor's degree or higher, percent ages 18-24, percent ages 65 and older, and percent registered Democrats. Group-district fixed effects indicate groups of similar turnout rates and ideology within the same pre-redistricting congressional district. We use state-specific quartiles of predicted turnout and of share of registered democrats to define groups. \*  $p < 0.1$ , \*\*  $p < 0.05$ , \*\*\*  $p < 0.01$ .

In Table E.6, we test if a change in competitiveness affects Democratic- versus Republican-leaning precincts differently and if there are underdog effects. In Columns 1 and 2, there is a statistically significant interaction between competitiveness and an indicator for whether a district is Democratic-leaning. The point estimates in Column 2 suggest that a 10 point increase in competitiveness

decreases turnout among Republican-leaning precincts by 0.6 p.p., but decreases turnout among Democrat-leaning precincts by 0.2 p.p.. To put these estimates in context, imagine that a gerrymanderer creates a highly competitive district that they expect to win with 51% of the votes. Suppose also that all voters experienced a 10 p.p. increase in competitiveness in the district. The estimates from Column 2 suggest that, after voters respond to the change in competitiveness, Democrats would expect to win with 50.9% of the votes.

In Columns 5 and 6, we test for underdog effects. The indicator *underdog<sub>pt</sub>* equals one if the precinct is not aligned with the district (e.g., the precinct is Democrat-leaning and the district is Republican-leaning). There are no statistically significant underdog effects, using either fixed effects specification or measure of competitiveness. The 95% confidence intervals from Columns 5-6 imply that if a precinct becomes an underdog (i.e., switches from a district in which it is aligned to one where it is not aligned), then turnout increases by no more than 0.2 to 0.6 percentage points. Turnout might decrease if a precinct becomes misaligned due to bandwagon effects. We can rule out any decrease in turnout greater than 1.3 p.p. in magnitude.

Overall, we estimate fairly precise null effects of competitiveness on turnout and of partisan alignment on turnout (underdog and bandwagon effects). We find evidence of heterogeneous effects of competitiveness for D- and R-leaning precincts. While small in magnitude, heterogeneous effects might nonetheless affect the optimal map. And, effects of competitiveness on turnout might differ across U.S. states and in other contexts. For both of these reasons, we study two models with endogenous turnout in Appendix C.

TABLE E.7. SUMMARY STATISTICS FOR PRECINCTS (N=96,307)

	Mean	SD	p1	p25	p50	p75	p99
<i>Population</i>							
Total population	1,977	1,973	87	837	1,390	2,363	9,630
<i>Voting Eligibility and Turnout</i>							
Percent voting age population	0.78	0.06	0.64	0.75	0.78	0.82	0.95
Percent citizen voting age population	0.71	0.13	0.36	0.63	0.72	0.81	0.98
Percent registered voters	0.64	0.14	0.22	0.56	0.66	0.74	0.94
Turnout rate	0.46	0.13	0.14	0.37	0.47	0.55	0.73

Note: Mean, Standard Deviation (SD) and percentiles (p) for precincts in all 25 in-sample states.

## E.5. Summary Statistics

Table E.7 reports summary statistics for all precincts. Figure E.2 shows the distribution of turnout rates for precincts with above- and below-median share of Registered Democrats for each state.

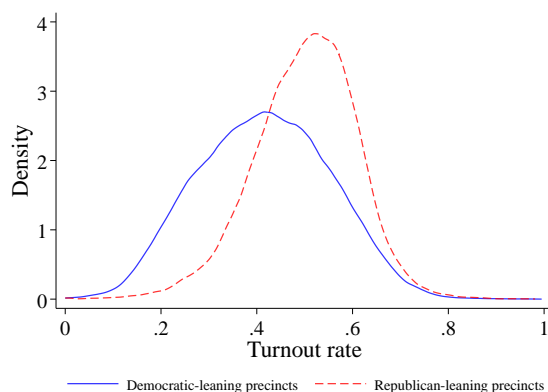


FIGURE E.2. TURNOUT RATE ACROSS PRECINCTS. This figure shows the distribution of turnout rates across precincts with above- and below-median share of registered Democrats for the state.

## F. Additional Empirical Evidence

### F.1. Partisan Redistricting Proposals

Figure F.1 shows the number of expected Democrat seats under each proposal. In 16 of the 25 states, Democrats expect to win strictly more seats under the Democrat proposal than the Republican proposal. In total, if all Democrat proposals were implemented there would be 30 more seats for Democrats than if all Republican proposals were implemented, a 12% swing in seats (there are 259 seats across the 25 states). Notably, if we were to use registered Democrats and Republicans to evaluate these maps, ignoring turnout data, then there would only be a 21-seat difference between Democrat and Republican proposals, an 8% swing in seats.

### F.2. Precinct-level Ideology and Partisan Lean

This section evaluates the robustness of results in Section 7.2 to alternative definitions of partisan lean. Recall that, within precincts of a given partisan-lean that are adjacent to previous congressional district borders, we find a negative correlation between a precinct turnout rate and the change in Democratic vote share of a district under the Democrat vs Republican proposal. In Table 1, we assume that there are four levels of partisan lean. Figure F.2 shows the distribution of the share of registered Democrats and the Democratic vote share across all precincts. The distributions are bi-modal and the median value is 0.52 and 0.48, respectively. Figure F.3 shows the distribution of the share of registered Democrats and Democratic vote shares by state. Using these two measures as proxies for the ideology of a precinct, we can divide each state into any number of equal-sized groups, using quantiles of ideology.

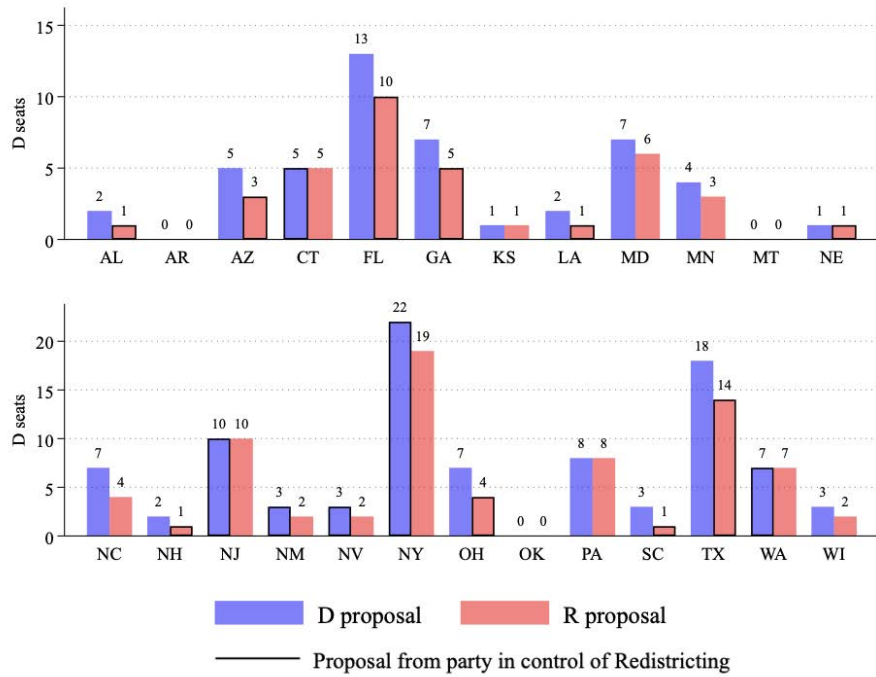


FIGURE F.1. EXPECTED DEMOCRAT SEATS UNDER BOTH PROPOSALS. This figure shows the expected number of seats won by Democrats under the Democratic and Republican proposals for U.S. Congressional districts. A seat is expected to be won by Democrats if the Democrat vote share is larger than the Republican vote share. Vote shares are measured using the average of the two presidential elections prior to the redistricting cycle (2016 and 2020). The party in control of redistricting is outlined in black. A party is in control of redistricting if both the majority party in the legislature and the party of the governor are aligned. Six states have split control: KS, MD, MN, NC, PA, and WI. Republicans have control in the states with zero expected Democratic seats (AR, MT, OK).

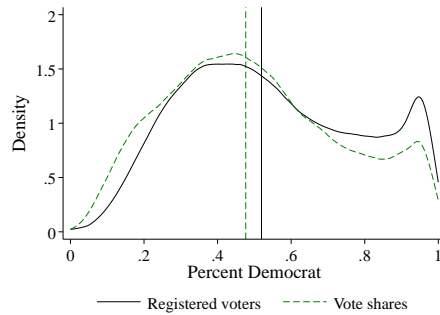


FIGURE F.2. DISTRIBUTION OF PERCENT REGISTERED DEMOCRATS AND DEMOCRATIC VOTE SHARE WITHIN PRECINCTS. Percent Democrat is either the two-party share of registered voters that are Democrats (black solid line) or the two-party vote share for Democrats (green dashed line). The vertical lines indicate the median values of 0.49 for Percent Registered Democrats and 0.45 for Democratic Vote Share.

We show OLS regression coefficients for the estimating Equation 9 using alternative definitions of partisan fixed effects, using either party registration (Figure F.4) or Democratic vote shares (Figure

F.5) to proxy for ideology. In each regression, we first choose the number of partisan-lean groups, ranging from two to ten. We divide each state into equal-sized partisan-lean groups using quantiles of the proxies for ideology (registered voters and vote shares). Then, we include a state fixed effect for each level of partisan-lean. We additionally include border fixed effects, as in the main specification reported in Table 1. The negative correlations in Table 1 are robust to these alternative fixed effects. Coefficients are also stable across specifications. We find no statistically significant differences between the coefficients from Table 1 (with 4 partisan-lean groups) and the corresponding coefficients in Figures F.4 and F.5 ( $p$ -values for  $t$ -tests are  $> 0.10$  for each pairwise comparison of estimated coefficients).

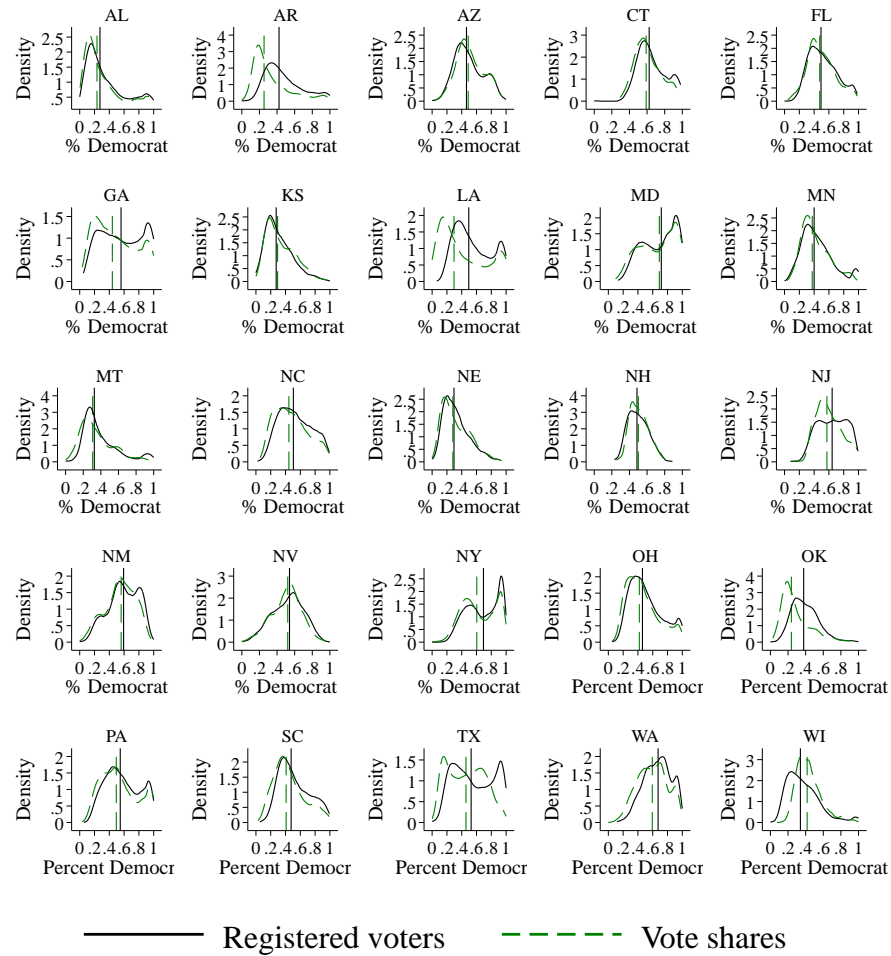


FIGURE F.3. DISTRIBUTION OF PERCENT REGISTERED DEMOCRATS AND DEMOCRATIC VOTE SHARE WITHIN PRECINCTS, BY STATE. Percent Democrat is either the two-party share of registered voters that are Democrats (black solid line) or the two-party vote share for Democrats (green dashed line). The vertical lines indicate the median values in each state.

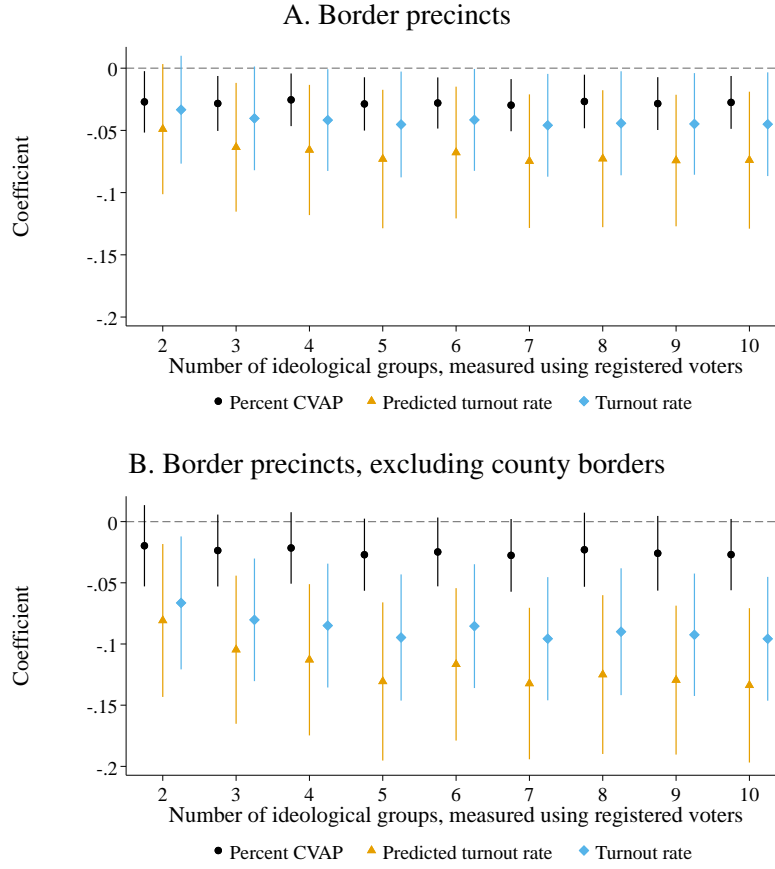


FIGURE F.4. CORRELATION BETWEEN TURNOUT AND CHANGE IN DEMOCRATIC VOTE SHARE BY THE NUMBER OF IDEOLOGICAL TYPES. This figure plots the regression coefficients from estimating Equation (9), using different numbers of ideological groups and hence partisan-lean fixed-effects. For each coefficient, we divide the sample of precincts into the number of ideological groups indicated on the x-axis, using quantiles of registered Democrats. The independent variable is one of three measures of turnout: percent Citizen Voting Age Population (CVAP), predicted turnout rate, or turnout rate. Each symbol is a point estimate from a separate regression. Vertical lines indicate 95% confidence intervals. Standard errors allow for arbitrary correlations between precincts within 50 kilometers.

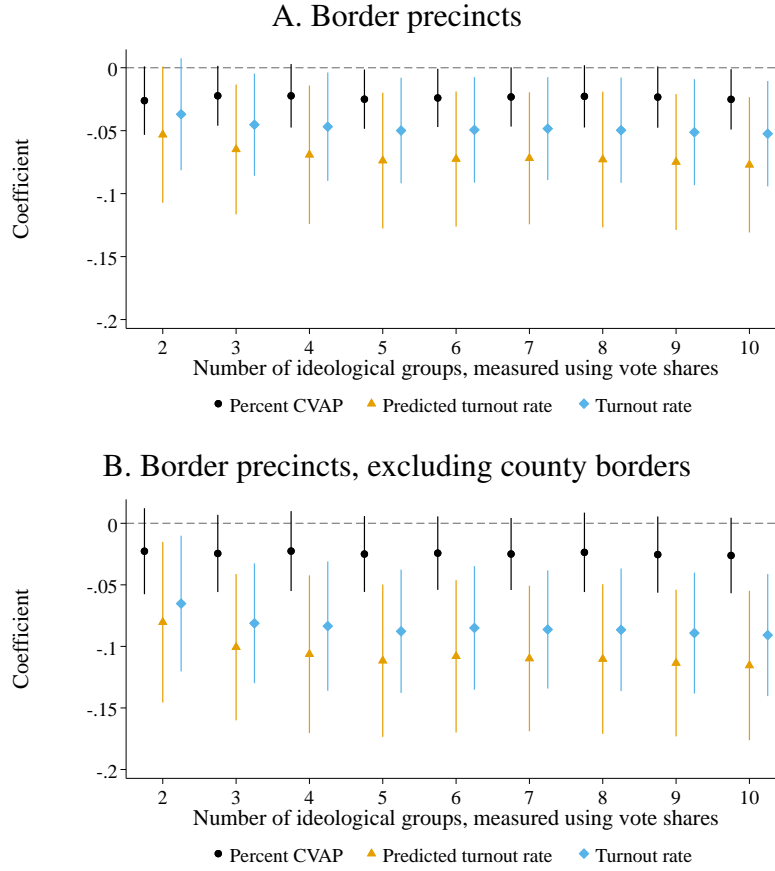


FIGURE F.5. CORRELATION BETWEEN TURNOUT AND CHANGE IN DEMOCRATIC VOTE SHARE BY NUMBER OF IDEOLOGICAL TYPES. This figure plots the regression coefficients from estimating Equation (9), using different numbers of ideological groups and therefore different partisan-lean fixed effects. For each coefficient, we divide the sample of precincts into the number of ideological groups indicated on the x-axis, using quantiles of Democratic vote shares in previous presidential elections. The independent variable is one of three measures of turnout: percent Citizen Voting Age Population (CVAP), predicted turnout rate, or turnout rate. Each symbol is a point estimate from a separate regression and vertical lines indicate 95% confidence intervals. Standard errors allow for arbitrary correlations between precincts within 50 kilometers.



### F.3. Definition of Movable Precincts

In Section 7.2, we restrict attention to a subset of precincts that are most likely to be movable. As described in Section 7.1, the empirical prediction may fail if we make inferences from precincts that the gerrymanderer had no control over. In Figure F.6, we show the distribution of the difference in the Democratic vote share under the Democratic proposal versus the Republican proposal (the outcome variable for the regressions in Table 1) for the full sample, the sample of precincts adjacent to a previous congressional district border, and the sample precincts adjacent to CD borders that are not county borders. The standard deviation increases in the border sample, relative to the whole sample, and especially after excluding county borders. This lends evidence to our hypothesis that precincts adjacent to previous district borders are more likely to be movable than others.

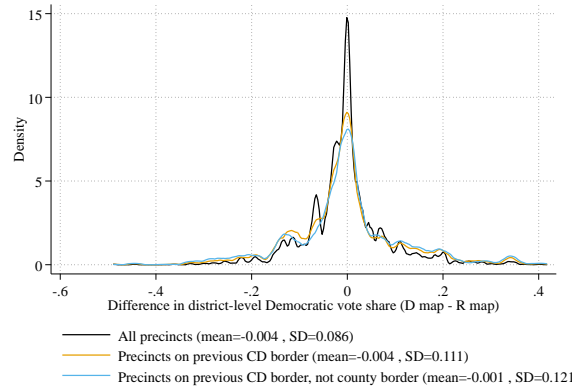


FIGURE F.6. DISTRIBUTION OF CHANGE IN DEMOCRATIC VOTE SHARE UNDER  $D$  VS  $R$  MAP. Democratic vote share is the two-party vote share from 2016 and 2020 presidential elections, aggregated to the level of the proposed district. We then take the difference between the  $D$  map and the  $R$  map.

To test sensitivity to this definition of movable, we estimate equation 9 for different sub-samples using an increasingly lenient definition of being movable. First we include precincts adjacent to border precincts (1 precinct from a border), then precincts that are 2 and 3 precincts from a border. Finally we report estimates for the full sample. The estimated coefficients are in Figure F.7. The negative correlation becomes smaller in magnitude as the definition of a movable precinct becomes more lenient. However, the negative correlation is robust to include precincts adjacent to border precincts, and the precincts adjacent to those, when using predicted and previous turnout measures. In contrast, the estimated coefficients for CVAP are stable across sub-samples and statistically insignificant. This might be because CVAP is a relatively noisy measure of expected turnout. The estimated correlation is statistically insignificant for all measures of turnout when using the full

sample of precincts. As explained in Section 7.1, estimates from the full sample might be biased because precincts that are not movable due to geographic and legal constraints are subject to spillover effects from precincts that are movable.

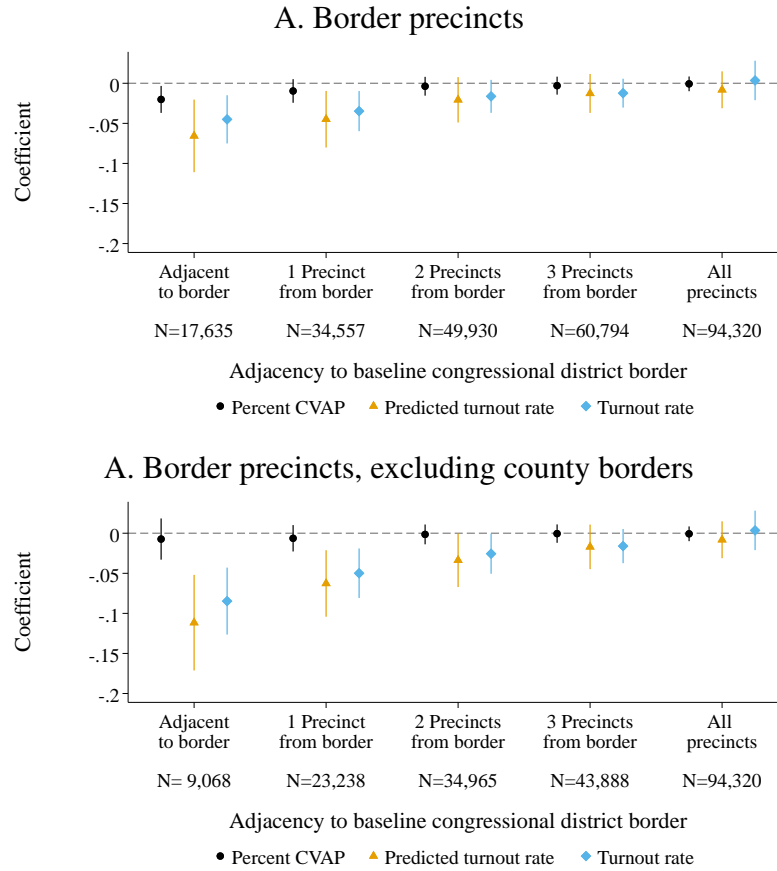


FIGURE F.7. CORRELATION BETWEEN TURNOUT AND CHANGE IN DEMOCRATIC VOTE SHARE BY SUB-SAMPLE OF MOVABLE PRECINCTS. This figure plots the regression coefficients from estimating Equation (9) using different definitions of movable precincts. Each symbol represents a point estimate from a separate regression, and the vertical lines indicate 95% confidence intervals. Standard errors are clustered within precincts, allowing for arbitrary correlations between precincts located within 50 kilometers.

#### F.4. Sensitivity to Selection of States

To test if the results are sensitive to the selection of states, we repeat the regressions in Table 1, leaving out one state at a time. Figure F.8 shows coefficients for estimates from each of the 25 samples. For the partisan-lean fixed effects, we use four quartiles defined by share of registered Democrats, as in Table 1.

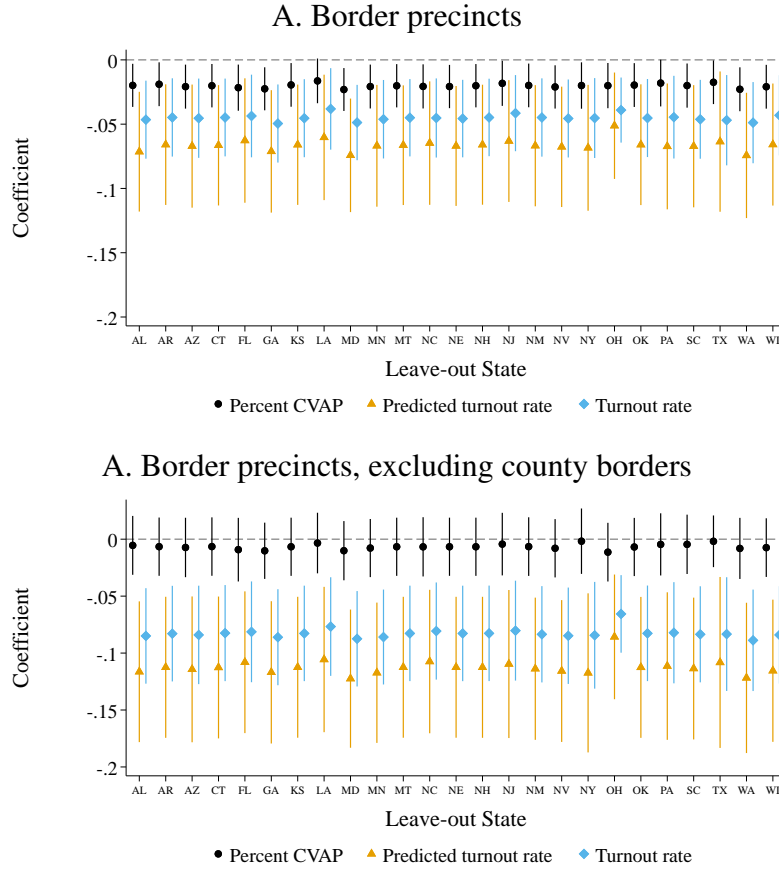


FIGURE F.8. CORRELATION BETWEEN TURNOUT AND CHANGE IN DEMOCRATIC VOTE SHARE BY SUB-SAMPLE OF MOVABLE PRECINCTS. This figure plots the regression coefficients from estimating Equation (9), using different samples of states. For each coefficient, we leave out the state indicated on the x-axis. Each symbol is a point estimate from a separate regression and vertical lines indicate 95% confidence intervals. Standard errors allow for arbitrary correlations between precincts within 50 kilometers.

### F.5. Calibrating the Standard Deviation of the Aggregate Shock

We use the standard deviation of two-party Democratic vote share from recent presidential elections (2008-2020) to calibrate  $\sigma_s$ , the standard deviation of the aggregate shock in a state. The average value of  $\sigma_s$  in the sample of precincts is 0.021.

TABLE F.1. STANDARD DEVIATION OF STATEWIDE PRESIDENTIAL DEMOCRAT VOTE SHARES, 2008-2020

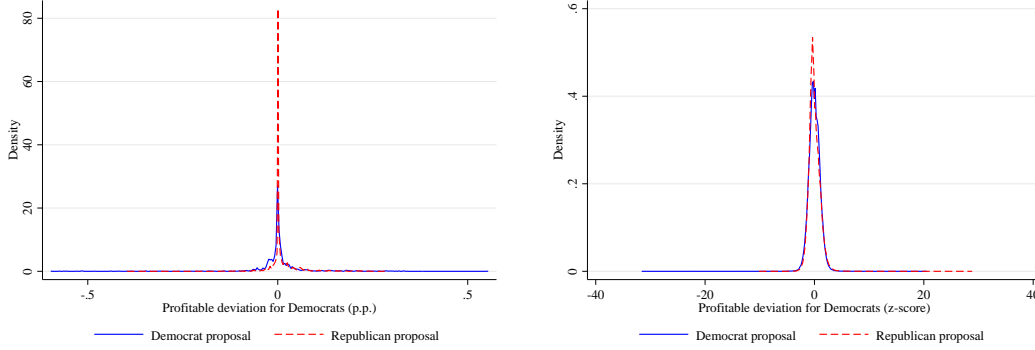
State	$\sigma_s$	State	$\sigma_s$	State	$\sigma_s$	State	$\sigma_s$
Alabama	0.016	Louisiana	0.006	New Jersey	0.007	South Carolina	0.012
Arkansas	0.02	Maryland	0.019	New Mexico	0.013	Texas	0.022
Arizona	0.08	Minnesota	0.019	Nevada	0.024	Washington	0.009
Connecticut	0.018	Montana	0.042	New York	0.021	Wisconsin	0.034
Florida	0.013	North Carolina	0.009	Ohio	0.035		
Georgia	0.017	Nebraska	0.025	Oklahoma	0.015		
Kansas	0.021	New Hampshire	0.02	Pennsylvania	0.025		

### F.6. Swapping Precincts at the Border: Robustness Checks

Most swaps have a negligible effect on the gerrymanderer's payoff function. In Figure 3, we plot the kernel density of the change in payoff for all swaps for Democrat and Republican proposals, for both the full sample of borders (Panel A) and for the subset of borders that do not overlap with county borders (Panel B). To compare the effects of swaps across boundaries and states, we also plot the distribution of the standardized effect of a swap (z-score), which is normalized by the border-specific mean and standard deviation. From these plots, it is easier to see that the most profitable swaps persist in the opponent's proposal, rather than a party's own proposal.

Next, we show that the patterns in Figure 3 are robust to alternative values of  $\sigma$ , the standard deviation of the zero-mean normal distribution for the aggregate shock. We plot the share of profitable deviations by  $\sigma$  in Figure F.10. In Panel A, we report the share of all swaps that are profitable ( $\hat{\pi}_1 + \hat{\pi}_2 - \pi_1 - \pi_2 > 0$ ) and in Panel B we report the share of all swaps that are profitable by at least 1 percentage point. We include all borders in this sensitivity analysis. While the data-implied values of  $\sigma$  lie between 0.01 and 0.02, depending on the state, the difference in the share of profitable deviations across proposals at first increases for larger values of  $\sigma$ , peaking between 0.05 and 0.1. For very large values of  $\sigma$ , the proposals tend to look more similar in terms of share of profitable deviations, approximating the case of the uniform aggregate shock.

### A. All borders



### B. Borders that do not overlap with county borders

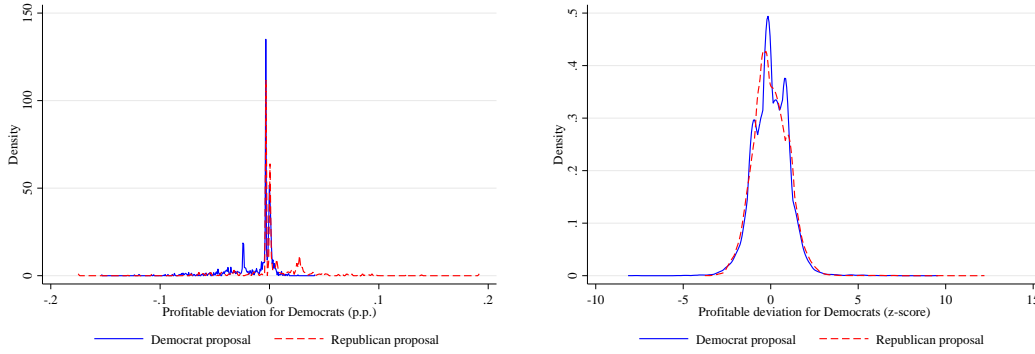
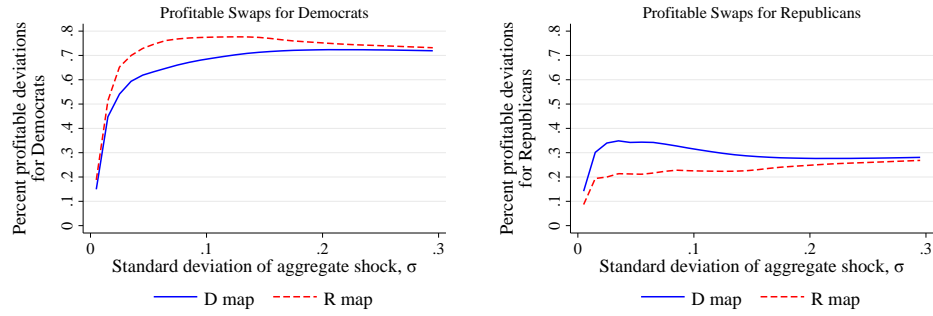


**FIGURE F.9. DISTRIBUTION OF THE EFFECT OF A SWAP ON THE PAYOFF FOR THE DEMOCRATIC GERRYMANDERER.** This figure plots the distribution of the effect of all counterfactual redistrictings, or swaps. The x-axis is the change in the payoff for the Democratic party, measured in percentage point gains to the Democrat's payoff function (left plots) or in standard deviations of the effect of swaps at a border (right plots). The solid blue line shows the distribution of the effect of swaps for the Democratic proposals, and the dashed red line shows the same for the Republican proposals.

Figure F.11 shows the share of profitable swaps using the ideology-only measure. These results are analogous to those shown in Figure 4, except we use vote shares to proxy for ideology rather than party registration.

Finally, we show that the patterns in Figure F.12 are not due to a single party nor to only the parties that have majority control over the legislature at the time of redistricting. We evaluate the share of swaps that are profitable for the party with majority control over the state legislature and the share of swaps that are profitable for the minority party in the state legislature. Parties have fewer profitable deviations under their own proposal when we look at borders that do not coincide with county borders, regardless of whether they are the majority or minority party in the state.

### A. All profitable deviations



### B. Profitable deviations at of 1 p.p. or higher

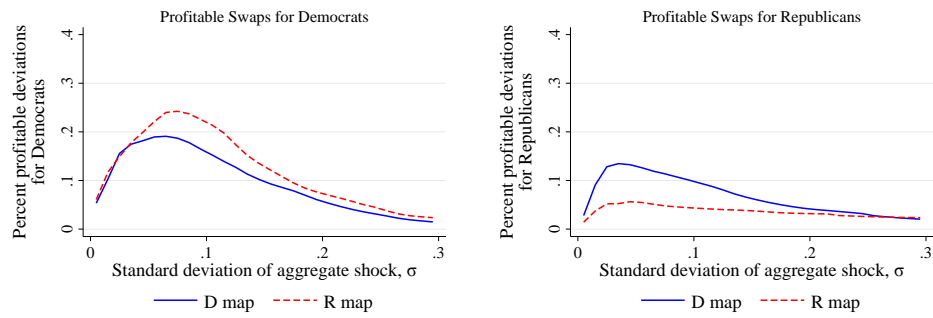
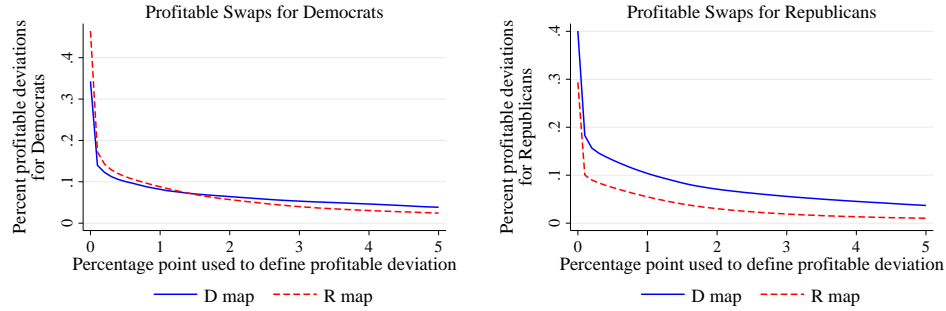


FIGURE F.10. SENSITIVITY ANALYSIS: profitable swaps by standard deviation of the aggregate shock ( $\sigma$ )

### A. Measure Payoffs with Ideology only: all borders



### B. Measure Payoffs with Ideology only: borders that do not coincide with counties

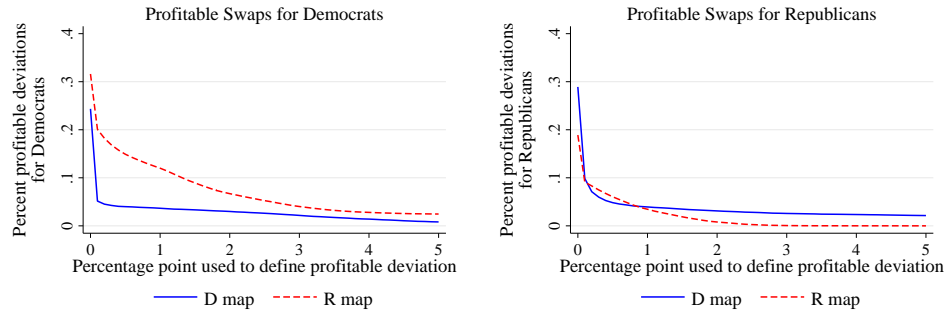
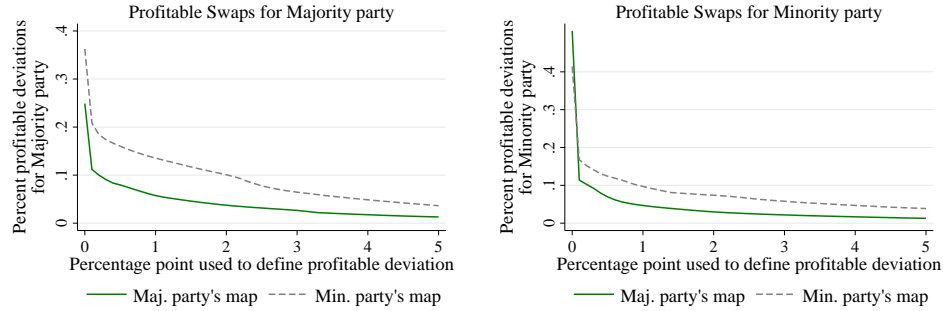


FIGURE F.11. SHARE OF SIGNIFICANTLY PROFITABLE SWAPS, MEASURING PAYOFFS WITH IDEOLOGY ONLY. The y-axis is the percent of feasible counterfactual maps ('swaps') that are profitable for Democrats (left) and Republicans (right). A swap is profitable if the change in payoff exceeds the threshold on the x-axis. The payoff is the expected number of seats. To compute the expected number of seats, we assume that the aggregate shock is normally distributed with mean zero and standard deviation calibrated using statewide presidential election returns from 2008-2020 (see Table F.1). For this exercise, we assume that the vote share of a district is the weighted average of the precinct-level ideology, where ideology is measured with precinct-level vote shares.

### A. All borders



### B. Borders that do not coincide with county borders

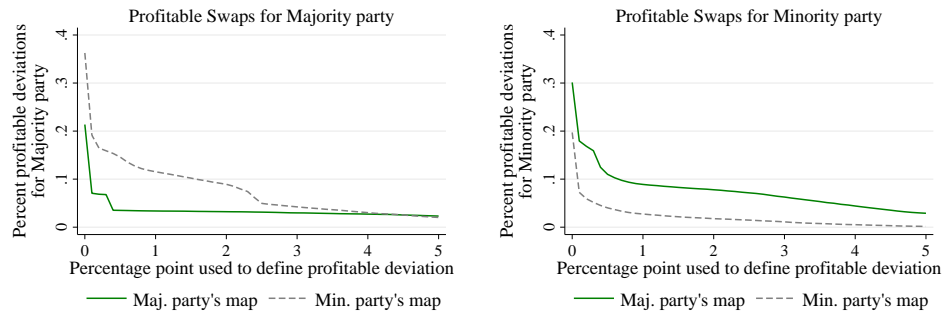


FIGURE F.12. SHARE OF SIGNIFICANTLY PROFITABLE SWAPS, COMPARING PROPOSALS FROM MAJORITY AND MINORITY PARTIES. The y-axis is the percent of feasible counterfactual maps ('swaps') that are profitable for the party that has majority control of both chambers of the state legislature (left) and for the minority party (right). A swap is profitable if the change in payoff exceeds the threshold on the x-axis. The payoff is the expected number of seats. To compute the expected number of seats we assume that the aggregate shock is normally distributed with mean zero and standard deviation calibrated using statewide presidential election returns from 2008-2020 (see Table F.1).